Acta Numerica (2023), pp. 1–80 Printed in the United Kingdom
doi:10.1017/S09624929XXXXXXXX

The Virtual Element Method

Lourenco Beirão da Veiga
Dipartimento di Matematica e Applicazioni, Università di Milano–Bicocca, Italy and IMATI-CNR, Pavia, Italy
E-mail: lourenco.beirao@unimib.it

Franco Brezzi
IUSS, Istituto Universitario di Studi Superiori, Pavia, Italy and IMATI-CNR, Pavia, Italy
E-mail: brezzi@imati.cnr.it

L. Donatella Marini
Dipartimento di Matematica, Università di Pavia, Italy, and IMATI-CNR, Pavia, Italy
E-mail: marini@imati.cnr.it

Alessandro Russo
Dipartimento di Matematica e Applicazioni, Università di Milano–Bicocca, Italy and IMATI-CNR, Pavia, Italy
E-mail: alessandro.russo@unimib.it

The present review paper points to several directions. As a first target it is meant to give a first idea of the general features of Virtual Element Methods (VEMs), that were introduced about a decade ago, in the field of Numerical Methods for Partial Differential Equations, in order to allow decompositions of the computational domain into polygons/polyhedra of a very general shape.

On the other hand, the paper is also addressed to people that already heard (and possibly read) about VEMs, and are interested in having more precise information, in particular concerning their application in specific subfields as: C^1 approximations of plate bending problems or approximations to problems in solid and fluid mechanics.

CONTENTS

1. Introduction

The Virtual Element Method (VEM) was introduced first in (Beirão da Veiga, Brezzi, Cangiani, Manzini, Marini and Russo 2013*b*, Beirão da Veiga, Brezzi, Marini and Russo 2014), as an alternative way of looking at Mimetic Finite Differences for the approximation of (systems of) Partial Differential Equations. The unknowns of the discretized problem, originally *nodal values*, in the VEM formulation became instead *functions* or, if convenient, *vector-valued functions*, individuated by a set of *degrees of freedom* that included *nodal values* or *moments* on edges and/or inside the element (referring to a two-dimensional problem). In Mimetic Finite Differences these values where used "as if they were related to a polynomial function", and the corresponding polynomial functions were used in the construction of the final discrete formulation. All this was done on polygons/polyhedra of very general shape, thus allowing the treatment of very general decompositions. The basic idea of Virtual Elements was "to associate with every suitable subset of degrees of freedom a corresponding function", and then write the discretized problem in terms of the corresponding functions, their values, their averages, and so on. Obviously, one could not expect to associate a *polynomial* function with every subset of degrees of freedom. Hence, the new (Virtual Element) strategy was: with every "set of degrees of freedom" we associate a function that is not necessarily a polynomial but rather a smooth function, solution of a PDE problem inside the element. These functions in general are not computable (one could not dream of solving a bunch of PDE problems inside each element of the decomposition!) but one would compute their *projections onto polynomial spaces* out of the degrees of freedom, and then use them in formulating the discretized problem. With time, the *internal PDE's problems* shifted from a simple Laplacian to more complex operators or systems of PDE's, connected (but, in general, not coincident) with the system of PDE's to be solved on the whole domain. Needless to say, all these element-by-element PDE's systems (with polynomial data) are *never* solved explicitly, but in the code one uses suitable projections of their solutions onto polynomial spaces.

The final outcome of this approach is a Galerkin method, having the same structure of the Finite Element Method. Furthermore, the two methods (VEM and FEM) are perfectly compatible, and can coexist on the same mesh. Moreover, somehow unexpectedly, some of the new techniques and ideas developed for polygonal elements proved to have some interest also on elements of classical shapes, like triangles or quadrilaterals, as shown in (Brezzi and Marini 2021).

In summary, the "general structure" of a VEM discretization amounts to:

i) generate a decomposition of the computational domain in polygons/polyhedra;
ii) define, inside each polygon/polyhedron, a finite dimensional space of functions, typically solutions of PDE problems with polynomial data (as for instance, a polynomial trace on each edge and a polynomial Laplacian);
iii) define a suitable set of degrees of freedom;
iv) individuate suitable polynomials, explicitly computable from the degrees of freedom, obtained by *projecting each of the above functions onto polynomial spaces*.

The above approach applies to an enormous variety of different PDE models, such as, for instance, Heat Diffusion, Elasticity, Plate Bending, Fluid Flows, Magnetic fields, and so on.

In the last decade, and soon after the publication of the first paper in 2013, Virtual Elements have seen an enormous growth of interest in the Applied Mathematics and in the Engineering community, thanks to their great ductility that makes them applicable to many different types of problems. The number of applications and variants is such that it would be difficult, if not prohibitive, to provide an exhaustive list. Here we decided to mention only few of them, chosen as samples among those that, to the best of our knowledge, appear to be particularly attractive in terms of number of papers and/or variety of groups of researchers. For each subject we will cite a couple of the most recent publications, and we refer to the references therein; more references are provided within each Section of the present paper.

For topology optimisation important contributions were given by G.H. Paulino and his group (Gain, Paulino, Duarte and Menezes 2015, Chi, Pereira, Menezes and Paulino 2020). Significant contributions to contact problems were given by P. Wriggers, B.D. Reddy and their groups (Wriggers, Rust and Reddy 2016, Cihan, Hudobivnik, Korelc and Wriggers 2022). For geophysical applications, and in particular for discrete fracture networks, S. Berrone and his group (Benedetto, Berrone, Borio, Pieraccini and Scialò 2016, Berrone and Raeli 2022) are worth mentioning. For Helmholtz problem we refer to I. Perugia & collaborators (Mascotto, Perugia and Pichler 2019).

A key ingredient in all VEM applications is the integration on general polygons and polyhedra; we refer to (Chin, Lasserre and Sukumar 2015, Chin and Sukumar 2021) for a detailed study of polytopal quadrature formulas.

For more methodology oriented papers we mention (Brenner, Guan and Sung 2017, Chen and Huang 2018) for results on a-priori estimates, (Mora, Rivera and Rodriguez 2017, Gardini, Manzini and Vacca 2019) for eigenvalue problems, (Beirão da Veiga, Chernov, Mascotto and Russo 2016, Chernov, Marcati and Mascotto 2021) for hp formulations, (Cangiani, Georgoulis, Pryer and Sutton 2017, Beirão da Veiga, Manzini and Mascotto 2019*a*) for a posteriori error analysis.

A "hot" subject regards the treatment of curved edges and faces, for which there are some results, still not completely satisfactory in (Bertoluzza, Pennacchio and Prada 2019, Beirão da Veiga, Russo and Vacca 2019*c*, Beirão da Veiga, Brezzi, Marini and Russo 2020, Dassi, Fumagalli, Scotti and Vacca 2022).

An update on the VEM-literature could be obtained through a non-conventional, although very effective, approach, consisting in looking (for instance in Google Scholar) at the most recent papers citing the original paper (Beirão da Veiga *et al.* 2013*b*).

In the present paper, following somehow the evolution and growth of the method and its applications, we will discuss the basic ideas, starting from the simplest Poisson problem, and then giving an overview on more general problems, namely, plate bending, elasticity, and fluid flows equations.

An outline of the whole presentation is as follows. After setting, in Section 2, the notation and some assumptions that will be used in the whole paper, in Section 3 we describe, on a simple Poisson problem, the basic approach to construct C^0-conforming approximations, in two and three dimensions. Section 4 is devoted to the C^0-non-conforming approximation of the same model problem, while Section 5 deals with C^1-conforming approximations, taking, as a reference problem, a plate bending problem. Section 6 is dedicated to the discretization of the spaces $H(\mathrm{div})$, $H(\mathrm{rot})$, and $H(\mathbf{curl})$. Two and three dimensional Face and Edge Virtual Elements are illustrated in detail, and are shown to form exact sequences. The last two Sections deal with specific problems: linear and nonlinear Elasticity in Section 7, Stokes and Navier-Stokes in Section 8. Suitable discrete spaces are presented and discussed, together with convergence results.

2. Preliminaries

In this Section we will define some common notation and introduce general assumptions that will be used throughout the paper. Other definitions and assumptions will be introduced as needed.

Computational domain and mesh

We will denote by $\Omega \subset \mathbb{R}^d$, $d = 2$ or $d = 3$, the computational domain of the differential problem under study. We assume that Ω can be decomposed into polygons (in two dimensions) or into polyhedra (in three dimensions). A generic polygon will be denoted by E and a generic polyhedron by P. We will use the general notation K to indicate a polygon or a polyhedron. The letter e will denote an edge (of a polygon or a polyhedron) and f a face (of a polyhedron).

The number of edges and vertices of a polygon or a polyhedron K will be denoted by $N_\mathrm{e}(K)$ and $N_V(K)$ respectively; the "(K)" will be omitted when no confusion can arise. Obviously for a polygon $N_{\mathrm{e}} = N_V$. Similarly, $N_{\mathrm{f}}(P)$ will indicate the number of faces of a polyhedron P.

The outward normal to K will be denoted by $\boldsymbol{n}_K$, sometimes with the superscript $^{\mathrm{f}}$ or $^{\mathrm{e}}$ to indicate that $\boldsymbol{n}_K$ belongs to the face f or the edge e respectively. When no confusion can arise, we will simply use the letter $\boldsymbol{n}$. Similarly, in three dimensions $\boldsymbol{n}_{\mathrm{f}}$ will denote the outward normal to the face f lying in the plane of f, and $\boldsymbol{n}_{\mathrm{f}}^{\mathrm{e}}$ will be that related to edge e. Tangent unit vectors will be denoted by $\boldsymbol{t}$; in particular, for an edge e, $\boldsymbol{t}_{\mathrm{e}}$ will be a unit vector parallel to e.

The diameter of an element K will be denoted by h_K; a family of decompositions of Ω will be denoted by $\{\mathcal{T}_h\}_h$, with $h = \max\{h_K, K \in \mathcal{T}_h\}$ being a measure of the size of the decomposition $\mathcal{T}_h$. On $\{\mathcal{T}_h\}_h$ we make the following assumption:

Assumption 2.1 (Mesh regularity). There exists a positive constant ϱ such that for any $K \in \{\mathcal{T}_h\}_h$:

- K is star-shaped with respect to a ball B_K of radius $\geq \varrho\, h_K$;
- (in three dimensions only) every face f of K is star-shaped with respect to a disk B_{f} of radius $\geq \varrho\, h_K$;
- any edge e of K has length $\geq \varrho\, h_K$.

We remark that the hypotheses above, though not too restrictive in many practical cases, could possibly be further relaxed, combining the present analysis with the studies in (Beirão da Veiga, Lovadina and Russo 2017*b*, Brenner *et al.* 2017, Brenner and Sung 2018, Cao and Chen 2018).

Polynomials

Given an integer $s \geq 0$ and a domain $\mathcal{O} \subset \mathbb{R}^d$ $(d = 1, 2, 3)$, $\mathbb{P}_s(\mathcal{O})$ will denote the space of polynomials of degree $\leq s$ restricted to $\mathcal{O}$; as usual, $\mathbb{P}_{-1} = \{0\}$. When no confusion is likely to occur, we will often use simply $\mathbb{P}_s$ instead of $\mathbb{P}_s(\mathcal{O})$. With a common abuse of language, we will often say "polynomial of degree s" meaning actually "polynomial of degree $\leq s$". If $\mathcal{O} = \mathbb{R}^d$ $(d = 1, 2, 3)$, its dimension $\pi_{s,d}$ is given by:

$$\pi_{s,1} = s + 1, \qquad \pi_{s,2} = \frac{(s+1)(s+2)}{2}, \qquad \pi_{s,3} = \frac{(s+1)(s+2)(s+3)}{6}.$$

When no confusion can occur, we will use the simpler notation π_k. For $s \geq 1$ we define

$$\mathbb{P}_s^0(\mathcal{O}) := \left\{ q_s \in \mathbb{P}_s(\mathcal{O}) \text{ such that } \int_{\mathcal{O}} q_s \,\mathrm{d}\mathcal{O} = 0 \right\}, \tag{2.1}$$

and

$$\mathbb{P}_s^{\mathrm{hom}}(\mathcal{O}) := \{\text{homogeneous polynomials of degree } s \text{ in the variables } (x_i - \bar{x}_i)\}$$

where $\bar{x}_i$ are the coordinates of the barycenter of $\mathcal{O}$. Next, for any non negative integers $m \leq n$, we denote by $\mathbb{P}_{n/m}$ any subspace (fixed once and for all) of $\mathbb{P}_n$ such that

$$\mathbb{P}_n = \mathbb{P}_m \oplus \mathbb{P}_{n/m}. \tag{2.2}$$

A common choice for $\mathbb{P}_{n/m}$ will be

$$\mathbb{P}_{n/m} = \mathbb{P}^{\text{hom}}_{m+1} \oplus \cdots \oplus \mathbb{P}^{\text{hom}}_{n}. \tag{2.3}$$

Differential operators

With a usual notation the symbols ∇ and Δ denote the gradient and the Laplacian for scalar functions, while div and **curl** are the divergence and the curl of a vector function. We recall that, in two dimensions, the **curl** operator has two incarnations (as ∇ and div) given by

$$\text{rot}(v_1, v_2) := \partial_x v_2 - \partial_y v_1 \qquad \textbf{rot}(\varphi) := (\partial_y \varphi, -\partial_x \varphi).$$

We will sometimes use the notation **grad** instead of ∇. Finally, for a vector $\boldsymbol{v} = (v_1, v_2)$ we indicate by $\boldsymbol{v}^\perp$ the vector $\boldsymbol{v}^\perp = (v_2, -v_1)$.

For a face f of a polyhedron P, the tangential differential operators will be denoted by the subscript 2, as in: div_2, rot_2, $\textbf{rot}_2$, $\textbf{grad}_2$, Δ_2 and so on.

Functional spaces

Throughout the paper we will follow the common notation for Sobolev spaces, scalar products, norms, and seminorms (see (Adams 1975)). For m integer ≥ 0 we define

$$H^m(\mathcal{O}) := \{v \text{ such that } D^\alpha v \in L^2(\mathcal{O}), \quad \forall |\alpha| \leq m\},$$

where

$$D^\alpha v = \frac{\partial^{|\alpha|} v}{\partial x_1^{\alpha_1} \cdots \partial x_n^{\alpha_n}}, \qquad |\alpha| = \alpha_1 + \cdots \alpha_n.$$

With $(v, w)_{0,\mathcal{O}}$ (sometimes, just $(v, w)_0$) and $\|v\|_{0,\mathcal{O}}$ (sometimes, just $\|v\|_0$) we will denote the $L^2(\mathcal{O})$ scalar product and norm, whereas $|v|_{m,\mathcal{O}}$ (sometimes, just $|v|_m$) and $\|v\|_{m,\mathcal{O}}$ (sometimes, just $\|v\|_m$) will denote, respectively, the H^m semi-norm and norm. In particular, we shall use $H^1(\mathcal{O})$ ($\mathcal{O} \subset \mathbb{R}^d,\ d = 2, 3$), $H^2(\mathcal{O})$ ($\mathcal{O} \subset \mathbb{R}^2$). Moreover, we will also need:

- For $\mathcal{O} \subset \mathbb{R}^2$:

$$H(\text{div}, \mathcal{O}) := \{\boldsymbol{v} \in [L^2(\mathcal{O})]^2 \text{ such that } \text{div}\,\boldsymbol{v} \in L^2(\mathcal{O})\},$$
$$H(\text{rot}, \mathcal{O}) := \{\boldsymbol{v} \in [L^2(\mathcal{O})]^2 \text{ such that } \text{rot}\,\boldsymbol{v} \in L^2(\mathcal{O})\}.$$

- For $\mathcal{O} \subset \mathbb{R}^3$:

$$H(\text{div}, \mathcal{O}) := \{\boldsymbol{v} \in [L^2(\mathcal{O})]^3 \text{ such that } \text{div}\,\boldsymbol{v} \in L^2(\mathcal{O})\},$$
$$H(\textbf{curl}, \mathcal{O}) := \{\boldsymbol{v} \in [L^2(\mathcal{O})]^3 \text{ such that } \textbf{curl}\,\boldsymbol{v} \in [L^2(\mathcal{O})]^3\}.$$

(2.4)

Projections onto polynomial spaces

- *L^2-projection*

  On $\mathcal{O}$ we will denote by $\Pi_s^{0,\mathcal{O}}$ (or simply by Π_s^0 when no confusion can occur) the $L^2(\mathcal{O})$-orthogonal projection operator onto $\mathbb{P}_s(\mathcal{O})$, defined, as usual, for every $\varphi \in L^2(\mathcal{O})$, by

$$\int_{\mathcal{O}} (\Pi_s^{0,\mathcal{O}} \varphi)\, p_s \,\mathrm{d}\mathcal{O} = \int_{\mathcal{O}} \varphi\, p_s \,\mathrm{d}\mathcal{O} \qquad \forall p_s \in \mathbb{P}_s(\mathcal{O}), \tag{2.5}$$

  with obvious extension for vector functions $\Pi_s^{0,\mathcal{O}} : [L^2(\mathcal{O}]^d \to [\mathbb{P}_n(\mathcal{O})]^d$ and tensor functions $\mathbf{\Pi}_s^{0,\mathcal{O}} : [L^2(\mathcal{O})]^{d\times d} \to [\mathbb{P}_s(\mathcal{O})]^{d\times d}$.

- *H_0^1-projection: the $\Pi_s^{\nabla,\mathcal{O}}$ operator*

  For every $\varphi \in H^1(\mathcal{O})$ we denote by $\Pi_s^{\nabla,\mathcal{O}}\varphi$ (or simply by $\Pi_s^{\nabla}\varphi$ when no confusion can occur) its projection onto the space $\mathbb{P}_s(\mathcal{O})$ with respect to the scalar product of $H^1(\mathcal{O})$, defined as the solution, in $\mathbb{P}_s(\mathcal{O})$, of

$$\begin{cases} \displaystyle\int_{\mathcal{O}} \nabla(\Pi_s^{\nabla,\mathcal{O}}\varphi) \cdot \nabla q_s \,\mathrm{d}\mathcal{O} = \int_{\mathcal{O}} \nabla\varphi \cdot \nabla q_s \,\mathrm{d}\mathcal{O} \quad \forall q_s \in \mathbb{P}_s(\mathcal{O}), \\ \displaystyle\int_{\partial\mathcal{O}} \Pi_s^{\nabla,\mathcal{O}}\varphi \,\mathrm{d}s = \int_{\partial\mathcal{O}} \varphi \,\mathrm{d}s. \end{cases} \tag{2.6}$$

Moreover, given a function $\psi \in L^2(\mathcal{O})$ and an integer $s \geq 0$, we recall that the *moments of order $\leq s$ of ψ on $\mathcal{O}$* are defined as:

$$\int_{\mathcal{O}} \psi\, q_s \,\mathrm{d}\mathcal{O} \qquad \text{for } q_s \in \mathbb{P}_s(\mathcal{O}).$$

Hence *to assign the moments of ψ up to the order s on $\mathcal{O}$* will amount to assign a number of conditions equal to the dimension of $\mathbb{P}_s(\mathcal{O})$. Typically this will be used when these moments are considered as *degrees of freedom*.

Remark 2.2. A quantity (depending on a function living in a discrete space with given degrees of freedom) is said to be **computable** if it can be determined directly out of information provided by the degrees of freedom. This would require to compute integrals of polynomials on polygonal and polyhedral domains (see, e.g., (2.5), and (2.6)). Among the various quadrature techniques we refer for instance to (Chin *et al.* 2015, Chin and Sukumar 2021).

3. H^1-conforming approximations

We will describe in this section the original Virtual Element Method (VEM), as first introduced in (Beirão da Veiga *et al.* 2013*b*). To fix ideas, we shall consider the following model problem:

$$-\Delta u = f \quad \text{in } \Omega, \qquad u = 0 \quad \text{on } \Gamma_D, \qquad \frac{\partial u}{\partial n} = g \ \text{ on } \Gamma_N. \tag{3.1}$$

In (3.1) $\Omega \subset \mathbb{R}^2$ is a polygonal domain, with boundary $\partial\Omega = \Gamma_D \cup \Gamma_N$ ($\Gamma_D \neq \emptyset$, $\mathring{\Gamma}_D \cap \mathring{\Gamma}_N = \emptyset$). The data f, g are given functions with $f \in L^2(\Omega)$, and g, say, in $L^2(\Gamma_N)$. Setting

$$
\begin{aligned}
&H^1_{0,\Gamma_D}(\Omega) := \{v \in H^1(\Omega) \text{ such that } v = 0 \text{ on } \Gamma_D\},\\
&a(u,v) := \int_\Omega \nabla u \cdot \nabla v \, dx,\\
&\ell(v) := (f,v)_{0,\Omega} + (g,v)_{0,\Gamma_N} = \int_\Omega f\, v\, dx + \int_{\Gamma_N} g\, v\, \mathrm{d}s,
\end{aligned}
\tag{3.2}
$$

the variational formulation of (3.1) is

$$
\text{find } u \in V := H^1_{0,\Gamma_D}(\Omega) \quad \text{such that} \quad a(u,v) = \ell(v) \quad \forall v \in V. \tag{3.3}
$$

Problem (3.3) has a unique solution thanks to Lax-Milgram Lemma. In particular, $a(\cdot,\cdot)$ is a symmetric bilinear form, continuous and elliptic, i.e.,

$$
\exists\, M > 0 \text{ such that } a(v,w) \le M \|v\|_{1,\Omega} \|w\|_{1,\Omega} \quad \forall v, w \in V, \tag{3.4}
$$

$$
\exists\, \alpha > 0 \text{ such that } a(v,v) \ge \alpha \|v\|^2_{1,\Omega} \quad \forall v \in V, \tag{3.5}
$$

and $\ell(\cdot)$ is a linear bounded functional, i.e.,

$$
\exists\, C > 0 \text{ such that } |\ell(v)| \le C(\|f\|_{0,\Omega} + \|g\|_{0,\Gamma_N})\|v\|_{1,\Omega} \quad \forall v \in V. \tag{3.6}
$$

The Virtual Element Method, as all Galerkin methods, uses all the classical ingredients needed for approximating variational formulations: a decomposition $\mathcal{T}_h$ of Ω into polygons E, and then an associated finite dimensional space $V_h \subset V$, a bilinear form $a_h(\cdot,\cdot)$, and a linear functional $\ell_h(\cdot)$. Then, the discrete problem reads

$$
\text{find } u_h \in V_h \text{ such that } a_h(u_h, v_h) = \ell_h(v_h) \quad \forall v_h \in V_h, \tag{3.7}
$$

and we have to define V_h, $a_h(\cdot,\cdot)$, and $\ell_h(\cdot)$ in such a way that problem (3.7) has a unique solution and optimal error estimates hold. This will be done in the next subsections, following the original approach of (Beirão da Veiga *et al.* 2013*b*).

3.1. An abstract convergence result

Let us recall the assumptions needed to prove the abstract convergence theorem. For every polygon $E \in \mathcal{T}_h$ of diameter h_E we denote by $V_{h|E}$, $a_h^E(\cdot,\cdot)$, and $a^E(\cdot,\cdot)$, respectively, the restriction to E of V_h, $a_h(\cdot,\cdot)$, and $a(\cdot,\cdot)$, i.e.,

$$
\begin{aligned}
a(v,w) &= \sum_{E \in \mathcal{T}_h} a^E(v,w) \quad \forall\, v,\, w \in V,\\
a_h(v_h,w_h) &= \sum_{E \in \mathcal{T}_h} a_h^E(v_h,w_h) \quad \forall\, v_h,\, w_h \in V_h.
\end{aligned}
\tag{3.8}
$$

On the bilinear form $a_h^E(\cdot,\cdot)$ we make the following assumption.

Assumption 3.1. There exists an integer $k \geq 1$ (that will be the order of accuracy) such that for all h, and for all E in $\mathcal{T}_h$, we have $\mathbb{P}_k(E) \subset V_{h|E}$ and

- *k*-**consistency**: for all $p_k \in \mathbb{P}_k(E)$ and for all $v_h \in V_{h|E}$,

$$a_h^E(p_k, v_h) = a^E(p_k, v_h) \tag{3.9}$$

- **stability**: there exist two positive constants α_* and α^*, independent of h and of E, such that

$$\forall v_h \in V_{h|E} \qquad \alpha_* \, a^E(v_h, v_h) \leq a_h^E(v_h, v_h) \leq \alpha^* \, a^E(v_h, v_h). \tag{3.10}$$

We notice that the symmetry of a_h^E, property (3.10), and the definition of a^E easily imply the continuity of a_h^E with

$$\begin{aligned} a_h^E(u_h, v_h) \leq & \left(a_h^E(u_h, u_h)\right)^{1/2} \left(a_h^E(v_h, v_h)\right)^{1/2} \\ \leq & \; \alpha^* \left(a^E(u_h, u_h)\right)^{1/2} \left(a^E(v_h, v_h)\right)^{1/2} \\ = & \; \alpha^* \, \|u_h\|_{1,E} \, \|v_h\|_{1,E} \quad \text{for all } u_h, v_h \in V_{h|E}. \end{aligned} \tag{3.11}$$

Theorem 3.2. Under Assumptions 3.1 the discrete problem (3.7) has a unique solution u_h. Moreover, for every approximation $u_I \in V_h$ of u, and for every approximation u_π of u that is piecewise in $\mathbb{P}_k$, we have

$$|u - u_h|_{1,\Omega} \leq C\Big(|u - u_I|_{1,\Omega} + |u - u_\pi|_{1,\mathcal{T}_h} + \mathfrak{F}_h\Big), \tag{3.12}$$

where C is a constant depending only on α_* and α^*, $|\cdot|_{1,\mathcal{T}_h}$ is the broken H^1-norm, and, for any h, $\mathfrak{F}_h$ is the smallest constant such that

$$\ell(v_h) - \ell_h(v_h) \leq \mathfrak{F}_h \, |v_h|_{1,\Omega} \quad \forall \, v_h \in V_h. \tag{3.13}$$

Proof. Existence and uniqueness of the solution of (3.7) are a consequence of

(3.10) and (3.5). Next, setting $\delta_h := u_h - u_I$ we have

$$
\begin{aligned}
\alpha_* |\delta_h|_1^2 &= \alpha_*\, a(\delta_h, \delta_h) \leq a_h(\delta_h, \delta_h) \\
&= a_h(u_h, \delta_h) - a_h(u_I, \delta_h) \text{ (use (3.7) and (3.8))} \\
&= \ell_h(\delta_h) - \sum_E a_h^E(u_I, \delta_h) \text{ (use } \pm u_\pi) \\
&= \ell_h(\delta_h) - \sum_E \left(a_h^E(u_I - u_\pi, \delta_h) + a_h^E(u_\pi, \delta_h) \right) \text{ (use (3.9))} \\
&= \ell_h(\delta_h) - \sum_E \left(a_h^E(u_I - u_\pi, \delta_h) + a^E(u_\pi, \delta_h) \right) \text{ (add } \pm u) \\
&= \ell_h(\delta_h) - \sum_E \left(a_h^E(u_I - u_\pi, \delta_h) + a^E(u_\pi - u, \delta_h) \right) - a(u, \delta_h) \text{ (use (3.7))} \\
&= \ell_h(\delta_h) - \sum_E \left(a_h^E(u_I - u_\pi, \delta_h) + a^E(u_\pi - u, \delta_h) \right) - \ell(\delta_h) \\
&= \ell_h(\delta_h) - \ell(\delta_h) - \sum_E \left(a_h^E(u_I - u_\pi, \delta_h) + a^E(u_\pi - u, \delta_h) \right).
\end{aligned}
$$

Now use (3.13), (3.11), and the continuity of each a^E to obtain

$$
|\delta_h|_{1,\Omega}^2 \leq C \left(\mathfrak{F}_h + |u_I - u_\pi|_{1,\mathcal{T}_h} + |u - u_\pi|_{1,\mathcal{T}_h} \right) |\delta_h|_{1,\Omega} \tag{3.14}
$$

for some constant C depending only on α_* and α^*. Then the result follows easily by the triangle inequality. □

3.2. *The local discrete spaces*

We first recall the definition of the discrete spaces from (Beirão da Veiga *et al.* 2013*b*). Let E be a generic polygon in $\mathcal{T}_h$. For k integer, $k \geq 1$, we define the local space $V_{h|E}$ as

$$
V_k(E) := \{ v \in C^0(\overline{E}) : \; v_{|\mathrm{e}} \in \mathbb{P}_k(\mathrm{e}) \; \forall \text{ edge } \mathrm{e} \subset \partial E, \; \Delta v \in \mathbb{P}_{k-2}(E) \}. \tag{3.15}
$$

Denoting by N_e the number of edges of E, the dimension of $V_k(E)$ is given by

$$
\dim V_k(E) = k N_\mathrm{e} + k(k-1)/2.
$$

We notice that the space (3.15) contains the space $\mathbb{P}_k(E)$, but is not reduced to it, except if E is a triangle and $k = 1$, as it can be seen by a simple dimensional count. The degrees of freedom for $v_h \in V_k(E)$ are given by

$$
\begin{aligned}
&(D_1) : \text{the values of } v_h \text{ at the vertices,} \\
&(D_2) : \text{for } k \geq 2 \text{ the moments } \int_\mathrm{e} v_h p_{k-2} \,\mathrm{d}s, \;\; \forall p_{k-2} \in \mathbb{P}_{k-2}(\mathrm{e}), \forall \text{ edge e} \\
&(D_3) : \text{for } k \geq 2 \text{ the moments } \int_E v_h p_{k-2} \,\mathrm{d}E \quad \forall p_{k-2} \in \mathbb{P}_{k-2}(E).
\end{aligned} \tag{3.16}
$$

Clearly, instead of the moments (D_2) one could use the values at $k-1$ distinct points on each edge, more in the spirit of Finite Elements:

$$(D_2'):\ \text{the value of } v_h \text{ at } k-1 \text{ distinct points on each edge e.}$$

We observe that it is convenient to scale the degrees of freedom so that they all have the same order of magnitude. The reason for this will be clear in the next subsection; here, however, we do not enter the details of this issue, and we refer to (Beirão da Veiga *et al.* 2014) for a more detailed discussion.

Remark 3.3. The classical definition of "degree of freedom" for a generic local finite element space $V_k(K)$ (as given for instance in Ciarlet (1978)), says that a degree of freedom is a linear functional $L : V_k(K) \to \mathbb{R}$, and a (finite) set $\{L_i\}$ of degrees of freedom is *unisolvent* if the set of linear equations $L_i(v) = b_i$ has a unique solution for any choice of the b_i's. Given a set of unisolvent degrees of freedom in $V_k(K)$, we can immediately define the corresponding dual basis $\{\varphi_i\}$ for $V_k(K)$ by requiring $L_i(\varphi_j) = \delta_{ij}$.

Here and in the rest of the paper we will associate with a polynomial space a set of degrees of freedom, in the sense that statements like (D_3) in (3.16) will mean that, *in practice*, one has to choose a basis $\{m_i\}$ for $\mathbb{P}_{k-2}(K)$ and then define the degrees of freedom

$$L_i(v_h) := \int_K v_h\, m_i \,\mathrm{d}K, \qquad v_h \in V_k(K). \tag{3.17}$$

These bases are typically chosen as shifted and scaled monomials (see for instance (Beirão da Veiga *et al.* 2014, Dassi and Vacca 2020)) or, for a better condition number behavior, in particular for high values of k, as suitable orthonormal polynomials (Chernov *et al.* 2021, Beirão da Veiga, Chernov, Mascotto and Russo 2016*e*).

Lemma 3.4. The degrees of freedom (3.16) are unisolvent for $V_k(E)$.

Proof. Since the number of dofs equals the dimension of $V_k(E)$, it is enough to show that a function v_h having all the dofs vanishing is identically zero. Since v_h is a polynomial of degree k on each edge, $(D_1) = 0$ and $(D_2) = 0$ imply that $v_h \equiv 0$ on ∂E. This, together with $(D_3) = 0$, gives

$$\int_E |\nabla v_h|^2 \,\mathrm{d}E = -\int_E v_h\, \Delta v_h \,\mathrm{d}E + \int_{\partial E} v_h \frac{\partial v_h}{\partial n}\,\mathrm{d}s = 0$$

since $\Delta v_h \in \mathbb{P}_{k-2}$. Hence, $\nabla v_h \equiv 0$, i.e., $v_h = \mathit{constant} = 0$ (since $v_h = 0$ on the boundary Γ_D). □

3.3. Construction of a computable discrete bilinear form

From the definition (3.15) we see that the functions of $V_k(E)$ are known on the boundary of ∂E but not inside, unless we are willing to solve a PDE on each element E, something that we do not want to do, not even in an approximate way. Then, in order to approximate $a^E(\cdot,\cdot)$ we use a projection onto $\mathbb{P}_k(E)$. We consider the operator Π_k^∇ defined in (2.6), for which we have the following Lemma.

Lemma 3.5. The operator Π_k^∇ is computable out of the degrees of freedom (3.16).

Proof. The left-hand side of (2.6) is a product of polynomials, and it is obviously computable. Integrating by parts the right-hand side we have

$$\int_E \nabla v_h \cdot \nabla q_k \, \mathrm{d}E = -\int_E v_h \, \Delta q_k \, \mathrm{d}E + \int_{\partial E} v_h \frac{\partial q_k}{\partial n} \, \mathrm{d}s, \tag{3.18}$$

and the two integrals are both computable from the degrees of freedom (3.16). □

Then, a discrete bilinear form can be constructed, in each element E, and for $v_h, w_h \in V_k(E)$, as

$$a_h^E(v_h, w_h) := a^E\left(\Pi_k^\nabla v_h, \Pi_k^\nabla w_h\right) + \mathcal{S}^E\left((I - \Pi_k^\nabla)v_h, (I - \Pi_k^\nabla)w_h\right), \tag{3.19}$$

where $\mathcal{S}^E$ is any symmetric bilinear form to be chosen in such a way that it scales like $a^E(\cdot,\cdot)$, and is positive on the kernel of Π_k^∇, i.e., there exist two positive constant c_1, c_2 such that

$$c_1 a^E(v_h, v_h) \le \mathcal{S}^E(v_h, v_h) \le c_2 a^E(v_h, v_h) \quad \forall v_h \text{ such that } \Pi_k^\nabla v_h = 0. \tag{3.20}$$

There are various recipes for $\mathcal{S}^E$, the most commonly used being the so-called *dofi-dofi*:

$$\mathcal{S}^E(v_h, w_h) := \sum_{i=1}^{\#\text{dofs}} dof_i(v_h)\, dof_i(w_h), \tag{3.21}$$

where dof_i is the i^{th} degree of freedom. As we already anticipated, for condition (3.20) to be satisfied, the degrees of freedom (3.16) must be properly scaled. Other choices can be convenient, for example,

$$\mathcal{S}^E(v_h, w_h) := h_E^{-1} \int_{\partial E} v_h \, w_h \, \mathrm{d}s, \tag{3.22}$$

(where h_E is still the diameter of the element E), or

$$\mathcal{S}^E(v_h, w_h) := h_E \int_{\partial E} \frac{\partial v_h}{\partial t} \frac{\partial w_h}{\partial t} \, \mathrm{d}s, \tag{3.23}$$

where $\partial/\partial t$ denotes the *tangential derivative*.

Lemma 3.6. The discrete bilinear form (3.19) is k-consistent and stable.

Proof. To prove consistency we observe that $\Pi_k^\nabla p_k \equiv p_k$ since Π_k^∇ is a projection. Hence, $\mathcal{S}^E\left((I - \Pi_k^\nabla)v_h, (I - \Pi_k^\nabla)p_k\right) \equiv 0, \forall v_h \in V_k(E)$ and $\forall p_k \in \mathbb{P}_k$. Then, using the definition (2.6) of Π_k^∇ we immediately have

$$a_h^E(v_h, p_k) = a^E(\Pi_k^\nabla v_h, p_k) = a^E(v_h, p_k). \tag{3.24}$$

To prove stability we use (3.20) and the definition (2.6) of Π_k^∇ to obtain

$$\begin{aligned} a_h^E(v_h, v_h) &\geq a^E(\Pi_k^\nabla v_h, \Pi_k^\nabla v_h) + c_1 a^E(v_h - \Pi_k^\nabla v_h, v_h - \Pi_k^\nabla v_h) \\ &= a^E(v_h, \Pi_k^\nabla v_h) + c_1 a^E(v_h - \Pi_k^\nabla v_h, v_h) \\ &\geq \min\{1, c_1\}(a^E(v_h, \Pi_k^\nabla v_h) + a^E(v_h - \Pi_k^\nabla v_h, v_h)) = \alpha_* a^E(v_h, v_h). \end{aligned}$$

Similarly,

$$\begin{aligned} a_h^E(v_h, v_h) &\leq a^E(\Pi_k^\nabla v_h, \Pi_k^\nabla v_h) + c_2 a^E(v_h - \Pi_k^\nabla v_h, v_h - \Pi_k^\nabla v_h) \\ &= a^E(v_h, \Pi_k^\nabla v_h) + c_2 a^E(v_h - \Pi_k^\nabla v_h, v_h) \\ &\leq \max\{1, c_2\}(a^E(v_h, \Pi_k^\nabla v_h) + a^E(v_h - \Pi_k^\nabla v_h, v_h)) = \alpha^* a^E(v_h, v_h). \end{aligned}$$

□

As a consequence of Lemma 3.6 we have that the abstract estimate (3.12) holds.

3.4. *Construction of a computable right-hand side*

We begin by recalling here the original approximation of the right-hand side, as introduced in (Beirão da Veiga *et al.* 2013*b*). In Section 3.7 we will present an alternative approach.

For the first integral in $\ell(v_h)$ (see (3.2)) we can define an approximation f_h of f directly computable from the degrees of freedom (D_1)-(D_3) as follows. Denoting by $\{V_i\}$ the N_V vertices of E, and recalling that Π_s^0 is the L^2-projection onto $\mathbb{P}_s$, we set:

$$(f_h, v_h)_{0,E} = \begin{cases} \text{for } k = 1 & \displaystyle\int_E (\Pi_0^0 f)\, \overline{v}_h \,\mathrm{d}E, \text{ with } \overline{v}_h = \frac{\sum_i v_h(V_i)}{N_V}, \\ \text{for } k \geq 2 & \displaystyle\int_E (\Pi_{k-2}^0 f)\, v_h \,\mathrm{d}E. \end{cases} \tag{3.25}$$

The case $k = 1$ needs a special treatment since in this case we do not have internal moments among the dofs to be used as for $k \geq 2$.

With the choice (3.25) optimal error estimates are guaranteed. For $k = 1$ we have, adding and subtracting $f\overline{v}_h$, and using the definition of the L^2-projection and standard approximation estimates:

$$\begin{aligned} (f, v_h)_{0,E} - (f_h, v_h)_{0,E} &= \int_E (f v_h - f\overline{v}_h + f\overline{v}_h - \Pi_0^0 f\, \overline{v}_h) \,\mathrm{d}E \\ &= \int_E (f v_h - f\overline{v}_h) \,\mathrm{d}E \leq C h_E \|f\|_{0,E} |v_h|_{1,E}. \end{aligned} \tag{3.26}$$

For $k \geq 2$, using again the definition of the L^2-projection, and standard approximation properties we have

$$
\begin{aligned}
(f, v_h)_{0,E} - (f_h, v_h)_{0,E} &= \int_E (f v_h - \Pi^0_{k-2} f\, v_h)\, \mathrm{d}E \\
&= \int_E (f - \Pi^0_{k-2} f)(v_h - \Pi^0_{k-2} v_h)\, \mathrm{d}E \\
&\leq C h_E^{k-1} \|f\|_{k-1,E}\, h_E |v_h|_{1,E} \\
&\leq C h_E^{k} \|f\|_{k-1,E}\, |v_h|_{1,E}.
\end{aligned}
\tag{3.27}
$$

The boundary integral poses no problems, since our functions are polynomials on each edge in Γ_N, and we might assume that we can compute the integrals to any chosen accuracy.

3.5. The global problem - Error estimates

The global space V_h is obviously defined as a patchwork of the spaces (3.15):

$$
V_h := \{ v_h \in H^1_{0,\Gamma_D}(\Omega) : \; v_{h|E} \in V_k(E) \; \forall E \in \mathcal{T}_h \}. \tag{3.28}
$$

The degrees of freedom in V_h are the natural extension of those defined in (3.16). The global bilinear form and right-hand side are defined, as in FEM, by summing over the elements of $\mathcal{T}_h$:

$$
\begin{aligned}
a_h(v_h, w_h) &:= \sum_{E \in \mathcal{T}_h} a_h^E(v_h, w_h), \\
\ell_h(v_h) &:= \sum_{E \in \mathcal{T}_h} (f_h, v_h)_{0,E} + \sum_{\mathrm{e} \subset \Gamma_N} (g, v_h)_{0,\mathrm{e}},
\end{aligned}
\tag{3.29}
$$

with $a_h^E(v_h, w_h)$ defined in (3.19), and $(f_h, v_h)_{0,E}$ in (3.25). The discrete problem is then

$$
\text{Find } u_h \in V_h \text{ such that } a_h(u_h, v_h) = \ell_h(v_h) \quad \forall v_h \in V_h. \tag{3.30}
$$

With these choices the assumptions of Theorem 3.2 are satisfied, so that (3.12) holds. In terms of order of convergence, the expected optimal order k holds, and we have the following Theorem.

Theorem 3.7. Let u be the solution of (3.3), and let u_h be the solution of (3.30). Under Assumptions 2.1 on the mesh it holds:

$$
|u - u_h|_{1,\Omega} \leq C h^k |u|_{k+1,\Omega}. \tag{3.31}
$$

Proof. From (3.26)-(3.27) we have

$$
\ell(v_h) - \ell_h(v_h) = \sum_{E \in \mathcal{T}_h} (f - f_h, v_h)_{0,E} \leq C\, h^k \|f\|_{k-1,\Omega}\, \|v_h\|_{1,\Omega} \quad \forall v_h \in V_h. \tag{3.32}
$$

For every element E, let $u_\pi \in \mathbb{P}_k(E)$ be defined as the L^2-projection of u onto

$\mathbb{P}_k(E)$:

$$u_\pi \in \mathbb{P}_k(E): \quad \int_E (u - u_\pi)\, p_k \,\mathrm{d}E = 0, \quad \forall E \in \mathcal{T}_h,\ \forall p_k \in \mathbb{P}_k(E). \tag{3.33}$$

Standard approximation properties (see (Brenner and Scott 2008)) give

$$\|u - u_\pi\|_{1,\mathcal{T}_h} \le C\, h^k |u|_{k+1,\Omega}. \tag{3.34}$$

Let now $u_I \in V_h$ be the interpolant of u, defined locally through the degrees of freedom (3.16):

$$\begin{aligned} & u_I = u \text{ at the vertices,} \\ & \text{for } k \ge 2 \quad \int_{\mathrm{e}} (u - u_I) p_{k-2} \,\mathrm{de} = 0 \quad \forall p_{k-2} \in \mathbb{P}_{k-2}(\mathrm{e}),\ \forall \text{ edge e} \\ & \text{for } k \ge 2 \quad \int_E (u - u_I) p_{k-2} \,\mathrm{d}E = 0 \quad \forall p_{k-2} \in \mathbb{P}_{k-2}(E). \end{aligned} \tag{3.35}$$

The following interpolation estimate was proved (see (Mora, Rivera and Rodríguez 2015), (Brenner *et al.* 2017), and (Chen and Huang 2018)):

$$\|u - u_I\|_{1,\Omega} \le C h^k |u|_{k+1,\Omega}. \tag{3.36}$$

Collecting (3.32), (3.34), and (3.36), from (3.12) we obtain the result. □

3.6. Enhanced and Serendipity Virtual Elements

A comparison with Finite Elements, in terms of number of degrees of freedom, and for a given degree k, shows that the boundary dofs are exactly the same, both on triangles and on quadrilaterals, as expected, since they have to guarantee the global continuity. Looking at (3.16) we see that the internal degrees of freedom for VEM are as many as the dimension of $\mathbb{P}_{k-2}$ for any polygon. Instead, the internal dofs for FEM are equal to the dimension of $\mathbb{P}_{k-3}$ on triangles, and to that of $\mathbb{Q}_{k-3}$ on quads, where we recall that $\mathbb{Q}_s$ are the polynomials of degree s separately in each variable. Hence, on triangles VEM use $k-1$ dofs more than FEM, while on quads FEM use $(k-1)(k-2)/2$ dofs more than VEM (see Figs. 3.1 and 3.2). The ideal situation would be to have the minimum number of necessary degrees of freedom, and hence it is desirable to eliminate as many as possible internal dofs. In this respect triangular FEM are already optimal, and quadrilateral FEM have been optimised through the serendipity procedure (see for instance (Arnold and Awanou 2011)). Following (Ahmad, Alsaedi, Brezzi, Marini and Russo 2013), and (Beirão da Veiga, Brezzi, Marini and Russo 2016*c*), in order to eliminate as many internal dofs as possible, and, at the same time, to allow the computation of all the moments of order $\le k$, we first define the local space

$$\widetilde{V}_k(E) := \{v_h \in C^0(\overline{E}):\ v_{h|\mathrm{e}} \in \mathbb{P}_k(\mathrm{e})\ \forall \mathrm{e} \subset \partial E,\ \Delta v_h \in \mathbb{P}_k(E)\}, \tag{3.37}$$

with the degrees of freedom

$$
\begin{aligned}
&(D_1) - (D_2) \qquad \text{(the same as in (3.16)),} \quad \text{plus} \\
&\text{the moments of order up to } k : \int_E v_h\, p_k \,\mathrm{d}E,\ \forall p_k \in \mathbb{P}_k(E).
\end{aligned}
\tag{3.38}
$$

Clearly the space (3.37) is bigger than (3.15), apparently in contradiction with our first aim, but now, thanks to the additional dofs in (3.38), the L^2-orthogonal projection onto $\mathbb{P}_k$ is directly available from the internal dofs. Then we begin by

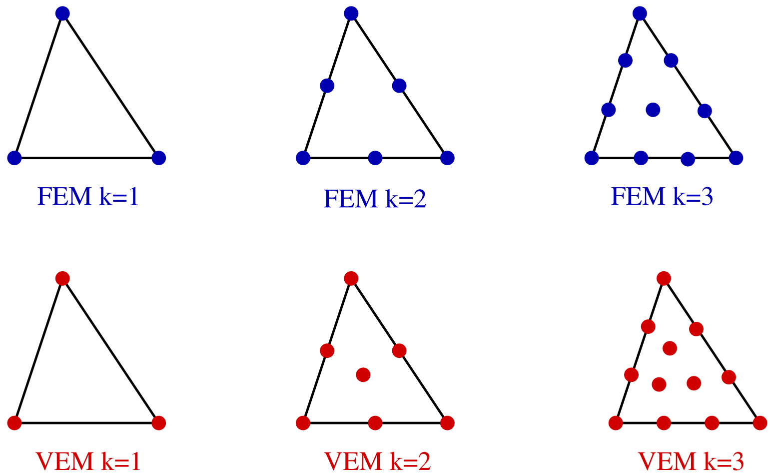

Figure 3.1. Triangles: dofs for FEM and original VEM

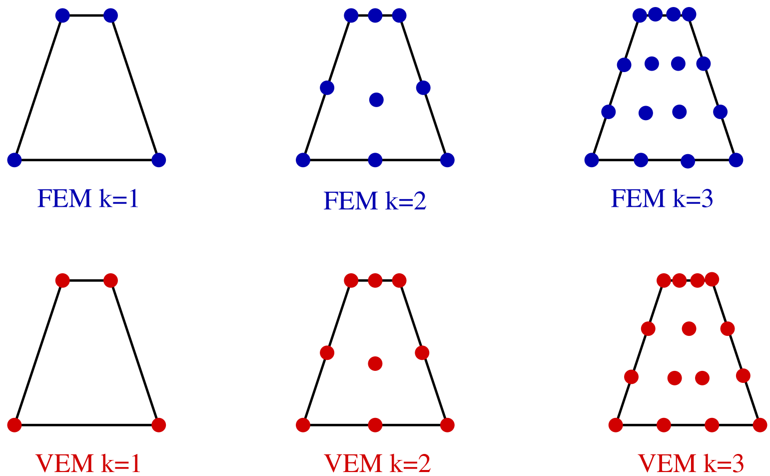

Figure 3.2. Quads: dofs for FEM and original VEM

defining locally a projection operator $\Pi_k : H^1(E) \rightarrow \mathbb{P}_k(E)$ as follows:

$$\Pi_k v \in \mathbb{P}_k(E) : \int_{\partial E} (\Pi_k v - v) q_k \, \mathrm{d}s = 0 \quad \forall q_k \in \mathbb{P}_k(E). \tag{3.39}$$

Clearly, system (3.39) has a unique solution unless $\mathbb{P}_k(E)$ contains polynomials that are identically zero on the boundary, i.e., unless $\mathbb{P}_k(E)$ contains bubbles. This happens for $k \geq 3$ on triangles (b_3 = product of the equations of the three edges) and for $k \geq 4$ on "true" quads (b_4 = product of the equations of the four edges). In these cases we need to add internal conditions, namely:

$$\underbrace{\int_E (\Pi_k v - v) q_s \, \mathrm{d}E = 0 \; \forall q_s \in \mathbb{P}_{k-3}}_{\text{on triangles}} \text{ or } \underbrace{\int_E (\Pi_k v - v) q_s \, \mathrm{d}E = 0 \; \forall q_s \in \mathbb{P}_{k-4},}_{\text{on quads}} \tag{3.40}$$

and then solve the system (3.39)-(3.40) in the least-squares sense. Once the polynomial $\Pi_k v$ has been computed, we define the new space by "copying" its moments. Namely, setting N = maximum degree of internal moments used to define Π_k (and clearly $N = -1$ in absence of internal moments), we introduce the new space

$$V_k^S(E) = \left\{ v_h \in \widetilde{V}_k(E) \text{ s. t.} \int_E (v_h - \Pi_k v_h) \, p_s \, \mathrm{d}E = 0 \; \forall p_s \in \mathbb{P}_s^{\mathrm{hom}}, \; N < s \leq k \right\}. \tag{3.41}$$

The degrees of freedom in (3.41) will be

$$(D_1) - (D_2) \qquad \text{(the same as in (3.16)), plus}$$

$$\text{the moments} \int_E v_h \, p \, \mathrm{d}E \quad \forall p \in \mathbb{P}_N(E).$$

Fig. 3.3 shows that, on triangles, serendipity VEM have the same number of dofs

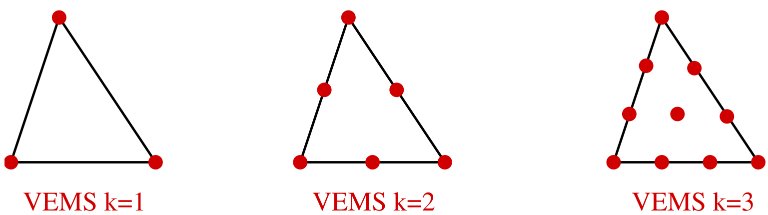

Figure 3.3. Triangles: dofs for serendipity VEM

as FEM (and actually the two spaces *coincide*), while Fig. 3.4 compares the dofs of serendipity VEM and FEM (see (Arnold and Awanou 2011)). The number is again the same, although serendipity FEM are known to suffer from element distortion (see (Arnold, Boffi and Falk 2002)), while VEM do not, as shown in (Beirão da Veiga *et al.* 2016*c*).

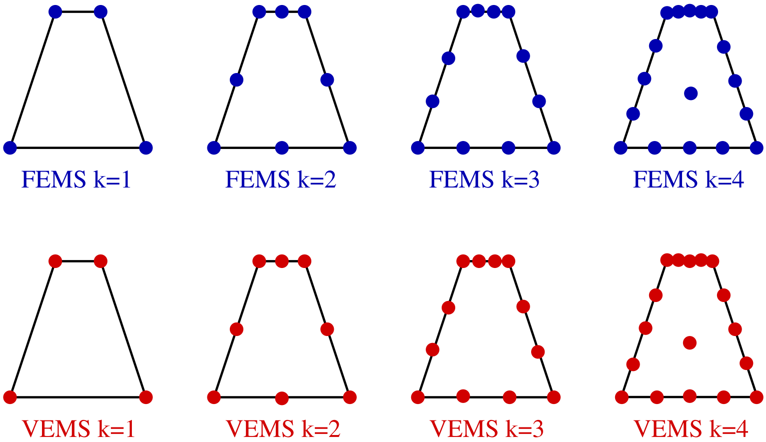

Figure 3.4. Quads: dofs for serendipity FEM and VEM

Figure 3.5. Fake triangles: a quad on the left, a pentagon on the right.

Remark 3.8. From the above discussion one might think that the number of internal moments necessary to define Π_k depends on k and on the number of edges: 3 for a triangle, 4 for a quad. This is true on *real* triangles and *real* quads. With the VEM approach the same geometrical entity (say, a triangle), might be considered as a polygon, a quad, or a pentagon or a hexagon, according to the number of points on its boundary that we consider as vertices (and then considering as edge the portion of the boundary between two consecutive vertices). See Fig. 3.5.

In the VEM terminology $\widetilde{Q}$ is a quad, while $\widetilde{P}$ is a pentagon, but the set of bubbles is the same, equal to that on triangles: $B_k = b_3 p_{k-3}$. What really counts is not the number of edges, but rather the number η of straight lines needed to cover the boundary (here $\eta = 3$ in both cases). Hence, the internal conditions necessary to compute Π_k, to be added to (3.39), are

$$\int_E (\Pi_k v - v) q_s \, \mathrm{d}E = 0 \; \forall q_s \in \mathbb{P}_{k-\eta}(E).$$

Remark 3.9. One might argue that static condensation could be a simpler procedure to reduce the number of internal degrees of freedom. This is true in two dimensional problems, but it is not anymore the case for three dimensional problems, where the reduction of dofs on faces is important. Static condensation on faces might turn into a nightmare, while the serendipity approach works very well.

A typical variant of this procedure can be identified in the original *enhancement trick* as designed first in (Ahmad *et al.* 2013). We consider again the space (3.37), with the degrees of freedom (3.38). Then, using the boundary dofs and the moments up to $k-2$ only, we construct the $\Pi_k^{\nabla,E}$ operator as in (2.6), and use it (mimicking (3.41), with $\Pi_k^{\nabla,E}$ instead of Π_k) to define the moments of v_h of order $k-1$ and k. Thus, the new space is

$$V_k^{\mathrm{enh}}(E) := \left\{ v_h \in \widetilde{V}_k(E) : \int_E (v_h - \Pi_k^\nabla v_h) p_s \,\mathrm{d}E = 0 \;\forall p_s \in \mathbb{P}_s^{\mathrm{hom}} \; s = k-1, k \right\}. \quad (3.42)$$

Remark 3.10. We observe that both Serendipity and Enhancement approach allow to compute the L^2-projection onto $\mathbb{P}_k$. This can be used to compute an approximation of the right-hand side simpler than the original one described in (3.25). Setting $f_h := \Pi_{k-1}^0 f$ we have

$$\begin{aligned}(f - f_h, v_h)_{0,E} &= \int_E (f - \Pi_{k-1}^0 f) v_h \,\mathrm{d}E = \int_E (f - \Pi_{k-1}^0 f)(v_h - \Pi_0^0 v_h)\mathrm{d}E \\ &\le C h_E^{k-1} \|f\|_{k-1,E} h_E |v_h|_{1,E} \le C h_E^k \|f\|_{k-1,E} |v_h|_{1,E}.\end{aligned} \quad (3.43)$$

3.7. L^2-projection of the gradient, and variable coefficients

From the degrees of freedom (3.16) we can compute, for any $v_h \in V_k(E)$, the L^2-projection of ∇v_h onto $[\mathbb{P}_{k-1}(E)]^2$, defined as

$$\int_E \Pi_{k-1}^0 \nabla v_h \cdot \mathbf{q}_{k-1} \,\mathrm{d}E = \int_E \nabla v_h \cdot \mathbf{q}_{k-1} \,\mathrm{d}E \quad \forall \mathbf{q}_{k-1} \in [\mathbb{P}_{k-1}(E)]^2. \quad (3.44)$$

In fact, the left-hand side is an integral of polynomials, and the right-hand side becomes, after integration by parts,

$$\int_E \nabla v_h \cdot \mathbf{q}_{k-1} \,\mathrm{d}E = -\int_E v_h \,\mathrm{div}\, \mathbf{q}_{k-1} \,\mathrm{d}E + \int_{\partial E} v_h \,\mathbf{q}_{k-1} \cdot \boldsymbol{n} \,\mathrm{d}s,$$

and both integrals on the right-hand side are computable.

As pointed out in (Beirão da Veiga, Brezzi, Marini and Russo 2016*d*), and experimentally verified, in presence of variable coefficients the Π_k^∇ operator produces a loss of order of convergence for $k \ge 3$. For this reason the consistency part of the discrete bilinear form needs to be changed. More precisely, if the problem to be approximated is $-\mathrm{div}(\kappa(x)\nabla u) = f$, we choose

$$a_h^E(v_h, w_h) = \int_E \kappa(x) \Pi_{k-1}^0 \nabla v_h \cdot \Pi_{k-1}^0 \nabla w_h \,\mathrm{d}E + \mathcal{S}^E((I - \Pi_k^\nabla) v_h, (I - \Pi_k^\nabla) w_h)$$

instead of (3.19). It can be easily seen that the two forms coincide for $k = 1$, but not for $k \ge 2$. In presence of variable coefficients the consistency property (3.9) cannot hold, but the consistency error can be controlled in terms of the right powers of h. In fact, from the properties of the L^2-projection we have, for any $v_h \in V_k(E)$ and $p_k \in \mathbb{P}_k(E)$,

$$\begin{aligned} a_h^E(v_h, p_k) - a^E(v_h, p_k) &= \int_E \kappa(x)(\Pi^0_{k-1}\nabla v_h - \nabla v_h)\cdot \nabla p_k \,\mathrm{d}E \\ &= \int_E (\Pi^0_{k-1}\nabla v_h - \nabla v_h)\cdot(\kappa(x)\nabla p_k - \Pi^0_{k-1}\kappa(x)\nabla p_k)\,\mathrm{d}E \\ &\le C h_E^k |\kappa \nabla p_k|_{k,E} |v_h|_{1,E}. \end{aligned}$$

This result will be used in the abstract convergence Theorem 3.2 with $p_k = u_\pi$. Consequently,

$$a_h^E(v_h, u_\pi) - a^E(v_h, u_\pi) \le C h_E^k |\kappa\nabla u_\pi|_{k,E}|v_h|_{1,E} \le C_\kappa h_E^k ||\nabla u||_{k,E} |v_h|_{1,E}.$$

Hence, as shown in (Beirão da Veiga *et al.* 2016*d*), the optimal estimate (3.31) holds true.

3.8. Extension to three dimensions

As a model problem, we take now the natural extension in three dimensions of problem (3.1).

The first attempt that comes to mind, given a polyhedron P and an integer $k \ge 1$, is to extend what we did in the two-dimensional case. Let $\mathcal{T}_h$ be a decomposition of Ω into polyhedra P. To begin with, we define the local spaces:

$$\begin{aligned} V_k(P) :=\{ v_h \in C^0(\overline{P}) :\ & v_{h|\mathrm{e}} \in \mathbb{P}_k(\mathrm{e})\ \forall \text{ edge } \mathrm{e} \subset \partial P, \\ & \Delta_2 v_{h|\mathrm{f}} \in \mathbb{P}_{k-2}(\mathrm{f})\ \forall \text{ face } \mathrm{f}\subset\partial P,\ \Delta_3 v_h \in \mathbb{P}_{k-2}(P)\}, \end{aligned} \tag{3.45}$$

with the degrees of freedom

$$\begin{aligned} &(D_1):\ \text{the values of } v_h \text{ at the vertices,} \\ &(D_2):\ \text{for } k\ge 2 \text{ the moments } \int_{\mathrm{e}} v_h\, p_{k-2}\,\mathrm{d}s,\ \forall p_{k-2}\in\mathbb{P}_{k-2}(\mathrm{e}), \forall \text{ edge e}, \\ &(D_3):\ \text{for } k\ge 2 \text{ the moments } \int_{\mathrm{f}} v_h\, p_{k-2}\,\mathrm{df},\ \forall p_{k-2}\in\mathbb{P}_{k-2}(\mathrm{f}), \forall \text{ face f}, \\ &(D_4):\ \text{for } k\ge 2 \text{ the moments } \int_{P} v_h\, p_{k-2}\,\mathrm{d}P,\ \forall p_{k-2}\in\mathbb{P}_{k-2}(P). \end{aligned} \tag{3.46}$$

Then, following the 2-dimensional path, for each $P \in \mathcal{T}_h$ and for each virtual element function v_h we can define its $H_0^1(P)$-projection $\Pi_k^{\nabla,P} v_h$ as in (2.6), that is, as the unique solution (up to a constant that can be easily fixed) in $\mathbb{P}_k(P)$ of

$$\int_P \nabla(\Pi_k^{\nabla,P} v_h)\cdot\nabla p_k\,\mathrm{d}P = \int_P \nabla v_h\cdot\nabla p_k\,\mathrm{d}P \quad \forall p_k\in\mathbb{P}_k(P). \tag{3.47}$$

Unfortunately, when we attempt *to compute* the right-hand side of (3.47) using the degrees of freedom (3.46), we have

$$\int_P \nabla v_h \cdot \nabla p_k \, \mathrm{d}P = \int_{\partial P} v_h \frac{\partial p_k}{\partial n} \, \mathrm{d}S - \int_P v_h \, \Delta p_k \, \mathrm{d}P. \tag{3.48}$$

Now, the second term in the right-hand side of (3.48) does not cause any trouble: for p_k in $\mathbb{P}_k$ we have that $\Delta p_k \in \mathbb{P}_{k-2}$ and the term can be computed using the degrees of freedom (D_4) in (3.46). But for the first term in the right-hand side of (3.48) we would need to know the moments of v_h on each face up to the order $k-1$ (the degree of $\frac{\partial p_k}{\partial n}$), while in (3.46) we have the moments only up to $k-2$. The way-out, as presented first in (Ahmad *et al.* 2013), is:

$$\begin{aligned} &\text{split } \frac{\partial p_k}{\partial n} \text{ as } \quad \frac{\partial p_k}{\partial n} = p_{k-2} + p_{k-1}^{\text{hom}}, \quad p_{k-2} \in \mathbb{P}_{k-2}, \; p_{k-1}^{\text{hom}} \in \mathbb{P}_{k-1}^{\text{hom}}, \\ &\text{and replace } \int_{\mathrm{f}} v_h \frac{\partial p_k}{\partial n} \, \mathrm{df} \; \text{ with } \int_{\mathrm{f}} v p_{k-2} \, \mathrm{df} + \int_{\mathrm{f}} (\Pi_k^{\nabla,\mathrm{f}} v_h) p_{k-1}^{\text{hom}} \, \mathrm{df}. \end{aligned} \tag{3.49}$$

In (3.49), $\Pi_k^{\nabla,\mathrm{f}} v_h$ is the two-dimensional projection of v_h, as defined in (2.6), whose computation, in turn, on each face f requires the moments of v_h on f only up to the order $k-2$. One might consider this as a typical use of the approach described in subsection 3.6, the so-called *enhancement trick*, which allows to have all the moments up to the order k, and consequently the L^2-projection onto $\mathbb{P}_k$. More precisely, the *enhancement trick* is the following.

- For each face f we consider the space $\widetilde{V}_k(\mathrm{f})$ defined in (3.37), with the degrees of freedom (3.38);
- In $\widetilde{V}_k(\mathrm{f})$ we can construct the operator $\Pi_k^{\nabla,\mathrm{f}}$, for which only the moments of degree up to $k-2$ are needed, and use its moments of degree $k-1$ and k to define the enhanced space $V_k^{\text{enh}}(\mathrm{f})$ on each face as in (3.42);
- Finally, the enhanced space on the polyhedron P is given by

$$V_k^{\text{enh}}(P) := \{v_h \in C^0(\overline{P}) : \; v_{h|\mathrm{f}} \in V_k^{\text{enh}}(\mathrm{f}) \; \forall \text{ face f}, \; \Delta_3 v_h \in \mathbb{P}_{k-2}(P)\}. \tag{3.50}$$

Once the operator $\Pi_k^{\nabla,P}$ has been computed, the local bilinear form can be defined, for each $P \in \mathcal{T}_h$ and for each $v_h, w_h \in V_k^{\text{enh}}(P)$, exactly as in (3.19):

$$a_h^P(v_h, w_h) := a^P(\Pi_k^{\nabla,P} v_h, \Pi_k^{\nabla,P} w_h) + S^P((I - \Pi_k^{\nabla,P})v_h, (I - \Pi_k^{\nabla,P})w_h). \tag{3.51}$$

Let us turn to the right-hand side. The first term in $\ell(v_h)$ (see (3.2)) is treated exactly as in (3.25), just by replacing the polygon E with the polyhedron P. Instead the treatment of the boundary term needs some care, since now the functions in $V_k^{\text{enh}}(P)$ are not known on the faces. Thanks to the *enhancement trick* we know their projections onto polynomials, in particular of degree $k-1$, on each face. Hence,

$$\int_{\mathrm{f}} g v_h \, \mathrm{df} \quad \text{can be replaced by} \quad \int_{\mathrm{f}} g \Pi_{k-1}^0 v_h \, \mathrm{df}, \quad \forall \text{face } \mathrm{f} \subset \Gamma_N. \tag{3.52}$$

Here too, like in the 2D-case, we assume that the integrals to the right of (3.52) can be computed exactly. Then, adding and subtracting $\Pi^0_{k-1}g$, and using the properties of the L^2-projection and classical estimates we obtain

$$
\begin{aligned}
&\int_{\mathrm{f}} g v_h \,\mathrm{df} - \int_{\mathrm{f}} g \Pi^0_{k-1} v_h \,\mathrm{df} \\
&= \int_{\mathrm{f}} (g - \Pi^0_{k-1} g) v_h \,\mathrm{df} + \int_{\mathrm{f}} ((\Pi^0_{k-1} g)\, v_h - g \Pi^0_{k-1} v_h) \,\mathrm{df} \\
&= \int_{\mathrm{f}} (g - \Pi^0_{k-1} g)(v_h - \Pi^0_{k-1} v_h) \,\mathrm{df} + 0 \\
&\le C\, h^{k-1/2} |g|_{k-1/2,\mathrm{f}}\, h^{1/2} |v_h|_{1/2,\mathrm{f}} \le C\, h^k |g|_{k-1/2,\mathrm{f}} \|v_h\|_{1,P}.
\end{aligned}
\tag{3.53}
$$

Finally, the global quantities are defined by collecting the local ones.

$$
\begin{aligned}
&V_h := \{v_h \in H^1_{0,\Gamma_D}(\Omega) \text{ such that } v_{h|P} \in V_k^{\mathrm{enh}}(P)\ \forall P \in \mathcal{T}_h\}, \\
&a_h(v_h, w_h) := \sum_{P \in \mathcal{T}_h} a_h^P(v_h, w_h) \quad \forall v_h, w_h \in V_h, \\
&\ell_h(v_h) := \sum_{P \in \mathcal{T}_h} (f_h, v_h)_{0,P} + \sum_{\mathrm{f} \subset \Gamma_N} (g, \Pi^0_{k-1} v_h)_{0,\mathrm{f}} \quad \forall v_h \in V_h.
\end{aligned}
\tag{3.54}
$$

4. H^1-nonconforming approximations

Nonconforming approximations for H^1 were first introduced and analyzed in (Ayuso de Dios, Lipnikov and Manzini 2016). In this section we will recall their approach, applied always to the continuous model problem (3.1), with some modifications in the treatment of the right-hand side. As for nonconforming Finite Element approximations, the discrete spaces that we are going to introduce are not subspaces of $H^1(\Omega)$, as they are made of functions which are only weakly continuous at the interelement boundaries. Therefore we need some preliminary notations. Let $\mathcal{T}_h$ be a decomposition of Ω into polygons E, and let

$$
H^1(\mathcal{T}_h) := \prod_{E \in \mathcal{T}_h} H^1(E).
$$

Let $\mathcal{E}_h$ be the set of edges of $\mathcal{T}_h$, $\mathcal{E}_h^o$ the set of internal edges, and $\mathcal{E}_h^\partial$ the set of boundary edges. For a function $v \in H^1(\mathcal{T}_h)$ (or a vector $\mathbf{v} \in [H^1(\mathcal{T}_h)]^2$) we define its averages and jumps on the edges as (see e.g. (Arnold, Brezzi, Cockburn and Marini 2001))

$$
\begin{aligned}
&\{v\}_{|\mathrm{e}} := \frac{v^+ + v^-}{2} \quad \text{on } \mathrm{e} \in \mathcal{E}_h^o, \qquad && \{v\}_{|\mathrm{e}} := v \quad \text{on } \mathrm{e} \in \mathcal{E}_h^\partial, \\
&[\![v]\!]_{|\mathrm{e}} := v^+ \boldsymbol{n}^+ + v^- \boldsymbol{n}^- \quad \text{on } \mathrm{e} \in \mathcal{E}_h^o, \qquad && [\![v]\!]_{|\mathrm{e}} := v \boldsymbol{n} \quad \text{on } \mathrm{e} \in \mathcal{E}_h^\partial,
\end{aligned}
\tag{4.1}
$$

where $v^\pm$ is the restriction of v to the elements $E^\pm$ having the edge e in common, and $\boldsymbol{n}^\pm$ is the outward unit normal to $E^\pm$. For an edge on the boundary, $\boldsymbol{n}$ is the outward unit normal to $\partial\Omega$. With these definitions the following useful formula holds for v and w in $H^1(\mathcal{T}_h)$ (see always (Arnold *et al.* 2001)):

$$\sum_{E\in\mathcal{T}_h}\int_{\partial E}\frac{\partial w}{\partial n}v\,\mathrm{d}s=\sum_{\mathrm{e}\in\mathcal{E}_h^o}\int_{\mathrm{e}}[[\,\nabla w\,]]\cdot\{v\}\,\mathrm{de}+\sum_{\mathrm{e}\in\mathcal{E}_h}\int_{\mathrm{e}}[[\,v\,]]\cdot\{\nabla w\}\,\mathrm{de}. \tag{4.2}$$

Let u be the solution of (3.1). By integrating by parts and applying (4.2), taking into account that $[[\,\nabla u\,]]_{|\mathrm{e}}=0$ on $\mathrm{e}\in\mathcal{E}_h^o$ we deduce, for all $v\in H^1(\mathcal{T}_h)$:

$$\begin{aligned}a(u,v)=\sum_{E\in\mathcal{T}_h}a^E(u,v)&=\sum_{E\in\mathcal{T}_h}\Big(\int_E-\Delta u\,v\,\mathrm{d}E+\int_{\partial E}\frac{\partial u}{\partial n}v\,\mathrm{d}s\Big)\\&=(f,v)_{0,\Omega}+\sum_{\mathrm{e}}\int_{\mathrm{e}}[[\,v\,]]\cdot\{\nabla u\}\,\mathrm{de}\\&=(f,v)_{0,\Omega}+\sum_{\mathrm{e}\subset\Gamma_N}\int_{\mathrm{e}}g\,v\,\mathrm{de}+\sum_{\mathrm{e}\not\subset\Gamma_N}\int_{\mathrm{e}}[[\,v\,]]\cdot\{\nabla u\}\,\mathrm{de}\\&=\ell(v)+\sum_{\mathrm{e}\not\subset\Gamma_N}\int_{\mathrm{e}}[[\,v\,]]\cdot\{\nabla u\}\,\mathrm{de}.\end{aligned} \tag{4.3}$$

The term

$$\mathcal{N}_h(u,v):=\sum_{\mathrm{e}\not\subset\Gamma_N}\int_{\mathrm{e}}[[\,v\,]]\cdot\{\nabla u\}\;\mathrm{d}s \tag{4.4}$$

is a measure of the nonconformity and needs to be estimated. To this end, we anticipate that the discrete VEM-spaces that we are going to build, made of functions weakly continuous at the interelements, will be subspaces of

$$H^{1,\mathrm{nc}}(\mathcal{T}_h):=\{v\in H^1(\mathcal{T}_h)\text{ s. t. }\int_{\mathrm{e}}[[\,v\,]]\cdot\boldsymbol{n}\,p_{k-1}\,\mathrm{d}s=0\,\forall\mathrm{e}\not\subset\Gamma_N,\,\forall p_{k-1}\in\mathbb{P}_{k-1}(\mathrm{e})\}.$$

We can prove now the following Lemma.

Lemma 4.1. Let u be the solution of problem (3.1). There exists a constant C independent of h such that the following estimate holds:

$$\mathcal{N}_h(u,v_h)\le C\,h^k\|u\|_{k+1,\Omega}\|v_h\|_{1,\mathcal{T}_h},\qquad\forall v_h\in H^{1,\mathrm{nc}}(\mathcal{T}_h). \tag{4.5}$$

Proof. We briefly sketch the proof, which is the same as for nonconforming Finite Elements. Using the properties of the L^2-projection and the definition of $H^{1,\mathrm{nc}}(\mathcal{T}_h)$ we have

$$\begin{aligned}\mathcal{N}_h(u,v_h)&:=\sum_{\mathrm{e}\not\subset\Gamma_N}\int_{\mathrm{e}}\{\nabla u\}\cdot[[\,v_h\,]]\,\mathrm{de}=\sum_{\mathrm{e}\not\subset\Gamma_N}\int_{\mathrm{e}}\big(\{\nabla u\}-\{\Pi^0_{k-1}\nabla u\}\big)\cdot[[\,v_h\,]]\,\mathrm{de}\\&=\sum_{\mathrm{e}\not\subset\Gamma_N}\int_{\mathrm{e}}\big(\{\nabla u\}-\{\Pi^0_{k-1}\nabla u\}\big)\cdot\big([[\,v_h\,]]-\Pi_0^{0,\mathrm{e}}([[\,v_h\,]])\big)\,\mathrm{de}\\&\le\sum_{\mathrm{e}\not\subset\Gamma_N}\|\{\nabla u\}-\{\Pi^0_{k-1}\nabla u\}\|_{0,\mathrm{e}}\cdot\|[[\,v_h\,]]-\Pi_0^{0,\mathrm{e}}([[\,v_h\,]])\|_{0,\mathrm{e}}\end{aligned}$$

where $\{\Pi^0_{k-1}\nabla u\}$ on an edge e is obtained by taking the average of $\Pi^{0,E^\pm}_{k-1}\nabla u$ with $E^\pm$ being the two elements having e as common edge.

Then, the trace inequality and standard approximation properties give the result. $\square$

We are now ready to introduce the nonconforming approximation of (3.1).

4.1. *The local discrete spaces and bilinear forms*

Let again E be a generic polygon in $\mathcal{T}_h$, and let $\boldsymbol{n}$ be, as usual, the unit outward normal to each edge, in the clockwise orientation of the boundary. For $k \geq 1$ we define

$$V_k^{\mathrm{nc}}(E) := \{v_h \in C^0(\overline{E}) : \frac{\partial v_h}{\partial n}_{|\mathrm{e}} \in \mathbb{P}_{k-1}(\mathrm{e}) \,\forall \text{ edge e} \subset \partial E,\ \Delta v_h \in \mathbb{P}_{k-2}(E)\}, \quad (4.6)$$

with the degrees of freedom given by

$$\begin{aligned} &(D_1): \text{ the moments } \int_{\mathrm{e}} v_h p_{k-1}\,\mathrm{de} \quad \forall p_{k-1} \in \mathbb{P}_{k-1}(\mathrm{e}),\ \forall \text{ edge e} \\ &(D_2): \text{ for } k \geq 2 \text{ the moments } \int_E v_h p_{k-2}\,\mathrm{d}E \quad \forall p_{k-2} \in \mathbb{P}_{k-2}(E). \end{aligned} \quad (4.7)$$

We underline that from the definition (4.6) it is clear that $\mathbb{P}_k(E) \subset V_k^{\mathrm{nc}}(E)$.

Lemma 4.2. The degrees of freedom (4.7) are unisolvent for $V_k^{\mathrm{nc}}(E)$.

Proof. Since the number of dofs equals the dimension of $V_k^{\mathrm{nc}}(E)$, it is enough to show that a function v_h having all the dofs vanishing is identically zero. Let then $v_h \in V_k^{\mathrm{nc}}(E)$ such that

$$\int_{\mathrm{e}} v_h p_{k-1}\,\mathrm{de} = 0 \,\forall p_{k-1} \in \mathbb{P}_{k-1}(\mathrm{e}) \,\forall \text{ edge e, and } \int_E v_h p_{k-2}\,\mathrm{d}E = 0 \,\forall p_{k-2} \in \mathbb{P}_{k-2}(E).$$

Since $\Delta v_h \in \mathbb{P}_{k-2}(E)$, and $\frac{\partial v_h}{\partial n}_{|\mathrm{e}} \in \mathbb{P}_{k-1}(\mathrm{e})\ \forall \mathrm{e}$, integration by parts gives

$$\int_E |\nabla v_h|^2\,\mathrm{d}E = -\int_E v_h\,\Delta v_h\,\mathrm{d}E + \int_{\partial E} v_h \frac{\partial v_h}{\partial n}\,\mathrm{d}s = 0.$$

Hence, $v_h = \textit{constant}$ which, together with $(D_1) = 0$, implies $v_h \equiv 0$. $\square$

Remark 4.3. The space (4.6) was the original space defined in (Ayuso de Dios *et al.* 2016). Here we will use instead an enhanced space, that simplifies significantly the treatment of the right-hand side. Without repeating the details of the *enhancement trick*, exactly the same to what we did in the previous section, we define the space

$$\widetilde{V}_k^{\mathrm{nc}}(E) := \{v_h \in C^0(\overline{E}) : \frac{\partial v_h}{\partial n}_{|\mathrm{e}} \in \mathbb{P}_{k-1}(\mathrm{e}) \,\forall \text{ edge e} \subset \partial E,\ \Delta v_h \in \mathbb{P}_{k}(E)\}, \quad (4.8)$$

with the degrees of freedom (4.7) plus the moments of order $k-1$ and k. After computing the Π_k^∇ operator as in (2.6) using only the degrees of freedom (4.7), we define the enhanced space as

$$V_k^{\rm nc,enh}(E) := \Big\{v_h \in \widetilde{V}_k^{\rm nc}(E) : \int_E (v_h - \Pi_k^\nabla v_h) p_s \,\mathrm{d}E = 0 \quad \forall p_s \in \mathbb{P}_s^{\rm hom}\ s = k-1, k\Big\}. \tag{4.9}$$

Once the local spaces $V_k^{\rm nc,enh}(E)$ have been defined, we follow the same path of the previous section in order to write the discrete problem. The local bilinear forms are constructed as in (3.19)–(3.21):

$$a_h^E(v_h, w_h) := a^E(\Pi_k^\nabla v_h, \Pi_k^\nabla w_h) + S^E((I - \Pi_k^\nabla)v_h, (I - \Pi_k^\nabla)w_h).$$

$k-$Consistency and stability hold with the same arguments as in Lemma 3.6.

4.2. *Construction of a computable right-hand side*

Thanks to the enhancement procedure of Remark 4.3 the approximation of the volume term in the right-hand side simplifies significantly with respect to the original one, and goes exactly as in (3.43) of Remark 3.10. Thus, with $f_h = \Pi_{k-1}^0 f$,

$$(f, v_h)_{0,E} - (f_h, v_h)_{0,E} \le C h_E^k \|f\|_{k,E} |v_h|_{1,E}. \tag{4.10}$$

For the term on the Neumann boundary, denoting by $\Pi_{k-1}^0 g$ the L^2-projection of g onto $\mathbb{P}_{k-1}(\mathrm{e})$ for each edge $\mathrm{e} \subset \Gamma_N$, and setting

$$g_{h|\mathrm{e}} = \Pi_{k-1}^0 g \quad \forall \mathrm{e} \subset \Gamma_N, \tag{4.11}$$

we obtain

$$\begin{aligned} &\int_\mathrm{e} g v_h \,\mathrm{de} - \int_\mathrm{e} \Pi_{k-1}^0 g v_h \,\mathrm{de} = \int_\mathrm{e} (g - \Pi_{k-1}^0 g)(v_h - \Pi_{k-1}^0 v_h) \,\mathrm{de} \\ &\le C\, h^{k-1/2} |g|_{k-1/2,\mathrm{e}}\, h^{1/2} |v_h|_{1/2,\mathrm{e}} \le C\, h^k |g|_{k-1/2,\mathrm{e}} \|v_h\|_{1,E}. \end{aligned} \tag{4.12}$$

4.3. *The global problem - Error estimates*

The global space is defined as a patchwork of the spaces (4.6), with the addition of a weak continuity condition at the interelements:

$$\begin{aligned} V_h^{\rm nc} : = \{v_h \in H^1(\mathcal{T}_h) :\ v_{h|E} \in V_k^{\rm nc,enh}(E)\ \forall E \in \mathcal{T}_h, \text{ and} \\ \int_\mathrm{e} [\![\, v_h \,]\!] \cdot \boldsymbol{n}\, p_{k-1} \,\mathrm{de} = 0\ \forall \mathrm{e} \not\subset \Gamma_N,\ \forall p_{k-1} \in \mathbb{P}_{k-1}(\mathrm{e})\}. \end{aligned} \tag{4.13}$$

The global bilinear form and right-hand side are defined, as usual, by summing over the elements of $\mathcal{T}_h$:

$$\begin{aligned} a_h(v_h, w_h) &:= \sum_{E \in \mathcal{T}_h} a_h^E(v_h, w_h), \\ \ell_h(v_h) &:= \sum_{E \in \mathcal{T}_h} (f_h, v_h)_{0,E} + \sum_{\mathrm{e} \subset \Gamma_N} (g_h, v_h)_{0,\mathrm{e}}, \end{aligned} \tag{4.14}$$

and the discrete problems is:

$$\text{Find } u_h \in V_h^{\text{nc}} \text{ such that } a_h(u_h, v_h) = \ell_h(v_h) \quad \forall v_h \in V_h^{\text{nc}}. \tag{4.15}$$

Theorem 4.4. The discrete problem (4.15) has a unique solution $u_h \in V_h^{\text{nc}}$. Moreover, under Assumptions 2.1 on the mesh it holds:

$$\|u - u_h\|_{1,\mathcal{T}_h} \le C h^k |u|_{k+1,\Omega}. \tag{4.16}$$

Proof. Since Assumptions 3.1 holds (the bilinear form is k-consistent and stable), problem (4.15) has a unique solution u_h. Moreover, an abstract estimate similar to (3.12) holds: for every approximation $u_I \in V_h^{\text{nc}}$ of u and for every approximation u_π of u that is piecewise in $\mathbb{P}_k$, we have

$$|u - u_h|_{1,\mathcal{T}_h} \le C\Big(|u - u_I|_{1,\mathcal{T}_h} + |u - u_\pi|_{1,\mathcal{T}_h} + \mathfrak{F}_h + \mathfrak{N}_h\Big), \tag{4.17}$$

where C is a constant independent of h, $|\cdot|_{1,\mathcal{T}_h}$ is the broken H^1-norm, and, for any h, $\mathfrak{F}_h$ and $\mathfrak{N}_h$ are, respectively, the smallest constants such that

$$|\ell(v_h) - \ell_h(v_h)| \le \mathfrak{F}_h\, |v_h|_{1,\mathcal{T}_h}, \quad |\mathcal{N}_h(u, v_h)| \le \mathfrak{N}_h\, |v_h|_{1,\mathcal{T}_h} \quad \forall\, v_h \in V_h^{\text{nc}}. \tag{4.18}$$

The proof of (4.17) goes like that of Theorem 3.2, with the addition of the non-conformity term (4.4). Setting $\delta_h = u_h - u_I$, without repeating all the steps of the proof, and using (4.3) we obtain

$$\begin{aligned}
\alpha_* |\delta_h|^2_{1,\mathcal{T}_h} &\le \ell_h(\delta_h) - \ell(\delta_h) - \sum_E \Big(a_h^E(u_I - u_\pi, \delta_h) + a^E(u_\pi - u, \delta_h)\Big) - \mathcal{N}_h(u, \delta_h) \\
&\le C\Big(\mathfrak{F}_h + \mathfrak{N}_h + |u_I - u_\pi|_{1,\mathcal{T}_h} + |u - u_\pi|_{1,\mathcal{T}_h}\Big)\, |\delta_h|_{1,\mathcal{T}_h},
\end{aligned}$$

and (4.17) follows by the triangle inequality. For the right-hand side we have, from (4.10)-(4.12),

$$\begin{aligned}
\ell(v_h) - \ell_h(v_h) &= \sum_{E \in \mathcal{T}_h} (f - f_h, v_h)_{0,E} + \sum_{\mathrm{e} \subset \Gamma_N} (g - g_h, v_h)_{\mathrm{e}} \\
&\le C\, h^k \Big(\|f\|_{k,\Omega} + \|g\|_{k-1/2,\Gamma_N}\Big)\, |v_h|_{1,\mathcal{T}_h} \quad \forall v_h \in V_h^{\text{nc}}.
\end{aligned} \tag{4.19}$$

From (4.5), (4.19), and classical approximation results (see, e.g., (Brenner and Scott 2008)) in (4.17) we finally have the optimal estimate (4.16). □

5. H^2-conforming approximations

With Virtual Elements it is quite easy to construct high-regularity approximations. Here we shall deal with C^1 approximations, having in mind, as an example of fourth order problem, a plate bending problem, in the Kirchoff-Love model:

$$D\Delta^2 w = f \quad \text{in } \Omega, \quad w = \frac{\partial w}{\partial n} = 0 \text{ on } \partial\Omega, \tag{5.1}$$

where $D = Et^3/12(1-\mu^2)$ is the bending rigidity, E the Young's modulus, t the thickness, μ is the Poisson's ratio, and we assumed that the plate is clamped all-over the boundary. In order to write the variational formulation of (5.1) we define

$$a(v,w) = D\Big[(1-\mu)\int_\Omega w_{/ij}v_{/ij}\,\mathrm{d}x + \mu\int_\Omega \Delta w \Delta v\,\mathrm{d}x\Big], \; < f, v >= \int_\Omega f v\,\mathrm{d}x. \quad (5.2)$$

In (5.2), $v_{/i} = \partial v/\partial x_i$, $i = 1, 2$, and we used the summation convention of repeated indices. Throughout this section $w_{/n}$ will denote the normal derivative, $w_{/t}$ the tangential derivative in the counterclockwise orientation of the boundary, and so on. When no confusion occurs we might also use w_n, w_t...

The variational formulation of (5.1) is then:

$$\begin{cases} \text{Find } w \in V := H^2_0(\Omega) \text{ such that} \\ a(w,v) =< f, v > \quad \forall v \in V. \end{cases} \quad (5.3)$$

In the following subsections we recall the discretization of (5.3) presented in (Brezzi and Marini 2013) and (Chinosi and Marini 2016). For other approaches we refer to (Zhao, Chen and Zhang 2016) and (Antonietti, Manzini and Verani 2018) for nonconforming approximations, to (Antonietti, Beirão da Veiga, Scacchi and Verani 2016) for application to Cahn-Hilliard equation, to (Brenner, Sung and Tan 2021) for optimal control problems, and to (Wang and Zhao 2021) for conforming and nonconforming approximations of contact problems.

5.1. The local VEM-spaces

Let E be a polygon in $\mathcal{T}_h$. The local spaces will depend on three integer indices (r, s, m), related to the degree of accuracy $k \geq 2$ by:

$$r = \max\{3, k\}, \quad s = k-1, \quad m = k-4. \quad (5.4)$$

We set

$$W_{r,s,m}(E) := \{w \in H^2(E) : w_{|\mathrm{e}} \in \mathbb{P}_r(\mathrm{e}),\ w_{n|\mathrm{e}} \in \mathbb{P}_s(\mathrm{e})\ \forall \text{ edge e},\ \Delta^2 w \in \mathbb{P}_m(E)\}. \quad (5.5)$$

The degrees of freedom in $W_{r,s,m}(E)$ are:

$$\begin{aligned} &(D_0) \text{ the values of } w, w_{/1} \text{ and } w_{/2} \text{ at the vertices,} \\ &(D_1) \text{ for } r \geq 4, \text{the moments } \int_{\mathrm{e}} w\, q_{r-4}\,\mathrm{de}\ \forall q_{r-4} \in \mathbb{P}_{r-4}(\mathrm{e}),\ \forall \mathrm{e} \subset \partial E, \\ &(D_2) \text{ for } s \geq 2, \text{ the moments } \int_{\mathrm{e}} w_{/n}\, q_{s-2}\,\mathrm{de}\ \forall q_{s-2} \in \mathbb{P}_{s-2}(\mathrm{e}),\ \forall \mathrm{e} \subset \partial E, \\ &(D_3) \text{ for } m \geq 0, \text{ the moments } \int_E w\, q_m\,\mathrm{d}E \quad \forall q_m \in \mathbb{P}_m(E). \end{aligned} \quad (5.6)$$

We note that the VEM space $W_{r,s,m}(E)$ will contain all polynomials $\mathbb{P}_k$ with

$$k = \min\{r, s+1, m+4\} \geq 2,$$

which will be the order of precision. We point out once more that the above degrees of freedom need to be properly scaled in such a way that they all have the same dimension. For a discussion and details on this issue we refer to (Brezzi and Marini 2013).

Lemma 5.1. The degrees of freedom (5.6) are unisolvent for $W_{r,s,m}(E)$.

Proof. The proof follows the usual path. Since the number of dofs equals the dimension of $W_{r,s,m}(E)$, it is enough to show that a function w having all the dofs vanishing is identically zero. We first observe that $(D_0) = 0$ implies that w and ∇w vanish at the vertices of E. Therefore, on each edge, w is a polynomial of degree r vanishing at the two endpoints with its tangential derivative. Hence, denoting by t the edge variable and by t_1 and t_2 the coordinates of the endpoints, w will have the expression $w = (t - t_1)^2(t - t_2)^2 q_{r-4}$. Then, from the vanishing of dofs (D_1) we deduce that $w \equiv 0$ on each edge. Similarly, from the vanishing of (D_0) and (D_2) we deduce that $w_{/n}$ vanishes identically on each edge. Indeed, on each edge $w_{/n}$ is a polynomial of degree s vanishing at the two endpoints. Its expression is then $w_{/n} = (t - t_1)(t - t_2)q_{s-2}$ which, together with $(D_2) = 0$, implies $w_{/n} \equiv 0$ on each edge. Consequently,

$$w \equiv 0 \quad w_{/n} \equiv 0 \quad \text{on } \partial E.$$

Finally, this, together with $(D_3) = 0$ and integration by parts twice give

$$\begin{aligned}\int_E (\Delta w)^2 \, \mathrm{d}E &= -\int_E \nabla w \cdot \nabla \Delta w \, \mathrm{d}E + \int_{\partial E} \frac{\partial w}{\partial n} \Delta w \, \mathrm{d}s \\ &= \int_E w \, \Delta^2 w \, \mathrm{d}E - \int_{\partial E} w \frac{\partial \Delta w}{\partial n} \, \mathrm{d}s + \int_{\partial E} \frac{\partial w}{\partial n} \Delta w \, \mathrm{d}s = 0\end{aligned}$$

since $\Delta^2 w \in \mathbb{P}_m(E)$. Then it follows that $\Delta w = 0$, and since $w = 0$ on the boundary we deduce that $w \equiv 0$ in E. □

5.2. *Construction of a computable discrete bilinear form*

Like we did in Section 3 we begin by defining, for $k \geq 2$, an operator $\Pi_k^\Delta : W_{r,s,m}(E) \longrightarrow \mathbb{P}_k(E) \subset W_{r,s,m}(E)$ defined as the solution of

$$\begin{cases} a^E(\Pi_k^\Delta \psi, q) = a^E(\psi, q) & \forall \psi \in W_{r,s,m}(E), \ \forall q \in \mathbb{P}_k(E) \\ \displaystyle\int_{\partial E} (\Pi_k^\Delta \psi - \psi) \, \mathrm{d}s = 0, & \displaystyle\int_{\partial E} \nabla(\Pi_k^\Delta \psi - \psi) \, \mathrm{d}s = 0. \end{cases} \tag{5.7}$$

We note that for $v \in \mathbb{P}_k(E)$ the first equation in (5.7) implies $(\Pi_k^\Delta v)_{/ij} = v_{/ij}$ for $i, j = 1, 2$, that joined with the second equation gives easily

$$\Pi_k^\Delta v = v \quad \forall v \in \mathbb{P}_k(E). \tag{5.8}$$

Hence, Π_k^Δ is a projector operator onto $\mathbb{P}_k(E)$. We also observe that Π_k^Δ is computable from the degrees of freedom (D_0)-(D_3), as it can be easily seen upon integration by parts twice of the term $a^E(\psi, q)$. Choosing $a_h^E(v,w) = a^E(\Pi_k^\Delta v, \Pi_k^\Delta w)$ would guarantee consistency, but not stability. Then, like we did in the previous section, we add a stabilizing term, and set

$$a_h^E(v,w) := a^E(\Pi_k^\Delta v, \Pi_k^\Delta w) + \mathcal{S}^E((I - \Pi_k^\Delta)v, (I - \Pi_k^\Delta)w), \tag{5.9}$$

where $\mathcal{S}^E$ is any symmetric bilinear form to be chosen in such a way that it scales like $a^E(\cdot,\cdot)$ and is positive on the kernel of Π_k^Δ, i.e., there exist two positive constant c_1, c_2 such that

$$c_1 a^E(v,v) \le \mathcal{S}^E(v,v) \le c_2 a^E(v,v) \quad \forall v \text{ such that } \Pi_k^\Delta v = 0.$$

Assuming, for example, that the degrees of freedom (5.6) are all scaled like the vertex values, we can take

$$\mathcal{S}^E(v,w) := h_E^{-2} \sum_{i=1}^{\#\text{dofs}} dof_i(v)\, dof_i(w). \tag{5.10}$$

Lemma 5.2. The discrete bilinear form (5.9) is k-consistent and stable.

Proof. The proof goes exactly as that of Lemma 3.6, and we do not repeat it. □

5.3. Construction of the right-hand side

In order to build an approximation of the term $< f, v >$ in a simple and easy way it is convenient to have internal degrees of freedom in $W_{r,s,m}(E)$, and this means, according to (5.4), that $k \ge 4$ is needed. In (Brezzi and Marini 2013) suitable choices were made for different values of k, enough to guarantee the proper order of convergence in H^2. Here we report the choice made in (Chinosi and Marini 2016) which makes use once more of the *enhancement trick* of (Ahmad *et al.* 2013). For that, we modify the definition (5.5). For $k \ge 2$, and r and s related to k by (5.4), let $\widetilde{W}_k(E)$ be the new local space, given by

$$\widetilde{W}_k(E) := \{v \in H^2(E) : \ v_{|e} \in \mathbb{P}_r(e),\ v_{n|e} \in \mathbb{P}_s(e)\ \forall e \subset \partial E,\ \Delta^2 v \in \mathbb{P}_{k-2}(E)\}.$$

The degrees of freedom in $\widetilde{W}_k(E)$ would be (5.6), plus the moments of degree $k-3$ and $k-2$, but for the construction of the operator Π_k^Δ only the dofs (5.6) are needed. Once Π_k^Δ has been constructed, we *copy* its moments. More precisely, we define:

$$\text{for } k = 2 \quad W_2(E) = \{v \in \widetilde{W}_2(E), \text{and} \int_E v \,\mathrm{d}E = \int_E \Pi_2^\Delta v \,\mathrm{d}E\}, \tag{5.11}$$

$$\begin{aligned}\text{for } k \ge 3 \quad W_k(E) = \{v \in \widetilde{W}_k(E),\ \text{and} \int_E v p_\alpha \,\mathrm{d}E = \int_E \Pi_k^\Delta v\, p_\alpha \,\mathrm{d}E,\\ p_\alpha \in \mathbb{P}_\alpha^{\text{hom}},\ \alpha = k-3, k-2\}.\end{aligned} \tag{5.12}$$

It can be checked that the dofs (5.6) are the same, but the added conditions on the moments allow now to compute the L^2–projection of any $v \in W_k$ onto $\mathbb{P}_{k-2}(E)$, and not only onto $\mathbb{P}_{k-4}(E)$ as before. Taking then, in each element, f_h as the L^2−projection of f onto the space of polynomials of degree $k-2$, i.e.,

$$f_{h|E} = \Pi^0_{k-2} f \quad \forall E \in \mathcal{T}_h,$$

we obtain

$$< f, v >_E - < f_h, v >_E = \int_E (f - \Pi^0_{k-2} f) v \, \mathrm{d}E \leq C h_E^{k-1} |f|_{k-1,E} \|v\|_{2,E}. \quad (5.13)$$

We are now ready to write the discrete problem.

5.4. The global problem - Error estimates

Let $\mathcal{T}_h$ be a decomposition of Ω into polygons, satisfying the Assumptions 2.1. The global space W_h is defined as a patchwork of the spaces (5.11) or (5.12), depending on the value of k:

$$W_h := \{ v \in H^2_0(\Omega) : \; v_{|E} \in W_k(E) \, \forall E \in \mathcal{T}_h \}. \quad (5.14)$$

The global bilinear form and right-hand side are defined by summing over the elements of $\mathcal{T}_h$:

$$a_h(v_h, w_h) := \sum_{E \in \mathcal{T}_h} a_h^E(v_h, w_h), \qquad < f_h, v_h > := \sum_{E \in \mathcal{T}_h} (\Pi^0_{k-2} f, v_h)_{0,E}, \quad (5.15)$$

and the discrete problem is

$$\text{find } w_h \in W_h \text{ such that } a_h(w_h, v_h) = < f_h, v_h > \quad \forall v_h \in W_h. \quad (5.16)$$

We have the analog of Theorem 3.2.

Theorem 5.3. Under Assumptions 3.1 the discrete problem (5.16) has a unique solution w_h. Moreover, for every approximation w_I of w in W_h and for every approximation w_π of w that is piecewise in $\mathbb{P}_k$, we have

$$|w - w_h|_{2,\Omega} \leq C \Big(|w - w_I|_{2,\Omega} + |w - w_\pi|_{2,\mathcal{T}_h} + \|f - f_h\|_{W_h'} \Big), \quad (5.17)$$

where C is a constant independent of h, $\| \cdot \|_{2,\mathcal{T}_h}$ is the broken H^2-norm, and

$$\|f - f_h\|_{W_h'} := \sup_{v_h \in W_h} \frac{< f - f_h, v_h >}{|v_h|_{2,\Omega}}. \quad (5.18)$$

Proof. Assumption 3.1 is satisfied thanks to Lemma 5.2. Following step by step the proof of the abstract Theorem 3.2 the result (5.17) follows easily. □

If w_I is the interpolant of w in W_h, defined through the degrees of freedom (5.6), thanks to the Assumptions 2.1 on the mesh we have

$$\|w - w_I\|_{2,\Omega} \leq C \, h^{k-1} \|w\|_{k+1,\Omega}. \quad (5.19)$$

Similarly,

$$\|w - w_\pi\|_{2,\mathcal{T}_h} \leq C \, h^{k-1} \|w\|_{k+1,\Omega}. \quad (5.20)$$

Finally the following convergence Theorem hold.

Theorem 5.4. Let w be the solution of problem (5.3), and let w_h be the solution of the discrete problem (5.16). The following holds true

$$\text{for } k \geq 2, \qquad \|w - w_h\|_{2,\Omega} \leq C\, h^{k-1} |w|_{k+1,\Omega}. \tag{5.21}$$

Proof. Using (5.19), (5.20), and (5.13) in (5.17) the result (5.21) follows. □

We conclude this section with a couple of remarks.

Remark 5.5. The lowest-order element of our family, corresponding to the choice $r = 3, s = 1, m = -2$, can be seen as the extension to polygons of the finite element composite triangle known as *reduced Hsieh-Clough-Tocher* element. On a triangle they have the same degrees of freedom ($w, w_{/x}, w_{/y}$ at the vertices), they both contain $\mathbb{P}_2$ and share the same order of accuracy, $k = 2$. Similar considerations apply to the next-to-the-lowest element of the family (corresponding to $r = 3, s = 2, m = -1$), that can be seen as the extension to polygons of the well known finite element composite *Hsieh-Clough-Tocher* triangle. On a triangle, the degrees of freedom are the same ($w, w_{/x}, w_{/y}$ at the vertices and $w_{/n}$ at the midpoints of the edges), $\mathbb{P}_3$ is included in the local spaces, and thus the order of precision is $k = 3$ for both.

6. $H(\mathbf{div})$, $H(\mathbf{rot})$, and $H(\mathbf{curl})$-conforming approximations

In a number of applicative problems, like for instance electromagnetism or diffusion problems in mixed form, spaces like L^2, H^1 or H^2 cannot be used alone. They must be suitably coupled with other functional spaces, like $H(\text{div})$, $H(\text{rot})$, and $H(\mathbf{curl})$. In the present section we will show how to design VEM-discretizations of such spaces.

Virtual Element spaces of $H(\text{div})$ type were initially introduced in (Brezzi, Falk and Marini 2014) and later improved in (Beirão da Veiga, Brezzi, Marini and Russo 2016*b*). Within the large literature involved in the application of such spaces to advanced diffusion problems we here mention (Benedetto, Borio and Scialò 2017, Benedetto, Borio, Kyburg, Mollica and Scialò 2022).

Afterwards, $H(\text{div})$ and $H(\mathbf{curl})$ VEM spaces in two and three dimensions were introduced in (Beirão da Veiga, Brezzi, Marini and Russo 2016*a*) and then improved in a series of papers (Beirão da Veiga, Brezzi, Dassi, Marini and Russo 2017*a*, 2018*b*,*a*), also dealing with the magneto-static equations as a model problem. Among the papers dealing with the application and extension of such spaces for more advanced problems we here mention (Dassi, Di Barba and Russo 2020*a*), (Beirão da Veiga, Dassi, Manzini and Mascotto 2022*b*,*a*) and (Cao, Chen, Guo and Lin 2022*b*, Cao, Chen and Guo 2022*a*).

Let us begin by introducing some further notation and definitions which will be useful in the sequel.

6.1. Polynomial spaces and exact sequences

In the following we will denote by i the mapping that to every real *number* c associates the constant *function* (zero-degree polynomial) identically equal to c, and by o the mapping that to every *function* (polynomial) associates the *number* 0.

Then we recall that we have the exactness of the following sequences:

- In dimension two:

$$\mathbb{R} \xrightarrow{\ i\ } \mathbb{P}_r \xrightarrow{\ \mathbf{grad}\ } [\mathbb{P}_{r-1}]^2 \xrightarrow{\ \mathrm{rot}\ } \mathbb{P}_{r-2} \xrightarrow{\ o\ } \mathbb{R} \tag{6.1}$$

  or equivalently:

$$\mathbb{R} \xrightarrow{\ i\ } \mathbb{P}_r \xrightarrow{\ \mathbf{rot}\ } [\mathbb{P}_{r-1}]^2 \xrightarrow{\ \mathrm{div}\ } \mathbb{P}_{r-2} \xrightarrow{\ o\ } \mathbb{R} \tag{6.2}$$

  are exact sequences.

- In dimension three:

$$\mathbb{R} \xrightarrow{\ i\ } \mathbb{P}_r \xrightarrow{\ \mathbf{grad}\ } [\mathbb{P}_{r-1}]^3 \xrightarrow{\ \mathbf{curl}\ } [\mathbb{P}_{r-2}]^3 \xrightarrow{\ \mathrm{div}\ } \mathbb{P}_{r-3} \xrightarrow{\ o\ } \mathbb{R} \tag{6.3}$$

  is an exact sequence.

We recall that *exact* means that *the image of every operator coincides with the kernel of the following one.* To better explain the consequences of these statements we introduce some additional notation. Given an integer s, we define the following polynomial spaces:

- in dimension two:

$$\mathcal{G}_s := \mathbf{grad}(\mathbb{P}_{s+1}) \subseteq [\mathbb{P}_s]^2, \qquad \mathcal{R}_s := \mathbf{rot}(\mathbb{P}_{s+1}) \subseteq [\mathbb{P}_s]^2, \tag{6.4}$$

- in dimension three:

$$\mathcal{G}_s := \mathbf{grad}(\mathbb{P}_{s+1}) \subseteq [\mathbb{P}_s]^3, \qquad \mathcal{R}_s := \mathbf{curl}([\mathbb{P}_{s+1}]^3) \subseteq [\mathbb{P}_s]^3. \tag{6.5}$$

We then set:

$$\begin{aligned} \mathcal{G}_s^{\mathrm{c}} &:= \text{a complement of } \mathcal{G}_s \text{ in } [\mathbb{P}_s]^d \\ \mathcal{R}_s^{\mathrm{c}} &:= \text{a complement of } \mathcal{R}_s \text{ in } [\mathbb{P}_s]^d. \end{aligned} \tag{6.6}$$

In the original paper (Beirão da Veiga *et al.* 2016*a*) we chose $\mathcal{G}_s^{\mathrm{c}}$ and $\mathcal{R}_s^{\mathrm{c}}$ as the L^2-orthogonal complements of $\mathcal{G}_s$ and $\mathcal{R}_s$, respectively. A more modern choice, described in (Beirão da Veiga *et al.* 2018*a*), is the following:

- in two dimensions:

$$\mathcal{G}_s^{\mathrm{c}} := \{\boldsymbol{x}^{\perp}\mathbb{P}_{s-1}\}, \quad \mathcal{R}_s^{\mathrm{c}} := \{\boldsymbol{x}\mathbb{P}_{s-1}\}, \tag{6.7}$$

- in three dimensions:

$$\mathcal{G}_s^{\mathrm{c}} := \{\boldsymbol{x} \wedge [\mathbb{P}_{s-1}]^3\}, \quad \mathcal{R}_s^{\mathrm{c}} := \{\boldsymbol{x}\mathbb{P}_{s-1}\}. \tag{6.8}$$

The choices (6.7), (6.8) are much easier to handle from the computational point of view. Finally, we recall (see (2.1)) that $\mathbb{P}^0_s$ are the polynomials of $\mathbb{P}_s$ having zero mean value.

The following properties are consequences of the exact sequences above.

- In two dimensions: (6.1) implies that for all integer s:

$$\begin{aligned} &\text{(i) } \mathbf{grad} \text{ is an isomorphism from } \mathbb{P}^0_s \text{ to } \mathcal{G}_{s-1}\\ &\text{(ii) } \boldsymbol{v} \in [\mathbb{P}_s]^2 \implies \operatorname{rot} \boldsymbol{v} = 0 \quad \text{if and only if } \boldsymbol{v} \in \mathcal{G}_s\\ &\text{(iii) } \operatorname{rot} \text{ is an isomorphism from } \mathcal{G}^c_s \text{ to the whole } \mathbb{P}_{s-1}, \end{aligned} \tag{6.9}$$

  and equivalently (6.2) implies that

$$\begin{aligned} &\text{(i) } \mathbf{rot} \text{ is an isomorphism from } \mathbb{P}^0_s \text{ to } \mathcal{R}_{s-1}\\ &\text{(ii) } \boldsymbol{v} \in [\mathbb{P}_s]^2 \implies \operatorname{div} \boldsymbol{v} = 0 \quad \text{if and only if } \boldsymbol{v} \in \mathcal{R}_s\\ &\text{(iii) } \operatorname{div} \text{ is an isomorphism from } \mathcal{R}^c_s \text{ to the whole } \mathbb{P}_{s-1}. \end{aligned} \tag{6.10}$$

- In three dimensions: (6.3) implies that

$$\begin{aligned} &\text{(i) } \boldsymbol{v} \in [\mathbb{P}_s]^3 \implies \mathbf{curl}\, \boldsymbol{v} = 0 \quad \text{if and only if } \boldsymbol{v} \in \mathcal{G}_s\\ &\text{(ii) } \boldsymbol{v} \in [\mathbb{P}_s]^3 \implies \operatorname{div} \boldsymbol{v} = 0 \quad \text{if and only if } \boldsymbol{v} \in \mathcal{R}_s\\ &\text{(iii) } \mathbf{grad} \text{ is an isomorphism from } \mathbb{P}^0_s \text{ to } \mathcal{G}_{s-1}\\ &\text{(iv) } \mathbf{curl} \text{ is an isomorphism from } \mathcal{G}^c_s \text{ to } \mathcal{R}_{s-1}\\ &\text{(v) } \operatorname{div} \text{ is an isomorphism from } \mathcal{R}^c_s \text{ to the whole } \mathbb{P}_{s-1}. \end{aligned} \tag{6.11}$$

Properties (ii) of (6.9) and (ii) of (6.10), as well as properties (i) and (ii) of (6.11), are just particular cases of well known results in Calculus.

From the definitions above (see also (Beirão da Veiga *et al.* 2016*a*)), we can easily deduce that

- in two dimensions:

$$\dim \mathcal{G}_k = \dim \mathcal{R}_k = \pi_{k+1,2} - 1, \quad \dim \mathcal{G}^c_k = \dim \mathcal{R}^c_k = \pi_{k-1,2} \tag{6.12}$$

- in three dimensions:

$$\begin{aligned} &\dim \mathcal{G}_k = \pi_{k+1,3} - 1, \quad \dim \mathcal{R}_k = 3\,\pi_{k+1,3} - \pi_{k+2,3} + 1,\\ &\dim \mathcal{G}^c_k = \dim \mathcal{R}_{k-1} = 3\,\pi_{k,3} - \pi_{k+1,3} + 1, \quad \dim \mathcal{R}^c_k = \pi_{k-1,3} \end{aligned} \tag{6.13}$$

For the sake of clarity we define $\gamma_{k,d} := \dim \mathcal{G}_k$ and $\varrho_{k,d} := \dim \mathcal{R}_k$.

6.2. *Spaces $H(div)$, $H(rot)$, and $H(\boldsymbol{curl})$*

The elements of our local Virtual Element spaces will be the solutions, within each element, of suitable *div-curl* systems. In view of that, it will be convenient to recall the *compatibility conditions* (between the data inside the element and those at the boundary) that are required in order to have a solution. We recall the spaces defined in (2.4), for a polygon E

$$H(\mathrm{div}; E) := \{\boldsymbol{v} \in [L^2(E)]^2 \text{ such that } \mathrm{div}\,\boldsymbol{v} \in L^2(E)\}, \tag{6.14}$$

$$H(\mathrm{rot}; E) := \{\boldsymbol{v} \in [L^2(E)]^2 \text{ such that } \mathrm{rot}\,\boldsymbol{v} \in L^2(E)\}, \tag{6.15}$$

and for a polyhedron P

$$H(\mathrm{div}; P) := \{\boldsymbol{v} \in [L^2(P)]^3 \text{ such that } \mathrm{div}\,\boldsymbol{v} \in L^2(P)\}, \tag{6.16}$$

$$H(\mathbf{curl}; P) := \{\boldsymbol{v} \in [L^2(P)]^3 \text{ such that } \mathbf{curl}\,\boldsymbol{v} \in [L^2(P)]^3\}. \tag{6.17}$$

We now assume that we are given, on a simply connected polygon E, two smooth functions f_d and f_r, and, on the boundary ∂E, two edge-wise smooth functions g_n and g_t. We recall that the problem:

$$\begin{cases} \text{find } \boldsymbol{v} \in H(\mathrm{div}; E) \cap H(\mathrm{rot}; E) \text{ such that:} \\ \mathrm{div}\,\boldsymbol{v} = f_d, \ \mathrm{rot}\,\boldsymbol{v} = f_r \qquad \text{in } E \\ \boldsymbol{v} \cdot \boldsymbol{n} = g_n \qquad \text{on } \partial E \end{cases} \tag{6.18}$$

has a unique solution if and only if

$$\int_E \mathrm{div}\,\boldsymbol{v}\,\mathrm{d}E = \int_{\partial E} g_n\,\mathrm{d}s. \tag{6.19}$$

Similarly the problem:

$$\begin{cases} \text{find } \boldsymbol{v} \in H(\mathrm{div}; E) \cap H(\mathrm{rot}; E) \text{ such that:} \\ \mathrm{div}\,\boldsymbol{v} = f_d, \ \mathrm{rot}\,\boldsymbol{v} = f_r \qquad \text{in } E \\ \boldsymbol{v} \cdot \boldsymbol{t} = g_t \qquad \text{on } \partial E \end{cases} \tag{6.20}$$

has a unique solution if and only if

$$\int_E \mathrm{rot}\,\boldsymbol{v}\,\mathrm{d}E = \int_{\partial E} g_t\,\mathrm{d}s. \tag{6.21}$$

In three dimensions, on a simply connected polyhedron P we assume that we are given a smooth scalar function f_d and a smooth vector valued function $\boldsymbol{f}_r$ with $\mathrm{div}\,\boldsymbol{f}_r = 0$. On the boundary ∂P we assume that we are given a face-wise smooth scalar function g_n and a face-wise smooth tangent vector field $\boldsymbol{g}_t$ whose tangential components are continuous at the edges of ∂P. Then we recall that the problem

$$\begin{cases} \text{find } \boldsymbol{v} \in H(\mathrm{div}; P) \cap H(\mathbf{curl}; P) \text{ such that:} \\ \mathrm{div}\,\boldsymbol{v} = f_d, \ \mathbf{curl}\,\boldsymbol{v} = \boldsymbol{f}_r \qquad \text{in } P \\ \boldsymbol{v} \cdot \boldsymbol{n} = g_n \qquad \text{on } \partial P \end{cases} \tag{6.22}$$

has a unique solution if and only if

$$\int_P \mathrm{div}\,\boldsymbol{v}\ \mathrm{d}P = \int_{\partial P} g_n\,\mathrm{d}s, \tag{6.23}$$

and similarly the problem:

$$\begin{cases} \text{find } \boldsymbol{v} \in H(\mathrm{div}; P) \cap H(\mathbf{curl}; P) \text{ such that:} \\ \mathrm{div}\, \boldsymbol{v} = f_d, \ \mathbf{curl}\, \boldsymbol{v} = \boldsymbol{f}_r \qquad \text{in } P \\ \boldsymbol{v}_t = \boldsymbol{g}_t \qquad \text{on } \partial P \end{cases} \tag{6.24}$$

has a unique solution if and only if

$$\boldsymbol{f}_r \cdot \boldsymbol{n} = \mathrm{rot}_2\, \boldsymbol{g}_t \text{ on } \partial P. \tag{6.25}$$

For more details concerning the solutions of the *div-curl system* we refer, for instance, to Auchmuty and Alexander (2001, 2005) and the references therein.

6.3. *Two-dimensional face elements*

These spaces are the same of Brezzi *et al.* (2014), although here we propose a different set of degrees of freedom.

On a polygon E, for k integer ≥ 1, we set:

$$\begin{aligned} V_{2,k}^{\mathrm{face}}(E) := \{ & \boldsymbol{v} \in H(\mathrm{div}; E) \cap H(\mathrm{rot}; E) \text{ such that:} \\ & \boldsymbol{v} \cdot \boldsymbol{n}_{|\mathrm{e}} \in \mathbb{P}_k(\mathrm{e}) \text{ for each edge e of } E, \\ & \mathrm{div}\, \boldsymbol{v} \in \mathbb{P}_{k-1}(E), \text{ and } \mathrm{rot}\, \boldsymbol{v} \in \mathbb{P}_{k-1}(E) \}. \end{aligned} \tag{6.26}$$

We recall from Subsection 6.2 that, given:

- a function g defined on ∂E such that $g_{|\mathrm{e}} \in \mathbb{P}_k(\mathrm{e})$ for all $\mathrm{e} \in \partial E$,
- a polynomial $f_d \in \mathbb{P}_{k-1}(E)$ such that

$$\int_E f_d \, \mathrm{d}E = \int_{\partial E} g \, \mathrm{d}s, \tag{6.27}$$

- a polynomial $f_r \in \mathbb{P}_{k-1}(E)$,

we can find a unique vector $\boldsymbol{v} \in V_{2,k}^{\mathrm{face}}(E)$ such that

$$\boldsymbol{v} \cdot \boldsymbol{n} = g \text{ on } \partial E, \quad \mathrm{div}\, \boldsymbol{v} = f_d \text{ in } E, \quad \mathrm{rot}\, \boldsymbol{v} = f_r \text{ in } E. \tag{6.28}$$

The dimension of $V_{2,k}^{\mathrm{face}}(E)$ is given by:

$$\begin{aligned} \dim V_{2,k}^{\mathrm{face}}(E) &= N_{\mathrm{e}} \dim \mathbb{P}_k(\mathrm{e}) + (\dim \mathbb{P}_{k-1}(E) - 1) + \dim \mathbb{P}_{k-1}(E) \\ &= N_{\mathrm{e}} \pi_{k,1} + \pi_{k-1,2} - 1 + \pi_{k-1,2} \\ &= N_{\mathrm{e}} \pi_{k,1} + 2\pi_{k-1,2} - 1. \end{aligned} \tag{6.29}$$

A convenient set of degrees of freedom for functions $\boldsymbol{v}$ in $V_{2,k}^{\text{face}}(E)$ will be:

$$
\begin{aligned}
&(D_1): \quad \int_{\mathrm{e}} \boldsymbol{v}\cdot\boldsymbol{n}\, p_k \,\mathrm{de} \quad \text{for all edges e, for all } p_k \in \mathbb{P}_k(\mathrm{e}),\\
&(D_2): \quad \int_E \boldsymbol{v}\cdot\boldsymbol{g}_{k-2}\,\mathrm{d}E \quad \text{for all } \boldsymbol{g}_{k-2}\in\mathcal{G}_{k-2},\\
&(D_3): \quad \int_E \boldsymbol{v}\cdot\boldsymbol{g}_k^{\mathrm{c}}\,\mathrm{d}E \quad \text{for all } \boldsymbol{g}_k^{\mathrm{c}}\in\mathcal{G}_k^{\mathrm{c}}.
\end{aligned}
\tag{6.30}
$$

Recalling (6.12) we easily see that the number of degrees of freedom (6.30) equals the dimension of $V_{2,k}^{\text{face}}(E)$ as given in (6.29).

Theorem 6.1. The degrees of freedom (6.30) are unisolvent for $V_{2,k}^{\text{face}}(E)$.

Proof. Since the number of degrees of freedom (6.30) equals the dimension of $V_{2,k}^{\text{face}}(E)$, to prove unisolvence we just need to show that if for a given $\boldsymbol{v}$ in $V_{2,k}^{\text{face}}(E)$ all the degrees of freedom (6.30) are zero, that is if

$$\int_{\mathrm{e}} \boldsymbol{v}\cdot\boldsymbol{n}\, p_k \,\mathrm{de} = 0 \quad \text{for all edges e, for all } p_k \in \mathbb{P}_k(\mathrm{e}), \tag{6.31}$$

$$\int_E \boldsymbol{v}\cdot\boldsymbol{g}_{k-2}\,\mathrm{d}E = 0 \quad \text{for all } \boldsymbol{g}_{k-2}\in\mathcal{G}_{k-2}, \tag{6.32}$$

$$\int_E \boldsymbol{v}\cdot\boldsymbol{g}_k^{\mathrm{c}}\,\mathrm{d}E = 0 \quad \text{for all } \boldsymbol{g}_k^{\mathrm{c}}\in\mathcal{G}_k^{\mathrm{c}}, \tag{6.33}$$

then we must have $\boldsymbol{v} = 0$. Assume that for a certain $\boldsymbol{v} \in V_{2,k}^{\text{face}}(E)$ we have (6.31)–(6.33). Since $\boldsymbol{v}\cdot\boldsymbol{n}_{|\mathrm{e}} \in \mathbb{P}_k(\mathrm{e})\ \forall \mathrm{e}$, (6.31) imply that $\boldsymbol{v}\cdot\boldsymbol{n} \equiv 0$ on ∂E. Using the fact that $\operatorname{div}\boldsymbol{v} \in \mathbb{P}_{k-1}$ and setting $q_{k-1} := \operatorname{div}\boldsymbol{v}$ we have from (6.32)

$$
\begin{aligned}
\int_E |\operatorname{div}\boldsymbol{v}|^2\,\mathrm{d}E &= \int_E \operatorname{div}\boldsymbol{v}\, q_{k-1}\,\mathrm{d}E\\
&= \int_{\partial E} \boldsymbol{v}\cdot\boldsymbol{n} q_{k-1}\,\mathrm{d}s - \int_E \boldsymbol{v}\cdot\mathbf{grad}\, q_{k-1}\,\mathrm{d}E = 0.
\end{aligned}
\tag{6.34}
$$

Hence we have that $\operatorname{div}\boldsymbol{v} = 0$ which, together with $\boldsymbol{v}\cdot\boldsymbol{n} \equiv 0$ on ∂E, gives

$$\int_E \boldsymbol{v}\cdot\mathbf{grad}\,\varphi\,\mathrm{d}E = 0 \quad \text{for all } \varphi \in H^1(E) \tag{6.35}$$

after an integration by parts. According to the definition of (6.26), $\operatorname{rot}\boldsymbol{v} \in \mathbb{P}_{k-1}$. Looking at (6.9; (iii)) we have then that $\operatorname{rot}\boldsymbol{v} = \operatorname{rot}\boldsymbol{q}_k^{\mathrm{c}}$ for some $\boldsymbol{q}_k^{\mathrm{c}} \in \mathcal{G}_k^{\mathrm{c}}$. Now the difference $\boldsymbol{v} - \boldsymbol{q}_k^{\mathrm{c}}$ satisfies $\operatorname{rot}(\boldsymbol{v} - \boldsymbol{q}_k^{\mathrm{c}}) = 0$, and as E is simply connected, it follows that $\boldsymbol{v} = \boldsymbol{q}_k^{\mathrm{c}} + \mathbf{grad}\,\varphi$ for some $\boldsymbol{q}_k^{\mathrm{c}} \in \mathcal{G}_k^{\mathrm{c}}$ and some $\varphi \in H^1(E)$. Then

$$\int_E |\boldsymbol{v}|^2\,\mathrm{d}E = \int_E \boldsymbol{v}\cdot(\boldsymbol{q}_k^{\mathrm{c}} + \mathbf{grad}\,\varphi)\,\mathrm{d}E = 0 \tag{6.36}$$

since the first term is zero by (6.33) and the second term is zero by (6.35). □

Remark 6.2. The degrees of freedom (D_1) in (6.30) are pretty obvious. A natural variant would be to use, on each edge e, the values of $\boldsymbol{v} \cdot \boldsymbol{n}$ at $k+1$ suitable points on e. Moreover, the degrees of freedom (D_2) in (6.30) could be replaced, after integration by parts, by

$$\int_E \operatorname{div} \boldsymbol{v}\, q_{k-1}\, \mathrm{d}E \qquad \text{for all } q_{k-1} \in \mathbb{P}^0_{k-1}. \tag{6.37}$$

Finally, the degrees of freedom (D_3) in (6.30) could be replaced by

$$\int_E \operatorname{rot} \boldsymbol{v}\, q_{k-1}\, \mathrm{d}E \qquad \text{for all } q_{k-1} \in \mathbb{P}_{k-1} \tag{6.38}$$

as we had in the original work Brezzi *et al.* (2014).

Computing the L^2 projection

As already said, the virtual functions are not explicitly known inside the elements, and their reconstruction is not straightforward. Hence, we use suitable projections onto polynomials. Here we show how to construct the L^2 projection onto $[\mathbb{P}_k(E)]^2$, which is possibly the most convenient, and surely the most commonly used. We point out that, thanks to the definition of the space $V^{\text{face}}_{2,k}(E)$, and to the degrees of freedom (D_3) in (6.30), the *enhancement trick* is not necessary here. Indeed, using the same integration by parts applied in (6.34), the degrees of freedom (D_1) and (D_2) in (6.30) allow us to compute $\int_E \operatorname{div} \boldsymbol{v}\, q_{k-1}\, \mathrm{d}E$ for all $q_{k-1} \in \mathbb{P}_{k-1}(E)$, and since $\operatorname{div} \boldsymbol{v} \in \mathbb{P}_{k-1}(E)$, we can compute exactly the divergence of any $\boldsymbol{v} \in V^{\text{face}}_{2,k}(E)$. In turn this implies, again by using an integration by parts and (D_1) in (6.30), that we are able to compute also

$$\int_E \boldsymbol{v} \cdot \boldsymbol{g}_k\, \mathrm{d}E \quad \forall \boldsymbol{g}_k \in \mathcal{G}_k, \tag{6.39}$$

and actually

$$\int_E \boldsymbol{v} \cdot \mathbf{grad}\, \varphi\, \mathrm{d}E \quad \forall \varphi \text{ polynomial on } E. \tag{6.40}$$

The above property, combined with (D_3) in (6.30), allows to compute the integrals against any $\boldsymbol{q}_k \in [\mathbb{P}_k(E)]^2$ and thus yields the following important result:

Theorem 6.3. The $L^2(E)$ projection operator

$$\Pi^0_k : V^{\text{face}}_{2,k}(E) \longrightarrow [\mathbb{P}_k(E)]^2 \tag{6.41}$$

is computable using the degrees of freedom (6.30).

The global two-dimensional face space

Given a polygonal domain Ω and a decomposition $\mathcal{T}_h$ of Ω into a finite number of polygonal elements E, we can now consider the *global* space

$$V^{\text{face}}_{2,k}(\Omega) := \{\boldsymbol{v} \in H(\operatorname{div};\Omega) \text{ such that } \boldsymbol{v}_{|E} \in V^{\text{face}}_{2,k}(E)\ \forall \text{ element } E \in \mathcal{T}_h\}. \tag{6.42}$$

Note that in (6.42) we assumed that the elements $\boldsymbol{v}$ of $V_{2,k}^{\text{face}}(\Omega)$ have a divergence that is *globally* (and not just element-wise) in $L^2(\Omega)$. Hence the normal component of vectors $\boldsymbol{v} \in V_{2,k}^{\text{face}}(\Omega)$ will have to be "continuous" (with obvious meaning) at the inter-element edges. The global degrees of freedom are the natural extension of the local degrees of freedom (6.30). It follows immediately that the dimension of $V_{2,k}^{\text{face}}(\Omega)$ is given by

$$\dim(V_{2,k}^{\text{face}}(\Omega)) = \pi_{k,1} \times \{\text{number of edges in } \mathcal{T}_h\} + \\ (2\pi_{k-1,2} - 1) \times \{\text{number of elements in } \mathcal{T}_h\}.$$

6.4. Two-dimensional Edge Elements

The edge elements in 2D correspond exactly to the face elements, just rotating everything by $\pi/2$. For the sake of completeness we just recall the definition of the spaces and the corresponding degrees of freedom.

On a polygon E we set

$$\begin{aligned} V_{2,k}^{\text{edge}}(E) := \{\boldsymbol{v} \in H(\text{div}; E) \cap H(\text{rot}; E) \text{ such that:} \\ \boldsymbol{v} \cdot \boldsymbol{t}_{|e} \in \mathbb{P}_k(\text{e}) \text{ for each edge e of } E, \\ \text{rot}\, \boldsymbol{v} \in \mathbb{P}_{k-1}(E), \text{ and } \text{div}\, \boldsymbol{v} \in \mathbb{P}_{k-1}(E)\}. \end{aligned} \tag{6.43}$$

A convenient set of degrees of freedom for elements $\boldsymbol{v} \in V_{2,k}^{\text{edge}}(E)$ is:

$$\begin{aligned} (D_1):& \quad \int_{\text{e}} \boldsymbol{v} \cdot \boldsymbol{t}\, p_k \,\text{de} \quad \text{for all edges e, for all } p_k \in \mathbb{P}_k(\text{e}), \\ (D_2):& \quad \int_E \boldsymbol{v} \cdot \boldsymbol{r}_{k-2} \,\text{d}E \quad \text{for all } \boldsymbol{r}_{k-2} \in \mathcal{R}_{k-2} \\ (D_3):& \quad \int_E \boldsymbol{v} \cdot \boldsymbol{r}_k^{\text{c}} \,\text{d}E \quad \text{for all } \boldsymbol{r}_k^{\text{c}} \in \mathcal{R}_k^{\text{c}}. \end{aligned} \tag{6.44}$$

Remark 6.4. Here too we could use alternative degrees of freedom, in analogy with those discussed in Remark 6.2. In particular we point out that we can identify uniquely an element $\boldsymbol{v}$ of $V_{2,k}^{\text{edge}}(E)$ by prescribing its tangential component $\boldsymbol{v} \cdot \boldsymbol{t}$ (in $\mathbb{P}_k(\text{e})$) on every edge, its rotation $\text{rot}\, \boldsymbol{v}$ (in $\mathbb{P}_{k-1}^0(E)$), and its divergence $\text{div}\, \boldsymbol{v}$ (in $\mathbb{P}_{k-1}(E)$).

Remark 6.5. Obviously, here too we can define the L^2-projection onto $\mathbb{P}_k$, exactly as we did before, with $\mathcal{R}_k^{\text{c}}$ taking the role of $\mathcal{G}_k^{\text{c}}$.

Given a polygonal domain Ω and a decomposition $\mathcal{T}_h$ of Ω into a finite number of polygonal elements E, we can now consider the *global* space

$$V_{2,k}^{\text{edge}}(\Omega) := \{\boldsymbol{v} \in H(\text{rot}; \Omega) \text{ such that } \boldsymbol{v}_{|E} \in V_{2,k}^{\text{edge}}(E)\ \forall \text{ element } E \in \mathcal{T}_h\}. \tag{6.45}$$

Note that the tangential component of vectors $\boldsymbol{v} \in V_{2,k}^{\text{edge}}(\Omega)$ will have to be "continuous" (with obvious meaning) at the inter-element edges. The degrees of freedom for $\boldsymbol{v} \in V_{2,k}^{\text{edge}}(\Omega)$ are the obvious extension of the local degrees of freedom (6.44), and the dimension of $V_{2,k}^{\text{edge}}(\Omega)$ is

$$\dim(V_{2,k}^{\text{edge}}(\Omega)) = \pi_{k,1} \times \{\text{number of edges in } \mathcal{T}_h\} + (2\pi_{k-1,2} - 1) \times \{\text{number of elements in } \mathcal{T}_h\}.$$

6.5. *Three-dimensional Face Elements*

The three-dimensional $H(\text{div})$-conforming spaces follow in a very natural way the path of their two-dimensional companions.

On a polyhedron P we set

$$\begin{aligned} V_{3,k}^{\text{face}}(P) := \{\boldsymbol{v} \in H(\text{div}; P) \cap H(\textbf{curl}; P) \text{ such that:} \\ \boldsymbol{v} \cdot \boldsymbol{n}_P^{\text{f}} \in \mathbb{P}_k(\text{f}) \ \text{ for all faces f of } P, \\ \text{div}\, \boldsymbol{v} \in \mathbb{P}_{k-1}(P), \ \text{and} \ \textbf{curl}\, \boldsymbol{v} \in \mathcal{R}_{k-1}(P)\}. \end{aligned} \tag{6.46}$$

The dimension of $V_{3,k}^{\text{face}}(P)$ is given by:

$$\dim(V_{3,k}^{\text{face}}(P)) = N_{\text{f}}\, \pi_{k,2} + \dim \mathcal{G}_{k-2} + \dim \mathcal{R}_{k-1} = N_{\text{f}}\, \pi_{k,2} + \gamma_{k-2,3} + \varrho_{k-1,3}. \tag{6.47}$$

The local degrees of freedom will be:

$$\begin{aligned} (D_1): &\quad \int_{\text{f}} \boldsymbol{v} \cdot \boldsymbol{n}_P^{\text{f}}\, p_k \, \text{df} \quad \text{for all faces f, for all } p_k \in \mathbb{P}_k(\text{f}), \\ (D_2): &\quad \int_P \boldsymbol{v} \cdot \boldsymbol{g}_{k-2} \, \text{d}P \quad \text{for all } \boldsymbol{g}_{k-2} \in \mathcal{G}_{k-2}, \\ (D_3): &\quad \int_P \boldsymbol{v} \cdot \boldsymbol{g}_k^{\text{c}} \, \text{d}P \quad \text{for all } \boldsymbol{g}_k^{\text{c}} \in \mathcal{G}_k^{\text{c}}. \end{aligned} \tag{6.48}$$

It is not difficult to check that the number of the above degrees of freedom is given by

$$N_{\text{f}}\, \pi_{k,2} + \dim \mathcal{G}_{k-2} + \dim \mathcal{G}_k^{\text{c}} \tag{6.49}$$

which equals the dimension of $V_{3,k}^{\text{face}}(P)$ as given in (6.47).

Lemma 6.6. The degrees of freedom (6.48) are unisolvent for the space $V_{3,k}^{\text{face}}(P)$.

Proof. The proof follows the same steps as in the two-dimensional case and is therefore omitted. □

Remark 6.7. We note that also in the three dimensional case there are alternative choices of degrees of freedom, similarly as in Remark 6.2.

Remark 6.8. Obviously, here too we can compute the L^2−projection onto $\mathbb{P}_k$, exactly as we did before (see Theorem 6.3).

The global three-dimensional-face space

Having now a polyhedral domain Ω and a decomposition $\mathcal{T}_h$ of Ω into a finite number of polyhedrons P, we can consider the global space:

$$V_{3,k}^{\text{face}}(\Omega) := \{\boldsymbol{v} \in H(\text{div};\Omega) \text{ such that } \boldsymbol{v}_{|P} \in V_{3,k}^{\text{face}}(P)\ \forall \text{ elements } P \in \mathcal{T}_h\}. \quad (6.50)$$

As we did for the 2D case, we note that the normal component of the elements of $V_{3,k}^{\text{face}}(\Omega)$ will be "continuous" at the inter-element face. The degrees of freedom for the global space $V_{3,k}^{\text{face}}(\Omega)$ are the obvious extension of the local ones already described, and the dimension of $V_{3,k}^{\text{face}}(\Omega)$ is

$$\dim(V_{3,k}^{\text{face}}(\Omega)) = \pi_{k,2} \times \{\text{number of faces in } \mathcal{T}_h\} + (\gamma_{k-2,3} + \varrho_{k-1,3}) \times \{\text{number of elements in } \mathcal{T}_h\}.$$

6.6. Three-dimensional Edge Elements

We begin by introducing some additional notation that will be useful in the sequel. For a smooth three-dimensional field $\boldsymbol{\varphi}$ on P, and for a face f with normal $\boldsymbol{n}_P^{\text{f}}$, we define the tangential component of $\boldsymbol{\varphi}$ as

$$\boldsymbol{\varphi}_{\text{f}} := \boldsymbol{\varphi} - (\boldsymbol{\varphi} \cdot \boldsymbol{n}_P^{\text{f}})\, \boldsymbol{n}_P^{\text{f}}, \quad (6.51)$$

while $\boldsymbol{\varphi}_{\boldsymbol{t}}$ denotes the vector field defined on the boundary of P whose restriction on each face f is $\boldsymbol{\varphi}_{\text{f}}$. Note that $\boldsymbol{\varphi}_{\text{f}}$ as defined in (6.51) is different from $\boldsymbol{\varphi} \wedge \boldsymbol{n}_P^{\text{f}}$; indeed, if for instance $\boldsymbol{n}_P^{\text{f}} = (0,0,1)$ and $\boldsymbol{\varphi} = (\varphi_1, \varphi_2, \varphi_3)$ then

$$\boldsymbol{\varphi}_{\text{f}} = (\varphi_1, \varphi_2, 0) \quad \text{while} \quad \boldsymbol{\varphi} \wedge \boldsymbol{n}_P^{\text{f}} = (\varphi_2, -\varphi_1, 0). \quad (6.52)$$

Both fields $\boldsymbol{\varphi}_{\text{f}}$ and $\boldsymbol{\varphi} \wedge \boldsymbol{n}_P^{\text{f}}$ can be considered as two-dimensional vectors in the plane of the face f.

We introduce moreover the following space.

Definition 6.9. We define the boundary space $\mathcal{B}(\partial P)$ as the space of $\boldsymbol{v}$ in $[L^2(\partial P)]^3$ such that $\boldsymbol{v}_{\text{f}} \in H(\text{div};\text{f}) \cap H(\text{rot};\text{f})$ on each face f of P, and such that on each edge e (common to the faces f_1 and f_2), $\boldsymbol{v}_{\text{f}_1} \cdot \boldsymbol{t}_{\text{e}}$ and $\boldsymbol{v}_{\text{f}_2} \cdot \boldsymbol{t}_{\text{e}}$ (where $\boldsymbol{t}_{\text{e}}$ is a unit tangential vector to e) coincide. Then we define $\mathcal{B}_t(\partial P)$ as the space of the tangential components of the elements of $\mathcal{B}(\partial P)$.

Definition 6.10. We now define the boundary VEM space $B_k^{\text{edge}}(\partial P)$ as

$$B_k^{\text{edge}}(\partial P) = \left\{\boldsymbol{v} \in \mathcal{B}_t(\partial P) \text{ such that } \boldsymbol{v}_{\text{f}} \in V_{2,k}^{\text{edge}}(\text{f}) \text{ on each face f} \in \partial P\right\}. \quad (6.53)$$

Recalling the previous discussion about the two-dimensional virtual elements $V_{2,k}^{\text{edge}}(\text{f})$, we can easily see that for a polyhedron with N_{e} edges and N_{f} faces the dimension β_k of $B_k^{\text{edge}}(\partial P)$ is given by

$$\beta_k = N_{\text{e}}\, \pi_{k,1} + N_{\text{f}}\, (2\pi_{k-1,2} - 1). \quad (6.54)$$

The local spaces

On a polyhedron P we set

$$V^{\text{edge}}_{3,k}(P) := \{\boldsymbol{v} \mid \boldsymbol{v}_t \in B^{\text{edge}}_k(\partial P),\quad \operatorname{div}\boldsymbol{v} \in \mathbb{P}_{k-1}(P), \text{ and } \mathbf{curl}\,\mathbf{curl}\,\boldsymbol{v} \in \mathcal{R}_{k-2}(P)\}. \tag{6.55}$$

In order to compute the dimension of the space $V^{\text{edge}}_{3,k}(P)$ we first observe that, given a vector $\boldsymbol{g}$ in $B^{\text{edge}}_k(\partial P)$, a function f_d in $\mathbb{P}_{k-1}$, and a vector $\boldsymbol{f}_r \in \mathcal{R}_{k-2}(P)$ we can find a unique $\boldsymbol{v}$ in $V^{\text{edge}}_{3,k}(P)$ such that

$$\boldsymbol{v_t} = \boldsymbol{g} \text{ on } \partial P,\ \operatorname{div}\boldsymbol{v} = f_d \text{ in } P, \text{ and } \mathbf{curl}\,\mathbf{curl}\,\boldsymbol{v} = \boldsymbol{f}_r \text{ in } P. \tag{6.56}$$

To prove it we consider the following auxiliary problems. The first is: find $\boldsymbol{H}$ in $H(\mathrm{div}; P) \cap H(\mathbf{curl}; P)$ such that

$$\mathbf{curl}\,\boldsymbol{H} = \boldsymbol{f}_r \text{ in } P, \operatorname{div}\boldsymbol{H} = 0 \text{ in } P, \text{ and } \boldsymbol{H}\cdot\boldsymbol{n} = \operatorname{rot}_2\boldsymbol{g} \text{ on } \partial P, \tag{6.57}$$

that is uniquely solvable since

$$\int_{\partial P} \operatorname{rot}_2\boldsymbol{g}\,\mathrm{d}S = 0. \tag{6.58}$$

The second is: find $\boldsymbol{\psi}$ in $H(\mathrm{div}; P) \cap H(\mathbf{curl}; P)$ such that

$$\mathbf{curl}\,\boldsymbol{\psi} = \boldsymbol{H} \text{ in } P, \operatorname{div}\boldsymbol{\psi} = 0 \text{ in } P, \text{ and } \boldsymbol{\psi}_t = \boldsymbol{g} \text{ on } \partial P, \tag{6.59}$$

that is also uniquely solvable since

$$\boldsymbol{H}\cdot\boldsymbol{n} = \operatorname{rot}_2\boldsymbol{g}. \tag{6.60}$$

The third problem is: find $\varphi \in H^1_0(P)$ such that:

$$\Delta\varphi = f_d \text{ in } P, \tag{6.61}$$

that also has a unique solution. Then it is not difficult to see that the choice

$$\boldsymbol{v} := \boldsymbol{\psi} + \mathbf{grad}\,\varphi \tag{6.62}$$

solves our problem. Indeed, it is clear that $(\mathbf{grad}\,\boldsymbol{\varphi})_{\boldsymbol{t}} = 0$, that $\operatorname{div}(\mathbf{grad}\,\boldsymbol{\varphi}) = f_d$ and that $\mathbf{curl}\,\mathbf{curl}(\mathbf{grad}\,\boldsymbol{\varphi}) = 0$; all these, added to (6.57) and (6.59), produce the right conditions. It is also clear that the solution $\boldsymbol{v}$ of (6.56) is unique.

Hence we can conclude that the dimension of $V^{\text{edge}}_{3,k}(P)$ is given by

$$\dim V^{\text{edge}}_{3,k}(P) = \beta_k + \pi_{k-1,3} + \varrho_{k-2,3} \tag{6.63}$$

where $\beta_k = \dim B^{\text{edge}}_k(\partial P)$ is defined in (6.54).

The local Degrees of Freedom

A possible set of degrees of freedom for the space $V^{\text{edge}}_{3,k}(P)$ are the following:

$$\left.\begin{array}{ll}
\bullet \text{ for every edge e:} & \\
(D_1): & \displaystyle\int_{\text{e}} \boldsymbol{v}\cdot\boldsymbol{t}\, p_k \,\text{de} \quad \text{for all } \; p_k \in \mathbb{P}_k(\text{e}), \\
\bullet \text{ for every face f:} & \\
(D_2): & \displaystyle\int_f \boldsymbol{v}\cdot\boldsymbol{r}^{\text{c}}_k \,\text{df for all } \boldsymbol{r}^{\text{c}}_k \in \mathcal{R}^{\text{c}}_k(\text{f}), \\
(D_3): & \displaystyle\int_f \boldsymbol{v}\cdot\boldsymbol{r}_{k-2} \,\text{df for all } \boldsymbol{r}_{k-2} \in \mathcal{R}_{k-2}(\text{f}), \\
\bullet \text{ and inside } P: & \\
(D_4): & \displaystyle\int_P \boldsymbol{v}\cdot\boldsymbol{r}^{\text{c}}_k \,\text{d}P \quad \text{for all } \boldsymbol{r}^{\text{c}}_k \in \mathcal{R}^{\text{c}}_k, \\
(D_5): & \displaystyle\int_P \boldsymbol{v}\cdot\boldsymbol{r}_{k-2} \,\text{d}P \quad \text{for all } \boldsymbol{r}_{k-2} \in \mathcal{R}_{k-2}.
\end{array}\right\} \tag{6.64}$$

The total number of degrees of freedom (6.64) is clearly equal to β_k as given in (6.54) and the number of degrees of freedom (D_5) is equal to $\varrho_{k-2,3}$. On the other hand, using [6.11;v)] we see that the number of degrees of freedom (D_4) is equal to $\pi_{k-1,3}$, so that the total number of degrees of freedom (6.64) equals the dimension of $V^{\text{edge}}_{3,k}(P)$ as computed in (6.63).

Lemma 6.11. The degrees of freedom (6.64) are unisolvent for the space $V^{\text{edge}}_{3,k}(P)$.

Proof. Having seen that the number of degrees of freedom (6.64) equals the dimension of $V^{\text{edge}}_{3,k}(P)$, in order to see their unisolvence we only need to check that a vector $\boldsymbol{v} \in V^{\text{edge}}_{3,k}(P)$ that satisfies

$$\int_{\text{e}} \boldsymbol{v}\cdot\boldsymbol{t}\, p_k \,\text{de} = 0 \quad \forall \text{ edge e of } P \text{ and } \forall\, p_k \in \mathbb{P}_k(\text{e}), \tag{6.65}$$

$$\int_f \boldsymbol{v}\cdot\boldsymbol{r}^{\text{c}}_k \,\text{df} = 0 \quad \forall \text{ face f of } P \text{ and } \forall\, \boldsymbol{r}^{\text{c}}_k \in \mathcal{R}^{\text{c}}_k(\text{f}), \tag{6.66}$$

$$\int_f \boldsymbol{v}\cdot\boldsymbol{r}_{k-2} \,\text{df} = 0 \quad \forall \text{ face f of } P \text{ and } \forall\, \boldsymbol{r}_{k-2} \in \mathcal{R}_{k-2}(\text{f}), \tag{6.67}$$

$$\int_P \boldsymbol{v}\cdot\boldsymbol{r}^{\text{c}}_k \,\text{d}P = 0 \quad \forall\, \boldsymbol{r}^{\text{c}}_k \in \mathcal{R}^{\text{c}}_k(P), \tag{6.68}$$

$$\int_P \boldsymbol{v}\cdot\boldsymbol{r}_{k-2} \,\text{d}P = 0 \quad \forall\, \boldsymbol{r}_{k-2} \in \mathcal{R}_{k-2}(P), \tag{6.69}$$

is necessarily equal to zero.

Actually, recalling the results of Section 6.4, it is pretty obvious that (6.65)-(6.67) imply that $\boldsymbol{v}_{\boldsymbol{t}} = 0$ on ∂P. Moreover, since $\mathbf{curl}\,\mathbf{curl}\,\boldsymbol{v} \in \mathcal{R}_{k-2}(P)$, we are allowed to take $\boldsymbol{r}_{k-2} = \mathbf{curl}\,\mathbf{curl}\,\boldsymbol{v}$ as a test function in (6.69). An integration by parts (using $\boldsymbol{v}_{\boldsymbol{t}} = 0$) gives

$$0 = \int_P \boldsymbol{v} \cdot \mathbf{curl}\,\mathbf{curl}\,\boldsymbol{v}\,\mathrm{d}P = \int_P (\mathbf{curl}\,\boldsymbol{v}) \cdot (\mathbf{curl}\,\boldsymbol{v})\,\mathrm{d}P \tag{6.70}$$

and therefore we get $\mathbf{curl}\,\boldsymbol{v} = 0$. Using this, and again $\boldsymbol{v}_{\boldsymbol{t}} = 0$, we easily check, integrating by parts, that

$$\int_P \boldsymbol{v} \cdot \mathbf{curl}\,\boldsymbol{\varphi}\,\mathrm{d}P = 0 \quad \forall \boldsymbol{\varphi} \in H(\mathbf{curl}; P). \tag{6.71}$$

Now we recall that from the definition (6.55) of $V^{\mathrm{edge}}_{3,k}(P)$ we have that $\mathrm{div}\,\boldsymbol{v}$ is in $\mathbb{P}_{k-1}$. From (6.11); v) we then deduce that there exists a $\boldsymbol{q}^{\mathrm{c}}_k \in \mathcal{R}^{\mathrm{c}}_k$ with $\mathrm{div}\,\boldsymbol{q}^{\mathrm{c}}_k = \mathrm{div}\,\boldsymbol{v}$, so that the divergence of $\boldsymbol{v} - \boldsymbol{q}^{\mathrm{c}}_k$ is zero, and then (since P is simply connected)

$$\boldsymbol{v} - \boldsymbol{q}^{\mathrm{c}}_k = \mathbf{curl}\,\boldsymbol{\varphi} \tag{6.72}$$

for some $\boldsymbol{\varphi} \in H(\mathbf{curl}; P)$. At this point we can use (6.71) and (6.72) to conclude as in (6.36)

$$\int_P |\boldsymbol{v}|^2\,\mathrm{d}P = \int_P \boldsymbol{v} \cdot (\boldsymbol{q}^{\mathrm{c}}_k + \mathbf{curl}\,\boldsymbol{\varphi})\,\mathrm{d}P = \int_P \boldsymbol{v} \cdot \boldsymbol{q}^{\mathrm{c}}_k\,\mathrm{d}P + \int_P \boldsymbol{v} \cdot \mathbf{curl}\,\boldsymbol{\varphi}\,\mathrm{d}P = 0.$$

□

Remark 6.12. As we did in the previous cases, we observe that the degrees of freedom (6.64) are not the only possible choice. To start with, we can change the degrees of freedom in each face, according to Remark 6.2. Moreover, in the spirit of (6.56) we could assign, instead of (D_4) and/or (D_5) in (6.64), $\mathbf{curl}\,\mathbf{curl}\,\boldsymbol{v}$ in $\mathcal{R}_{k-2}(P)$ and/or $\mathrm{div}\,\boldsymbol{v}$ in $\mathbb{P}_{k-1}(P)$, respectively.

The global three-dimensional-edge space is defined as

$$V^{\mathrm{edge}}_{3,k}(\Omega) := \{\boldsymbol{v} \in H(\mathbf{curl}; \Omega) \text{ s. t. } \boldsymbol{v}_{|P} \in V^{\mathrm{edge}}_{3,k}(P)\ \forall \text{ element } P \in \mathcal{T}_h\}. \tag{6.73}$$

and the degrees of freedom are the natural extension of the local ones defined in (6.64). The dimension of $V^{\mathrm{edge}}_{3,k}(\Omega)$ is

$$\begin{aligned}\dim(V^{\mathrm{edge}}_{3,k}(\Omega)) = \pi_{k,1} &\times \{\text{number of edges in } \mathcal{T}_h\}\\ &+ (2\pi_{k-1,2} - 1) \times \{\text{number of faces in } \mathcal{T}_h\}\\ &\qquad + (\pi_{k-1,3} + \varrho_{k-1,3}) \times \{\text{number of polyhedra in } \mathcal{T}_h\}.\end{aligned}$$

6.7. *Virtual exact sequences*

We show now that, for the obvious choices of the polynomial degrees, the set of virtual spaces introduced in this Section constitutes an exact sequence. We start with the (simpler) two-dimensional case. Let $V_{2,k}^{\text{vert}}(\Omega)$ denote the same H^1 conforming space introduced in (3.28), and

$$V_{2,k}^{\text{elem}}(\Omega) = \{v \in L^2(\Omega) \text{ such that } v_{|E} \in \mathbb{P}_k(E)\,\forall \text{ element } E \in \mathcal{T}_h\}. \tag{6.74}$$

Then, we have the following theorem:

Theorem 6.13. Let $k \geq 2$, and assume that Ω is a simply connected polygon, decomposed in a finite number of polygons E. Then the sequences

$$\mathbb{R} \xrightarrow{\;i\;} V_{2,k}^{\text{vert}}(\Omega) \xrightarrow{\;\mathbf{grad}\;} V_{2,k-1}^{\text{edge}}(\Omega) \xrightarrow{\;\text{rot}\;} V_{2,k-2}^{\text{elem}}(\Omega) \xrightarrow{\;o\;} 0 \tag{6.75}$$

and

$$\mathbb{R} \xrightarrow{\;i\;} V_{2,k}^{\text{vert}}(\Omega) \xrightarrow{\;\mathbf{rot}\;} V_{2,k-1}^{\text{face}}(\Omega) \xrightarrow{\;\text{div}\;} V_{2,k-2}^{\text{elem}}(\Omega) \xrightarrow{\;o\;} 0 \tag{6.76}$$

are both exact sequences.

Proof. We note first that the two sequences are practically the same, up to a rotation of $\pi/2$. Hence we will just show the exactness of the sequence (6.75). Essentially, the only non-trivial part will be to show that

- **a.1** for every $\boldsymbol{v} \in V_{2,k-1}^{\text{edge}}(\Omega)$ with $\text{rot}\,\boldsymbol{v} = 0$ there exists a $\varphi \in V_{2,k}^{\text{vert}}(\Omega)$ such that $\mathbf{grad}\,\varphi = \boldsymbol{v}$.
- **a.2** for every $q \in V_{2,k-2}^{\text{elem}}(\Omega)$ there exists a $\boldsymbol{v} \in V_{2,k-1}^{\text{edge}}(\Omega)$ such that $\text{rot}\,\boldsymbol{v} = q$.

We start with **a.1**. As Ω is simply connected, we have that the condition $\text{rot}\,\boldsymbol{v} = 0$ implies that there exists a function $\varphi \in H^1(\Omega)$ such that $\mathbf{grad}\,\varphi = \boldsymbol{v}$ in Ω. On every edge e of $\mathcal{T}_h$ such φ will obviously satisfy, as well:

$$\frac{\partial \varphi}{\partial \boldsymbol{t}_{\text{e}}} = \boldsymbol{v} \cdot \boldsymbol{t}_{\text{e}} \in \mathbb{P}_{k-1}(\text{e}). \tag{6.77}$$

Then the restriction of φ to each $E \in \mathcal{T}_h$ verifies:

$$\varphi_{|e} \in \mathbb{P}_k(\text{e})\;\forall e \in \partial E; \qquad \Delta\varphi \equiv \text{div}\,\boldsymbol{v} \;\in \mathbb{P}_{k-2}(E) \tag{6.78}$$

so that clearly $\varphi \in V_{2,k}^{\text{vert}}(\Omega)$.

To deal with **a.2**, we first construct a $\boldsymbol{\varphi}$ in $[H^1(\Omega)]^2$ such that $\text{rot}\,\boldsymbol{\varphi} = q$ and

$$\boldsymbol{\varphi} \cdot \boldsymbol{t} = \frac{\int_\Omega q \,\text{d}\Omega}{|\partial\Omega|} \quad \text{on } \partial\Omega, \tag{6.79}$$

where $\boldsymbol{t}$ is the unit counterclockwise tangent vector to $\partial\Omega$ and $|\partial\Omega|$ is the length of $\partial\Omega$. Then we consider the element $\boldsymbol{v} \in V_{2,k-1}^{\text{edge}}(\Omega)$ such that

$$\boldsymbol{v} \cdot \boldsymbol{t}_{\text{e}} := \Pi_{k-1}^0(\boldsymbol{\varphi} \cdot \boldsymbol{t}_{\text{e}})\;\forall \text{ edge } e \text{ in } \mathcal{T}_h \tag{6.80}$$

and, within each element E:

$$\text{rot}\,\boldsymbol{v} = \text{rot}\,\boldsymbol{\varphi} = q, \qquad \text{div}\,\boldsymbol{v} = 0. \tag{6.81}$$

Clearly such a $\boldsymbol{v}$ solves the problem. □

Remark 6.14. The construction in the proof of **a.2** could also be done if the two-dimensional domain Ω is a *closed surface*, obtained as union of polygons. To fix the ideas, assume that we deal with the boundary ∂P of a polyhedron P, and that we are given on every face f of P a polynomial q_{f} of degree $k-2$, in such a way that

$$\sum_{\mathrm{f}\in\partial P} \int_{\mathrm{f}} q_{\mathrm{f}}\,\mathrm{df} = 0. \tag{6.82}$$

Then there exists an element $\boldsymbol{v} \in B^{\mathrm{edge}}_{k-1}(\partial P)$ such that on each face f we have $\mathrm{rot}_2(\boldsymbol{v}_{|f}) = q_{\mathrm{f}}$. To see that this is true, we define first, for each face f, the number

$$\tau_{\mathrm{f}} := \int_{\mathrm{f}} q_{\mathrm{f}}\,\mathrm{df}.$$

Then we fix, on each edge e, an orientation $\boldsymbol{t}_{\mathrm{e}}$, we orient each face f with the outward normal, and we define, *for each edge* e *of* f, the counterclockwise tangent unit vector $\boldsymbol{t}^{\mathrm{f}}_c$. Then we consider the *combinatorial problem* (defined on the topological decomposition $\mathcal{T}_h$) of finding for each edge e a real number σ_{e} such that for each face f

$$\sum_{\mathrm{e}\subset\partial\mathrm{f}} \sigma_{\mathrm{e}}\,\boldsymbol{t}_{\mathrm{e}}\cdot\boldsymbol{t}^{\mathrm{f}}_c = \tau_{\mathrm{f}}. \tag{6.83}$$

This could be solved using the same approach used in the above proof, applied on a flat polygonal decomposition that is topologically equivalent to the decomposition of ∂P without one face. The last face will fit automatically, due to (6.82). Then we take $\boldsymbol{v}$ such that on each edge $\boldsymbol{v}\cdot\boldsymbol{t} \in \mathbb{P}_{k-1}$ with $\int_{\mathrm{e}} \boldsymbol{v}\cdot\boldsymbol{t}_{\mathrm{e}}\,\mathrm{de} = \sigma_{\mathrm{e}}$, and for each face, $\mathrm{div}\,\boldsymbol{v}_{\mathrm{f}} = 0$, $\mathrm{rot}\,\boldsymbol{v}_{\mathrm{f}} = q_{\mathrm{f}}$.

We are now ready to consider the three-dimensional case. Let $V^{\mathrm{vert}}_{3,k}(\Omega)$ denote the H^1-conforming space obtained by gluing together the local spaces introduced in (3.45), and let

$$V^{\mathrm{elem}}_{3,k}(\Omega) := \{v \in L^2(\Omega) \text{ such that } v_{|P} \in \mathbb{P}_k(P)\,\forall \text{ element } P \in \mathcal{T}_h\}. \tag{6.84}$$

Then, we have the following theorem:

Theorem 6.15. Let $k \geq 3$, and assume that Ω is a simply connected polyhedron, decomposed in a finite number of polyhedra P. Then the sequence

$$\mathbb{R} \xrightarrow{\ i\ } V^{\mathrm{vert}}_{3,k}(\Omega) \xrightarrow{\ \mathbf{grad}\ } V^{\mathrm{edge}}_{3,k-1}(\Omega) \xrightarrow{\ \mathbf{curl}\ } V^{\mathrm{face}}_{3,k-2}(\Omega) \xrightarrow{\ \mathrm{div}\ } V^{\mathrm{elem}}_{3,k-3}(\Omega) \xrightarrow{\ o\ } 0 \tag{6.85}$$

is exact.

Proof. It is pretty much obvious, looking at the definitions of the spaces, that

- a constant function is in $V^{\mathrm{vert}}_{3,k}(\Omega)$ and has zero gradient,

- the gradient of a function of $V^{\text{vert}}_{3,k}(\Omega)$ is in $V^{\text{edge}}_{3,k-1}(\Omega)$ and has zero **curl**,
- the **curl** of a vector in $V^{\text{edge}}_{3,k-1}(\Omega)$ is in $V^{\text{face}}_{3,k-2}(\Omega)$ and has zero divergence,
- the divergence of a vector of $V^{\text{face}}_{3,k-2}(\Omega)$ is in $V^{\text{elem}}_{3,k-3}(\Omega)$.

Hence, essentially, we have to prove that:

- **b.1** for every $\boldsymbol{v} \in V^{\text{edge}}_{3,k-1}(\Omega)$ with $\mathbf{curl}\,\boldsymbol{v} = 0$ there exists a $\varphi \in V^{\text{vert}}_{3,k}(\Omega)$ such that $\mathbf{grad}\,\varphi = \boldsymbol{v}$.
- **b.2** for every $\boldsymbol{\tau} \in V^{\text{face}}_{3,k-2}(\Omega)$ with $\operatorname{div}\boldsymbol{\tau} = 0$ there exists a $\boldsymbol{\varphi} \in V^{\text{edge}}_{3,k-1}(\Omega)$ such that $\mathbf{curl}\,\boldsymbol{\varphi} = \boldsymbol{\tau}$
- **b.3** for every $q \in V^{\text{elem}}_{3,k-3}(\Omega)$ there exists a $\boldsymbol{\sigma} \in V^{\text{face}}_{3,k-2}(\Omega)$ such that $\operatorname{div}\boldsymbol{\sigma} = q$.

The proof of **b.1** is immediate, as in the two-dimensional case **a.1**: the function (unique up to a constant) φ such that $\mathbf{grad}\,\varphi = \boldsymbol{v}$ will verify (6.77) on each edge. Moreover, its restriction $\boldsymbol{\varphi}_{\text{f}}$ to each face f will satisfy $\mathbf{grad}_2\,\boldsymbol{\varphi}_{\text{f}} = \boldsymbol{v}_{\text{f}}$, and so on.

Let us therefore look at **b.2**. Given $\boldsymbol{\tau} \in V^{\text{face}}_{3,k-2}(\Omega)$ with $\operatorname{div}\boldsymbol{\tau} = 0$ we first consider (as in Remark 6.14) the element $\boldsymbol{g} \in B^{\text{edge}}_{k-1}(\partial\Omega)$ such that, on each face $\text{f} \subset \partial\Omega$

$$\operatorname{rot}_2(\boldsymbol{g}_{|\text{f}}) = \boldsymbol{\tau}\cdot\boldsymbol{n}\ (\in \mathbb{P}_{k-2}(\text{f})). \tag{6.86}$$

Note that

$$\sum_{\text{f}\subset\partial\Omega}\int_{\text{f}}\boldsymbol{\tau}\cdot\boldsymbol{n}^{\text{f}}_{\Omega}\,\text{df} = \int_{\Omega}\operatorname{div}\boldsymbol{\tau}\,\text{d}\Omega \;=\; 0, \tag{6.87}$$

so that the compatibility condition (6.82) is satisfied. Then we solve in Ω the *Div-Curl* problem

$$\operatorname{div}\boldsymbol{\psi} = 0 \quad \text{and} \quad \mathbf{curl}\,\boldsymbol{\psi} = \boldsymbol{\tau} \quad \text{in } \Omega, \qquad \text{with} \quad \boldsymbol{\psi}_t = \boldsymbol{g} \quad \text{on } \partial\Omega. \tag{6.88}$$

The (unique) solution of (6.88) has enough regularity to take the trace of its tangential component on each edge e, and therefore, after deciding an orientation $\boldsymbol{t}_{\text{e}}$ for every edge e in $\mathcal{T}_h$, we can take

$$\eta_{\text{e}} := \Pi^0_{k-1}(\boldsymbol{\psi}\cdot\boldsymbol{t}_{\text{e}}) \qquad \text{on each edge e in } \mathcal{T}_h. \tag{6.89}$$

At this point, for each element P we construct $\boldsymbol{\varphi} \in B^{\text{edge}}_{k-1}(\partial P)$ by requiring that

$$\begin{aligned} &\boldsymbol{\varphi}\cdot\boldsymbol{t}_{\text{e}} = \eta_{\text{e}} \ \text{ on each edge e,}\\ &\operatorname{rot}_2\boldsymbol{\varphi}_{\text{f}} = \boldsymbol{\tau}\cdot\boldsymbol{n}^{\text{f}}_P \ \text{and}\ \operatorname{div}\boldsymbol{\varphi}_{\text{f}} = 0 \ \text{ in each face } \text{f}\subset\partial P. \end{aligned} \tag{6.90}$$

Then we can define $\boldsymbol{\varphi}$ inside each element by choosing, together with (6.90),

$$\mathbf{curl}\,\boldsymbol{\varphi} = \boldsymbol{\tau} \ \text{and}\ \operatorname{div}\boldsymbol{\varphi} = 0 \quad \text{in each element } P. \tag{6.91}$$

It is easy to see that the boundary conditions given in (6.90) are *compatible* with the requirement $\mathbf{curl}\,\boldsymbol{\varphi} = \boldsymbol{\tau}$, so that the solution of (6.91) exists. Moreover it is easy to see that all the necessary orientations fit, in such a way that $\mathbf{curl}\,\boldsymbol{\varphi}$ is globally in $[L^2(\Omega)]^3$, so that actually $\boldsymbol{\varphi} \in V^{\text{edge}}_{3,k-1}(\Omega)$.

Finally, we have to prove **b.3**. The proof follows very closely the two dimensional case: given $q \in V^{\text{elem}}_{3,k-3}(\Omega)$, we first choose $\boldsymbol{\beta} \in [H^1(\Omega)]^3$ such that

$$\operatorname{div} \boldsymbol{\beta} = q \quad \text{in } \Omega \qquad \text{and } \boldsymbol{\beta} \cdot \boldsymbol{n}_\Omega = \frac{\int_\Omega q \, \mathrm{d}\Omega}{|\partial\Omega|} \tag{6.92}$$

where, now, $|\partial\Omega|$ is obviously the *area* of $\partial\Omega$. Then on each face f of $\mathcal{T}_h$ we take

$$\boldsymbol{\sigma} \cdot \boldsymbol{n}^{\mathrm{f}}_\Omega = \Pi^0_{k-2}(\boldsymbol{\beta} \cdot \boldsymbol{n}^{\mathrm{f}}_\Omega) \tag{6.93}$$

and inside each element P we take $\operatorname{div} \boldsymbol{\sigma} = q$ and $\mathbf{curl}\, \boldsymbol{\sigma} = 0$. Note again that condition $\operatorname{div} \boldsymbol{\sigma} = q$ is *compatible* with the boundary conditions (6.93) and the orientations will fit in such a way that actually $\operatorname{div} \boldsymbol{\sigma} \in L^2(\Omega)$, so that $\boldsymbol{\sigma} \in V^{\text{face}}_{3,k-2}(\Omega)$.

□

Remark 6.16. Although here we are not dealing with applications, we point out that, as is well known (see e.g. Bossavit (1988), Mattiussi (1997), Hiptmair (2001), Arnold, Falk and Winther (2006*b*)), the exactness of the above sequences are of paramount importance in proving several properties (as the various forms of *inf-sup*, the ellipticity in the kernel, etc.) that are crucial in the study of convergence of mixed formulations (see e.g. Boffi, Brezzi and Fortin (2013)).

6.8. *A hint on more general cases*

As already pointed out in the final part of Brezzi *et al.* (2014) for the particular case of 2D face elements, we observe here that actually in all four cases considered in this paper (face elements and edge elements in 2D and in 3D), we have at least three parameters to play with in order to create variants of our elements.

For instance, considering the case of 3D face elements, we could choose three different integers k_b, k_r and k_d (all ≥ -1) and consider, instead of (6.46) the spaces

$$V^{\text{face}}_{3,\boldsymbol{k}}(P) := \{\boldsymbol{v} \in H(\operatorname{div}; P) \cap H(\mathbf{curl}; P) \text{ such that}$$
$$\boldsymbol{v} \cdot \boldsymbol{n}^{\mathrm{f}}_P \in \mathbb{P}_{k_b}(\mathrm{f})\, \forall \text{ face f of } P, \operatorname{div} \boldsymbol{v} \in \mathbb{P}_{k_d}(P),\ \mathbf{curl}\, \boldsymbol{v} \in \mathcal{R}_{k_r}(P)\}, \tag{6.94}$$

where obviously $\boldsymbol{k}$ is given by $\boldsymbol{k} := (k_b, k_d, k_r)$. Taking, for a given integer k, the three indices as $k_b = k$, $k_d = k-1$, $k_r = k-1$ we re-obtain the elements in (6.46), that in turn are the natural extension of the BDM $H(\text{div})$-conforming elements. Taking instead $k_b = k$, $k_d = k$, $k_r = k-1$, for $k \geq 0$ we would rather mimic the Raviart-Thomas elements. In particular, on simplices and for $k = 0$ we recover exactly the RT_0 element.

We also point out that if we know a priori that (say, in a mixed formulation) the *vector part* of the solution of our problem will be a gradient, we could consider the choice $k_b = k$, $k_d = k-1$, $k_r = -1$ obtaining a space that contains all polynomial vectors in $\mathcal{G}_k$ (that is: vectors that are gradients of some scalar polynomial of degree

$\leq k+1$), a space that is rich enough to provide an optimal approximation of our unknown.

Similarly, for the spaces in (6.55) one can consider the variants

$$V_{3,\boldsymbol{k}}^{\text{edge}}(P) := \{\boldsymbol{v}|\ \boldsymbol{v}_t \in B_{k_b}^{\text{edge}}(\partial P), \quad \operatorname{div}\boldsymbol{v} \in \mathbb{P}_{k_d}(P), \text{ and } \mathbf{curl}\,\mathbf{curl}\,\boldsymbol{v} \in \mathcal{R}_{k_r-1}(P)\}. \tag{6.95}$$

On the other hand, for nodal VEMs we can play with two indices, say k_b and k_Δ, to have

$$V_{3,\boldsymbol{k}}^{\text{vert}}(P) := \{v \mid v_{|\partial P} \in B_{k_b}^{\text{vert}}(\partial P) \text{ and } \Delta v \in \mathbb{P}_{k_\Delta-2}(P)\}, \tag{6.96}$$

and, needless to say, in the definition of $B_{k_b}^{\text{vert}}(\partial P)$, the degree of Δ_2 in each face could be different from k_b.

6.9. Serendipity elements

Some of the discrete spaces appearing in the diagram (6.75) are not suitable for practical computations. Indeed, as discussed in Section 3.8 for the space $V_{3,k}^{\text{vert}}(\Omega)$, the chosen set of degrees of freedom only allows to compute projections of sub-optimal order. A simple way out would be to enlarge the spaces and add degrees of freedom, in the spirit of (3.37), but this would result in high computational costs. The best choice is instead to make use of Serendipity variants of the above spaces, which allow to reduce the number of degrees of freedom and still be able to compute projections of the required order. An example of this strategy was shown in Section 3.6, but here we have the additional difficulty that the involved Serendipity projections need to be compatible with the exact sequence structure. Such Serendipity sequences constitute the current state of the art of Virtual Elements discrete complexes, and we refer the reader to (Beirão da Veiga *et al.* 2017*a*), (Beirão da Veiga *et al.* 2018*b*), (Beirão da Veiga *et al.* 2018*a*) for a detailed description. Here we limit ourselves to show a brief example in the two dimensional case, where the aim is to build the serendipity exact sequence (6.76).

In the following part we focus on a single sample element E, the global version following trivially. Furthermore, for simplicity of exposition we assume that $\eta > k$, so that no polynomial bubbles exist on the polygon E (see Section 3.6).

For k integer, $k \geq 1$, we begin by enlarging the original scalar VEM-space (3.15) as we did in (3.37), that we recall here (with a different notation):

$$W_k^{\text{node}}(E) := \Big\{v \in C^0(\overline{E}) :\ v_{|\mathrm{e}} \in P_k(\mathrm{e})\ \forall \mathrm{e} \subset \partial E,\ \Delta v \in P_k(E)\Big\}, \tag{6.97}$$

with the degrees of freedom

$$
\begin{aligned}
&(D_1): && \text{the values of } v \text{ at the vertices of } E,\\
&(D_2): && \text{for each edge e, the moments } \int_{\mathrm{e}} v\, p_{k-2}\,\mathrm{d}s \quad \forall p_{k-2} \in \mathbb{P}_{k-2}(\mathrm{e}),\\
&(D_3): && \int_E (\nabla v \cdot \boldsymbol{x})\, p_k\,\mathrm{d}E \quad \forall p_k \in \mathbb{P}_k(E).
\end{aligned}
\tag{6.98}
$$

Note that, using an integration by parts, it is easy to check that the set of degrees of freedom (6.98) is equivalent to the set (3.38), where the moments $\int_E v p_k\,\mathrm{d}E$ are assigned instead of (D_3). We associate with the above space the enlarged edge-space $W^{\mathrm{edge}}_{k-1}(E)$

$$
\begin{aligned}
W^{\mathrm{edge}}_{k-1}(E) := \Big\{ \boldsymbol{v} \in [L^2(E)]^2 \ :\ &\operatorname{div} \boldsymbol{v} \in P_k(E),\ \operatorname{rot} \boldsymbol{v} \in P_{k-1}(E),\\
&\boldsymbol{v}_{|\mathrm{e}} \cdot \boldsymbol{t}_{\mathrm{e}} \in P_{k-1}(\mathrm{e})\ \forall \mathrm{e} \subset \partial E \Big\},
\end{aligned}
\tag{6.99}
$$

with the degrees of freedom

$$
\begin{aligned}
&(D_1): \text{ the moments } \int_{\mathrm{e}} (\boldsymbol{v} \cdot \boldsymbol{t}_{\mathrm{e}}) p_{k-1}\,\mathrm{d}s\ \forall p_{k-1} \in \mathbb{P}_{k-1}(\mathrm{e}),\ \forall \text{ edge e},\\
&(D_2): \text{ the moments } \int_E \boldsymbol{v} \cdot \boldsymbol{x}\, p_k\,\mathrm{d}E \quad \forall p_k \in \mathbb{P}_k(E),\\
&(D_3): \int_E \operatorname{rot} \boldsymbol{v}\, p^0_{k-1}\,\mathrm{d}E \quad \forall p^0_{k-1} \in \mathbb{P}^0_{k-1}(E).
\end{aligned}
\tag{6.100}
$$

It can be easily checked that such spaces form an exact sequence

$$
\mathbb{R} \xrightarrow{\ i\ } W^{\mathrm{node}}_k(E) \xrightarrow{\ \boldsymbol{\nabla}\ } W^{\mathrm{edge}}_{k-1}(E) \xrightarrow{\ \mathrm{rot}\ } \mathbb{P}_{k-1}(E) \xrightarrow{\ o\ } 0. \tag{6.101}
$$

On the other hand, $W^{\mathrm{node}}_k(E)$ and $W^{\mathrm{edge}}_{k-1}(E)$ have a large number of internal degrees of freedom, a particularly cumbersome situation when planning to use such spaces on the faces of a polyhedron (in order to design their three dimensional counterparts). We therefore introduce the following Serendipity variants. Let us introduce the projection operator $\Pi^{\mathrm{node}}_S : W^{\mathrm{node}}_k(E) \to \mathbb{P}_k(E)$, defined by

$$
\begin{cases}
\displaystyle\int_{\partial E} \partial_t (q - \Pi^{\mathrm{node}}_S q) \partial_t p\,\mathrm{d}s = 0 \quad \forall p \in \mathbb{P}_k(E),\\
\displaystyle\int_{\partial E} (\boldsymbol{x} \cdot \boldsymbol{n})(q - \Pi^{\mathrm{node}}_S q)\,\mathrm{d}s = 0.
\end{cases}
\tag{6.102}
$$

It can be proven, see (Beirão da Veiga *et al.* 2017*a*), that the above operator is well defined. We can then introduce the Serendipity nodal space as:

$$
SV^{\mathrm{node}}_k(E) := \Big\{ q \in W^{\mathrm{node}}_k(E) : \int_E \nabla(q - \Pi^{\mathrm{node}}_S q) \cdot \boldsymbol{x}\, p_k\,\mathrm{d}E = 0\,\forall p_k \in \mathbb{P}_k \Big\}. \tag{6.103}
$$

Clearly, a set of degree of freedom for $SV^{\mathrm{node}}_k(E)$ is given by $(D_1) - (D_2)$ in (6.98);

the set (D_3) is not needed anymore. Analogously, after defining the space

$$S_{k-1}^{\text{edge}} := \textbf{grad}\, \mathbb{P}_k \oplus \boldsymbol{x}^{\perp}\mathbb{P}_{k-1}, \tag{6.104}$$

we introduce the well defined operator $\Pi_S^{\text{edge}} : W_{k-1}^{\text{edge}}(E) \to S_{k-1}^{\text{edge}}$:

$$\int_{\partial E} [(\boldsymbol{v} - \Pi_S^{\text{edge}}\boldsymbol{v}) \cdot \boldsymbol{t}][\nabla p \cdot \boldsymbol{t}]\, \mathrm{d}s = 0 \quad \forall p \in \mathbb{P}_k(E), \tag{6.105}$$

$$\int_{\partial E} (\boldsymbol{v} - \Pi_S^{\text{edge}}\boldsymbol{v}) \cdot \boldsymbol{t}\, \mathrm{d}s = 0, \tag{6.106}$$

$$\int_{E} \mathrm{rot}(\boldsymbol{v} - \Pi_S^{\text{edge}}\boldsymbol{v}) p_{k-1}^0\, \mathrm{d}E = 0 \quad \forall p_{k-1}^0 \in \mathbb{P}_{k-1}^0(E). \tag{6.107}$$

We can now define **the Serendipity edge space** as:

$$SV_{k-1}^{\text{edge}}(E) = \left\{\boldsymbol{v} \in W_{k-1}^{\text{edge}}(E) \colon \int_{E} (\boldsymbol{v} - \Pi_S^{\text{edge}}\boldsymbol{v}) \cdot \boldsymbol{x}\, p_k\, \mathrm{d}E = 0 \quad \forall p_k \in \mathbb{P}_k\right\}. \tag{6.108}$$

A set of dofs for $SV_{k-1}^{\text{edge}}(E)$ is given by (D_1) and (D_3) in (6.100). The above projections have been carefully chosen so that the Serendipity spaces still form an exact sequence:

$$\mathbb{R} \xrightarrow{\;i\;} SV_k^{\text{node}}(E) \xrightarrow{\;\boldsymbol{\nabla}\;} SV_{k-1}^{\text{edge}}(E) \xrightarrow{\;\mathrm{rot}\;} \mathbb{P}_{k-1}(E) \xrightarrow{\;o\;} 0 \tag{6.109}$$

When compared with their counterparts in (6.101), the above spaces are smaller but allow the same computability in terms of projection operators and have the same approximation properties. We finally observe that interpolation and stability estimates for Serendipity edge and face VEM spaces can be found in (Beirão da Veiga, Mascotto and Meng 2022) and (Beirão da Veiga and Mascotto 2022).

7. The Elasticity problem

In the present section we introduce the Virtual Element Method for linear and nonlinear elasticity, with particular attention in dealing with almost-incompressible materials. After the development of the H^1-conforming VEM of order k (Beirão da Veiga *et al.* 2013*b*), it was immediately recognized that (for $k \geq 2$) such discrete space was also suitable for building a simple and effective displacement/pressure inf-sup stable pair for incompressible elasticity. This observation lead to the contribution (Beirão da Veiga, Brezzi and Marini 2013*a*) where the authors introduced a Virtual Element family for linear elasticity in primal form, robust in the incompressible limit.

The main part of this section is indeed based on (Beirão da Veiga *et al.* 2013*a*), but with a more modern viewpoint on many details, such as the construction used in the bilinear forms and the adoption of enhanced VE spaces. In particular, we also present a different viewpoint on the same method, which sets the basic background for generalization to nonlinear problems. In the final part of this section (mainly inspired from (Beirão da Veiga, Lovadina and Mora 2015), see also (Artioli, Beirão da Veiga, Lovadina and Sacco 2017*b*)) we describe the VE discretization of nonlinear elasticity problems in small deformations and comment briefly on more complex problems such as inelasticity and large deformations (Chi, Beirao da Veiga and Paulino 2017).

The present section constitutes only a brief introduction to the very wide research area of VEM for Solid Mechanics. The main motivations of the success of VEM in the solid mechanics engineering community were (1) the ease of combining/embedding the method with existing FEM codes, (2) the robustness to large mesh distortions, (3) the possibility to automatically handle hanging nodes, (4) the simplicity and efficiency of the formulation for the lowest order (1-gauss-node-per-element) case. Among the many advances in the literature, we here mention (in addition to the above) only a few sample papers regarding topology optimization (Gain *et al.* 2015, Chi *et al.* 2020), contact problems (Wriggers *et al.* 2016), Hellinger-Reissner elasticity (Artioli, de Miranda, Lovadina and Patruno 2018, Dassi, Lovadina and Visinoni 2020*b*), fracture and crack propagation (Hussein, Aldakheel, Hudobivnik, Wriggers, Guidault and Allix 2019, Artioli, Marfia and Sacco 2020), elastodynamics (Park, Chi and Paulino 2020), elasticity and plasticity for finite deformations (Wriggers, Reddy, Rust and Hudobivnik 2017, Wriggers and Hudobivnik 2017).

7.1. *The linear elasticity problem*

We consider the deformation problem of a linearly elastic body subjected to a volume load and with given boundary conditions, under the hypothesis of small deformations. In the main part of this section we will focus on the two-dimensional case, while hints on the 3D (which is essentially analogous) will be given at the end. Let Ω be a polygonal domain, and let Γ be its boundary. Let λ and μ be positive coefficients (Lamé coefficients) and let $\boldsymbol{f}$ be a vector valued function belonging to $[L^2(\Omega)]^2$. For the sake of simplicity we will use (homogeneous) Dirichlet boundary conditions. The strong form of the equations read

$$A_{\lambda,\mu}\boldsymbol{u} = \boldsymbol{f} \ \text{ in } \Omega \qquad \text{and} \qquad \boldsymbol{u} = 0 \ \text{ on } \Gamma\,,$$

where the linear elliptic operator $A_{\lambda,\mu}$ is given by

$$A_{\lambda,\mu}\boldsymbol{u} := -\begin{pmatrix} 2\mu(u_{1,xx} + \frac{1}{2}(u_{1,yy} + u_{2,xy})) + \lambda(u_{1,xx} + u_{2,yx}) \\ 2\mu(\frac{1}{2}(u_{1,yx} + u_{2,xx}) + u_{2,yy}) + \lambda(u_{1,xy} + u_{2,yy}) \end{pmatrix}.$$

In order to introduce the corresponding variational formulation, we consider the space

$$\boldsymbol{V} := [H^1_0(\Omega)]^2 \tag{7.1}$$

and the bilinear form

$$a(\boldsymbol{u},\boldsymbol{v}) := 2\mu \int_\Omega \boldsymbol{\varepsilon}(\boldsymbol{u}) : \boldsymbol{\varepsilon}(\boldsymbol{v})\,\mathrm{d}\Omega + \lambda \int_\Omega \mathrm{div}\,\boldsymbol{u}\ \mathrm{div}\,\boldsymbol{v}\,\mathrm{d}\Omega \equiv 2\mu a_\mu(\boldsymbol{u},\boldsymbol{v}) + \lambda a_\lambda(\boldsymbol{u},\boldsymbol{v})\,, \tag{7.2}$$

where $\boldsymbol{\varepsilon}(\boldsymbol{u}) = (\nabla\boldsymbol{u} + \nabla^T\boldsymbol{u})/2$ represents as usual the *symmetric gradient operator*.

It is easy to see (possibly using Korn inequality in the presence of more general boundary conditions) that there exist two constants, $M > 0$ and $\alpha > 0$, depending only on Ω, λ and μ, such that

$$\alpha\,\|\boldsymbol{v}\|^2_{\boldsymbol{V}} \le a(\boldsymbol{v},\boldsymbol{v}) \le M\,\|\boldsymbol{v}\|^2_{\boldsymbol{V}} \qquad \forall\,\boldsymbol{v}\in\boldsymbol{V}. \tag{7.3}$$

We note that $\boldsymbol{f}\in\boldsymbol{V}'$, and we denote by $<\boldsymbol{f},\boldsymbol{v}>$ the corresponding duality pairing (that here coincides with the usual L^2 inner product). Then the variational form of the problem reads:

$$\begin{cases}\text{Find } \boldsymbol{u}\in\boldsymbol{V} \text{ such that}\\ a(\boldsymbol{u},\boldsymbol{v}) =< \boldsymbol{f},\boldsymbol{v}> \quad \forall\,\boldsymbol{v}\in\boldsymbol{V}\end{cases} \tag{7.4}$$

that clearly has a unique solution, that belongs at least to $[H^s(\Omega)]^2$ for some $s > 3/2$ depending on the maximum angle in Γ.

Remark 7.1. As it is well known, when the parameter $\lambda >> \mu$, we fall into the range of the so called "almost-incompressible" materials. In such case the coercivity and continuity constants in (7.3) diverge. Unless specific care is taken in the discretization, the accuracy of numerical methods will degenerate in such situations; there is a large FEM literature in this respect (see for instance (Boffi *et al.* 2013) and the references therein). The VEM scheme here proposed will be robust also in the almost-incompressible limit.

7.2. The discrete spaces and problem

The method here described is taken from (Beirão da Veiga *et al.* 2013*a*) but with a more modern viewpoint on some aspects. We refer also to (Artioli, Beirão da Veiga, Lovadina and Sacco 2017*a*) for a more engineering oriented introduction. In order to introduce the discrete VEM space for the displacement field, we start by the same scalar "enhanced" spaces introduced in section 3.6, that we recall here. For $k \ge 1$ we set

$$\begin{aligned} V_k(E) :=\{ & v\in C^0(\overline{E}) \text{ such that } v_{|\mathrm{e}}\in\mathbb{P}_k(\mathrm{e})\ \forall \mathrm{e}\in\partial E,\ \Delta v\in\mathbb{P}_k(E),\\ & \text{and } \int_E (v-\Pi_k^{\nabla,E}v)\,p_s\,\mathrm{d}E = 0 \quad \forall p_s\in\mathbb{P}_s^{\mathrm{hom}}(E), s=k-1,k\}, \end{aligned} \tag{7.5}$$

where the operator $\Pi_k^{\nabla,E}$ has been defined in (2.6). Note that also the simpler space (3.15) could be chosen, but at the price of a less accurate load approximation. The local VEM displacement space is then simply

$$\boldsymbol{V}_k(E) = [V_k(E)]^2\,, \tag{7.6}$$

with the corresponding degrees of freedom

$$
\begin{aligned}
&(\mathbf{D_1}) : \text{the values of } \boldsymbol{v} \text{ at the vertexes of the polygon } E;\\
&(\mathbf{D_2}) : \text{for } k \geq 2, \text{ the moments } \int_{\mathrm{e}} \boldsymbol{v} \cdot \boldsymbol{p} \, \mathrm{de} \quad \forall \boldsymbol{p} \in [\mathbb{P}_{k-2}(\mathrm{e})]^2 \ \ \forall \mathrm{e} \subset \partial E; \\
&(\mathbf{D_3}) : \text{for } k \geq 2, \text{ the moments } \int_E \boldsymbol{v} \cdot \boldsymbol{p} \, \mathrm{d}E \quad \forall \boldsymbol{p} \in [\mathbb{P}_{k-2}(E)]^2.
\end{aligned}
\tag{7.7}
$$

It is easy to check that $[\mathbb{P}_k(E)]^2 \subseteq \boldsymbol{V}_k(E)$. Furthermore, by similar arguments as in Section 3, we have that the following projection operators are computable in terms of the dofs (7.7):

$$
\begin{aligned}
\Pi_k^{\nabla,E} &: \boldsymbol{V}_k(E) \to [\mathbb{P}_k(E)]^2\,,\\
\Pi_k^{0,E} &: \boldsymbol{V}_k(E) \to [\mathbb{P}_k(E)]^2\,,\\
\boldsymbol{\Pi}_{k-1}^{0,E} &: \boldsymbol{\nabla} \boldsymbol{V}_k(E) \to [\mathbb{P}_{k-1}(E)]^{2\times 2}\,,\\
\Pi_{k-1}^{0,E} &: \operatorname{div} \boldsymbol{V}_k(E) \to \mathbb{P}_{k-1}(E)\,.
\end{aligned}
\tag{7.8}
$$

The global discrete displacement space is given by

$$
\boldsymbol{V}_h = \left\{ \boldsymbol{v} \in \boldsymbol{V} \text{ such that } \boldsymbol{v}|_E \in \boldsymbol{V}_k(E) \ \forall E \in \mathcal{T}_h \right\}
$$

and the associated global dofs are trivially deduced from the local ones in the standard FEM fashion.

We now define the local bilinear forms approximating the forms $a_\mu(\cdot,\cdot)$ and $a_\lambda(\cdot,\cdot)$ in (7.2) at the element level. We will introduce such bilinear forms written in the most explicit way, which makes it easier to understand the particular treatment for the volumetric term and the ensuing robustness in the incompressible limit. Later we will show a different description of the same forms which is better suited for generalization to nonlinear problems and for the implementation in an engineering perspective.

For all $E \in \mathcal{T}_h$ and all $\boldsymbol{v}_h, \boldsymbol{w}_h \in \boldsymbol{V}_k(E)$ we define

$$
\begin{aligned}
a_{\mu,h}^E(\boldsymbol{v}_h, \boldsymbol{w}_h) &:= 2\mu \int_E \boldsymbol{\Pi}_{k-1}^{0,E} \boldsymbol{\varepsilon}(\boldsymbol{v}_h) : \boldsymbol{\Pi}_{k-1}^{0,E} \boldsymbol{\varepsilon}(\boldsymbol{w}_h) \, \mathrm{d}E \\
&\qquad + \mu\, \mathcal{S}^E((I - \Pi_k^{\nabla,E})\boldsymbol{v}_h, (I - \Pi_k^{\nabla,E})\boldsymbol{w}_h)\,,\\
a_{\lambda,h}^E(\boldsymbol{v}_h, \boldsymbol{w}_h) &:= \lambda \int_E \Pi_{k-1}^{0,E}(\operatorname{div} \boldsymbol{v}_h)\, \Pi_{k-1}^{0,E}(\operatorname{div} \boldsymbol{w}_h) \, \mathrm{d}E,
\end{aligned}
\tag{7.9}
$$

where the stabilizing form $\mathcal{S}^E(\cdot,\cdot)$ is any symmetric and computable bilinear form on $\boldsymbol{V}_k(E)$ that satisfies (cfr (3.20))

$$
c_1 |\boldsymbol{v}_h|_{1,E}^2 \leq \mathcal{S}^E(\boldsymbol{v}_h, \boldsymbol{v}_h) \leq c_2 |\boldsymbol{v}_h|_{1,E}^2 \quad \forall \boldsymbol{v}_h \in \boldsymbol{V}_k(E) \text{ with } \Pi_k^{\nabla,E} \boldsymbol{v}_h = 0 \tag{7.10}
$$

uniformly in the mesh elements. The form $\mathcal{S}^E(\cdot,\cdot)$ can be taken equal to the (vector version of) the choices already discussed in Section 3 (see (3.21)–(3.23)) directly on the (properly scaled) dofs or on some boundary integrals. We note that the absence of a stabilizing term for the volumetric form $a_{\lambda,h}^E(\cdot,\cdot)$ is aimed to obtain a scheme that is robust also in the incompressible limit. Indeed, such choice corresponds to a relaxation of the volumetric constraint when $\lambda >> \mu$, as it happens in PSRI Finite Elements or mixed approaches to elasticity (Boffi *et al.* 2013). The global versions of the above forms are obtained as usual: for all $\boldsymbol{v}_h, \boldsymbol{w}_h$ in V_h

$$a_{\mu,h}(\boldsymbol{v}_h, \boldsymbol{w}_h) := \sum_{E \in \mathcal{T}_h} a^E_{\mu,h}(\boldsymbol{v}_h, \boldsymbol{w}_h), \quad a_{\lambda,h}(\boldsymbol{v}_h, \boldsymbol{w}_h) := \sum_{E \in \mathcal{T}_h} a^E_{\lambda,h}(\boldsymbol{v}_h, \boldsymbol{w}_h),$$
$$a_h(\boldsymbol{v}_h, \boldsymbol{w}_h) := a_{\mu,h}(\boldsymbol{v}_h, \boldsymbol{w}_h) + a_{\lambda,h}(\boldsymbol{v}_h, \boldsymbol{w}_h).$$

Finally, the discrete loading term is defined by

$$< \boldsymbol{f}_h, \boldsymbol{v}_h >:= \sum_{E \in \mathcal{T}_h} \int_E \Pi^{0,E}_k(\boldsymbol{f}) \cdot \boldsymbol{v}_h \, \mathrm{d}E = \sum_{E \in \mathcal{T}_h} \int_E \boldsymbol{f} \cdot \Pi^{0,E}_k(\boldsymbol{v}_h) \, \mathrm{d}E. \tag{7.11}$$

We are now able to present the VEM method for the linear elasticity problem

$$\begin{cases} \text{Find } \boldsymbol{u}_h \in \boldsymbol{V}_h \text{ such that} \\ a_h(\boldsymbol{u}_h, \boldsymbol{v}_h) =< \boldsymbol{f}_h, \boldsymbol{v}_h > \quad \forall \, \boldsymbol{v}_h \in \boldsymbol{V}_h. \end{cases} \tag{7.12}$$

It is easy to check that the form $a_h(\cdot,\cdot)$ is coercive on $\boldsymbol{V}_h$ so that the above problem has a unique solution.

Remark 7.2. An alternative form found in the literature (see, e.g. (Beirão da Veiga *et al.* 2013*a*)) for $a^E_{\mu,h}(\cdot,\cdot)$ is

$$a^E_{\mu,h}(\boldsymbol{v}_h, \boldsymbol{w}_h) := 2\mu \int_E \boldsymbol{\varepsilon}(\Pi^{\nabla,E}_k \boldsymbol{v}_h) : \boldsymbol{\varepsilon}(\Pi^{\nabla,E}_k \boldsymbol{w}_h) \, \mathrm{d}E$$
$$+ \, \mu \, \mathcal{S}^E((I - \Pi^{\nabla,E}_k)\boldsymbol{v}_h, (I - \Pi^{\nabla,E}_k)\boldsymbol{w}_h) \, .$$

The more modern choice (7.9) is more appropriate for generalizations (such as variable coefficients or, as we will see below, nonlinear problems).

An equivalent form of the same scheme

As already anticipated, we here introduce a different description of the same bilinear form $a_h(\cdot,\cdot)$ which is better suited for generalization to nonlinear problems and for the implementation in an engineering perspective. In the following we will denote the Cauchy stress (associated to the present linearly elastic constitutive law)

$$\boldsymbol{\sigma}\big(\boldsymbol{\varepsilon}(\boldsymbol{v})\big) := 2\mu\boldsymbol{\varepsilon}(\boldsymbol{v}) + \lambda \, \mathrm{tr}\, \boldsymbol{\varepsilon}(\boldsymbol{v}) I \qquad \forall \boldsymbol{v} \in H^1(\Omega) \, ,$$

and recall that the continuous bilinear form (7.2) can be written as

$$a(\boldsymbol{v}, \boldsymbol{w}) = \int_\Omega \boldsymbol{\sigma}\big(\boldsymbol{\varepsilon}(\boldsymbol{v})\big) : \boldsymbol{\varepsilon}(\boldsymbol{w}) \, \mathrm{d}\Omega. \tag{7.13}$$

We consider the local elastic form ($E \in \mathcal{T}_h$)

$$a^E_h(\boldsymbol{v}_h, \boldsymbol{w}_h) := a^E_{\mu,h}(\boldsymbol{v}_h, \boldsymbol{w}_h) + a^E_{\lambda,h}(\boldsymbol{v}_h, \boldsymbol{w}_h), \tag{7.14}$$

see (7.9). By trivial calculations and definition of the L^2 projection, for any $\boldsymbol{v}_h \in \boldsymbol{V}_k(E)$,

$$\lambda\, \Pi^{0,E}_{k-1}(\operatorname{div} \boldsymbol{v}_h) = \lambda\, \Pi^{0,E}_{k-1}\big(\operatorname{tr} \boldsymbol{\varepsilon}(\boldsymbol{v}_h)\big) = \lambda \operatorname{tr} \boldsymbol{\Pi}^{0,E}_{k-1}\big(\boldsymbol{\varepsilon}(\boldsymbol{v}_h)\big)\,,$$

where tr denotes the trace operator. Furthermore, by identical arguments, for all $\boldsymbol{v}_h \in \boldsymbol{V}_k(E)$

$$\Pi^{0,E}_{k-1}(\operatorname{div} \boldsymbol{v}_h) = \operatorname{tr} \boldsymbol{\Pi}^{0,E}_{k-1}\big(\boldsymbol{\varepsilon}(\boldsymbol{v}_h)\big) = \boldsymbol{\Pi}^{0,E}_{k-1}\big(\boldsymbol{\varepsilon}(\boldsymbol{v}_h)\big) : I\,,$$

with I denoting the 2×2 identity tensor and $A : B = \sum_{i,j} A_{ij} B_{ij}$ for all square matrixes A, B. We now combine the two above identities in the definition of $a^E_{\lambda,h}(\boldsymbol{v}_h, \boldsymbol{w}_h)$, cfr (7.9). With some simple manipulation we obtain

$$\begin{aligned} a^E_{\lambda,h}(\boldsymbol{v}_h, \boldsymbol{w}_h) &= \int_E \lambda \Pi^{0,E}_{k-1}(\operatorname{div} \boldsymbol{v}_h)\, \Pi^{0,E}_{k-1}(\operatorname{div} \boldsymbol{w}_h)\, \mathrm{d}E \\ &= \int_E \lambda \operatorname{tr} \boldsymbol{\Pi}^{0,E}_{k-1}\big(\boldsymbol{\varepsilon}(\boldsymbol{v}_h)\big) I : \boldsymbol{\Pi}^{0,E}_{k-1}\big(\boldsymbol{\varepsilon}(\boldsymbol{w}_h)\big)\, \mathrm{d}E \end{aligned} \tag{7.15}$$

Therefore, the form (7.14) can be written as

$$\begin{aligned} a^E_h(\boldsymbol{v}_h, \boldsymbol{w}_h) &= \int_E \Big(2\mu \boldsymbol{\Pi}^{0,E}_{k-1}\big(\boldsymbol{\varepsilon}(\boldsymbol{v}_h)\big) + \lambda \operatorname{tr} \boldsymbol{\Pi}^{0,E}_{k-1}\big(\boldsymbol{\varepsilon}(\boldsymbol{v}_h)\big) I\Big) : \boldsymbol{\Pi}^{0,E}_{k-1}\big(\boldsymbol{\varepsilon}(\boldsymbol{w}_h)\big)\, \mathrm{d}E \\ &\qquad + \mu\, \mathcal{S}^E((I - \Pi^{\nabla,E}_k)\boldsymbol{v}_h, (I - \Pi^{\nabla,E}_k)\boldsymbol{w}_h) \\ &= \int_E \boldsymbol{\sigma}\Big(\boldsymbol{\Pi}^{0,E}_{k-1}\big(\boldsymbol{\varepsilon}(\boldsymbol{v}_h)\big)\Big) : \boldsymbol{\Pi}^{0,E}_{k-1}\big(\boldsymbol{\varepsilon}(\boldsymbol{w}_h)\big)\, \mathrm{d}E \\ &\qquad + \mu\, \mathcal{S}^E((I - \Pi^{\nabla,E}_k)\boldsymbol{v}_h, (I - \Pi^{\nabla,E}_k)\boldsymbol{w}_h). \end{aligned} \tag{7.16}$$

The above form is to be compared with the local version of (7.13). The expression (7.16) is equivalent to the original discrete form of the previous section, but underlines that the VEM discretization is obtained simply by projecting the strains on a local polynomial space and then applying the constitutive law. The expression (7.16) is therefore suitable to easily generalize the present construction to small and large deformation nonlinear problems, as it suggests the following systematic approach: project the strains on a polynomial space and then apply the (nonlinear) constitutive law before integrating on the element. More details will be given in Section 7.4.

Finally, it is important to underline that the stabilization depends only on the parameter μ (and is therefore unaffected by large values of λ), which is what makes the scheme robust in the incompressible limit. Also this idea is easily extendable to more complex problems, by making the stabilizing form dependent only on the deviatoric part of the stresses. See also, for instance, (Park, Chi and Paulino 2021).

Extension to the 3D case

We here comment briefly on the three dimensional case. The extension of the method here presented to 3D problems is quite straightforward, in light of the previous developments for the scalar case. We simply replace the 2D scalar space (7.5) with the scalar space described in Section 3.8, and then set

$$\boldsymbol{V}_k(P) = [V_k(P)]^3 \tag{7.17}$$

for each polyhedron P in the mesh $\mathcal{T}_h$. The local degrees of freedom are the trivial vector valued version of those in (3.46). By the same arguments, it can be checked that the 3D analogs of the projections appearing in (7.8) are still computable. The rest of the construction (global space and related dofs, discrete bilinear form, load approximation) is essentially identical. Although many results of the next sections apply also to the 3D case with minor modifications, in the following we will continue to work in the bi-dimensional framework for ease of presentation.

7.3. Convergence and robustness in the incompressible limit

The interpolation estimates for the scalar space discussed in Section 3 (formulae (3.34) and (3.36) immediately apply also to the vector valued version (7.6). Since also (7.12) is a classical linear elliptic problem, deriving error estimates for the method would, in principle, follow the same identical steps (and obtain analogous results) as for the Laplace problem. On the other hand such approach would not lead to error estimates that are robust in the incompressible limit, i.e. in which the constant involved in the error does not depend on the parameter λ. In order to obtain such estimates, one needs to resort to a mixed interpretation of (7.12), in which an important role is played by the pressure variable $p = \lambda \operatorname{div} \boldsymbol{u}$.

We here show the main intermediate results leading to the final convergence Corollary 7.7, and refer to (Beirão da Veiga *et al.* 2013*a*) for the proofs. In the rest of the section we assume the same mesh assumption 2.1 already stated in Section 2, which could be relaxed following the ideas in (Beirão da Veiga *et al.* 2017*b*, Brenner and Sung 2018).

Let the (piecewise polynomial) auxiliary space

$$Q_h := \left\{ q_h \in L^2_0(\Omega) \text{ such that } q_h \in \mathbb{P}_{k-1}(E) \; \forall E \in \mathcal{T}_h \right\} .$$

We have the following inf-sup lemma.

Lemma 7.3. Let $k \geq 2$ and let the mesh assumptions 2.1 hold. Then there exists a strictly positive constant β, independent of h, such that

$$\sup_{\boldsymbol{v}_h \in \boldsymbol{V}_h} \frac{\int_\Omega (\operatorname{div} \boldsymbol{v}_h) q_h \, \mathrm{d}\Omega}{\|\boldsymbol{v}_h\|_{1,\Omega}} \geq \beta \|q_h\|_{0,\Omega} \qquad \forall q_h \in Q_h.$$

Remark 7.4. For the particular case $k = 1$ the validity of the above inf-sup condition is not assured and depends on the mesh family considered (for instance, for $k = 1$ on a triangular mesh we obtain the famous pair $\mathbb{P}_1/\mathbb{P}_0$ which is well known to fail in such respect). Positive results for a class of polygonal meshes can be obtained by extending the ideas in (Beirao da Veiga and Lipnikov 2010). In order to obtain inf-sup stability for any class of (shape-regular) meshes one would need to add edge-bubbles, which would imply a simple modification of the space with the addition of one degree of freedom per edge to the displacement space. We do not dwell here on this variants, and assume in the following that $k \geq 2$.

By classical arguments borrowed from mixed FEM, cfr (Boffi *et al.* 2013), Lemma (7.3) implies the existence of a Fortin-like operator, that is (in particular) an optimal approximant in H^1 which "preserves" the projected divergence.

Lemma 7.5. Let $k \geq 2$ and let the mesh assumptions 2.1 hold. Then there exists a positive constant C, independent of h, such that the following holds: For all $\boldsymbol{v}$ in the broken Sobolev space $[H^s(\mathcal{T}_h)]^2$, $1 \leq s \leq k+1$, there exists $\boldsymbol{v}_I \in \boldsymbol{V}_h$ that satisfies

$$\|\boldsymbol{v} - \boldsymbol{v}_I\|_1 \leq C h^{s-1} |\boldsymbol{v}|_{s,\mathcal{T}_h} ,$$
$$\int_\Omega (\operatorname{div} \boldsymbol{v}_I) q_h \,\mathrm{d}\Omega = \int_\Omega (\operatorname{div} \boldsymbol{v}) q_h \,\mathrm{d}\Omega \qquad \forall q_h \in Q_h ,$$

where by $|\cdot|_{s,\mathcal{T}_h}$ we denote the corresponding H^s broken Sobolev semi-norm.

The following convergence result bounds the error $\boldsymbol{u} - \boldsymbol{u}_h$ in terms of the interpolation error $\boldsymbol{u} - \boldsymbol{u}_I$. There is also a load approximation term (which is typically neglected in FEM analysis by assuming exact integration of the right hand side), a polynomial approximation term (stemming from the VEM approximation of the involved bilinear forms) and an explicit volumetric term.

Theorem 7.6. Let $k \geq 2$ and let the mesh assumptions 2.1 hold. Let $\boldsymbol{u}$ be the solution of problem (7.4) and $\boldsymbol{u}_h$ the solution of problem (7.12). Let $p = \lambda \operatorname{div} \boldsymbol{u}$ and p_I be its L^2 projection in Q_h. Let $\boldsymbol{u}_I$ be as defined in Lemma 7.5, and let u_π be any approximant of $\boldsymbol{u}$ piecewise in $[\mathbb{P}_k]^2$. Then there exists a positive constant C, independent of h and λ, such that

$$\|\boldsymbol{u} - \boldsymbol{u}_h\|_1 \leq C \left(\|\boldsymbol{u} - \boldsymbol{u}_I\|_1 + \|\boldsymbol{u} - \boldsymbol{u}_\pi\|_{1,\mathcal{T}_h} + \|p - p_I\|_0 + h\|\boldsymbol{f} - \boldsymbol{f}_h\|_0 \right) .$$

By combining the above theorem with Lemma 7.5 and standard polynomial approximation estimates, we obtain the following convergence result.

Corollary 7.7. Let the same assumptions as in Theorem 7.6 hold. Let furthermore $\boldsymbol{u}, \boldsymbol{f}$ be in the broken Sobolev space $[H^s(\mathcal{T}_h)]^2$ and p be in the the broken Sobolev space $H^{s-1}(\mathcal{T}_h)$, $1 \leq s \leq k+1$. Then it exists a constant C, independent of h and λ, such that

$$\|\boldsymbol{u} - \boldsymbol{u}_h\|_1 \leq C\, h^{s-1} \left(|\boldsymbol{u}|_{s,\mathcal{T}_h} + h^2 |\boldsymbol{f}|_{s,\mathcal{T}_h} + |p|_{s-1,\mathcal{T}_h} \right) .$$

It is important to observe that also the auxiliary variable p is uniformly bounded independently of λ (see for instance Remark 3.1 in (Beirão da Veiga *et al.* 2013*a*)), therefore the above result is indeed robust in the volumetric limit. We refer to Lemma 2.4 in (Beirão da Veiga *et al.* 2013*a*) for the corresponding error estimate $\|\boldsymbol{u} - \boldsymbol{u}_h\|_0$.

7.4. *Nonlinear elasticity*

In the present section we briefly present the extension of the previous ideas to the nonlinear case, focusing on small deformation elasticity and providing references on further extensions. The main results of this section are based on (Beirão da Veiga *et al.* 2015), see also (Artioli *et al.* 2017*b*) for a more engineering oriented approach. As in the previous part of this section we assume homogeneous Dirichlet boundary conditions for simplicity of exposition, the extension to more general kind of boundary conditions (and loading types) being trivial.

Assuming a regime of small deformations and an elastic material, we are now given a (general) constitutive law for the material at every point $x \in \Omega$, relating strains to stresses $\boldsymbol{\sigma}$, through the function

$$\boldsymbol{\sigma} = \boldsymbol{\sigma}(\boldsymbol{x}, \nabla \boldsymbol{u}(\boldsymbol{x})) \in \mathbb{R}^{d\times d}_{\text{symm}} . \tag{7.18}$$

Given the law (7.18), the deformation problem reads

$$\begin{cases} -\operatorname{div} \boldsymbol{\sigma} = \boldsymbol{f} & \text{in } \Omega, \\ \boldsymbol{u} = 0 & \text{on } \partial\Omega . \end{cases} \tag{7.19}$$

Let now $\boldsymbol{V}$ denote the space of admissible displacements, which will, in particular, satisfy homogeneous Dirichlet boundary conditions on $\partial\Omega$ and be equal to the space of its variations. The variational formulation of the elastic deformation problem reads

$$\begin{cases} \text{Find } \boldsymbol{u} \in \boldsymbol{V} \text{ such that} \\ \displaystyle\int_\Omega \boldsymbol{\sigma}(\boldsymbol{x}, \nabla \boldsymbol{u}(\boldsymbol{x})) : \nabla \boldsymbol{v}(\boldsymbol{x}) \,\mathrm{d}\Omega = \int_\Omega \boldsymbol{f}(\boldsymbol{x}) \cdot \boldsymbol{v}(\boldsymbol{x}) \,\mathrm{d}\Omega \quad \forall \boldsymbol{v} \in \boldsymbol{V} \end{cases} \tag{7.20}$$

The VEM discretization of problem (7.20) follows the same approach discussed previously for obtaining (7.16). We refer, for instance, to the book (Simo and Hughes 2006) for a review on standard tools and terms in computational (small deformation) solid mechanics. We here limit ourselves in recalling that typical computational codes combine a finite element construction with a constitutive algorithm, that is applied point-wise and, given the strains, computes the ensuing stresses. Such algorithm also gives the constitutive tangent, which is the algorithmically consistent tangent $\partial\sigma/\partial\nabla\boldsymbol{u}$ and is needed in the Newton iterations.

We consider the same space $\boldsymbol{V}_h$ in (7.6) of discrete displacements (or its 3D variant) and write the discrete (nonlinear) problem

$$\begin{cases} \text{Find } \boldsymbol{u}_h \in \boldsymbol{V}_h \text{ such that} \\ a_{\sigma,h}(\boldsymbol{u}_h; \boldsymbol{u}_h, \boldsymbol{v}_h) = \displaystyle\int_\Omega \boldsymbol{f}_h \cdot \boldsymbol{v}_h \,\mathrm{d}\Omega \quad \forall \boldsymbol{v}_h \in \boldsymbol{V}_h. \end{cases} \tag{7.21}$$

where the loading term is approximated as in (7.11), and the form is given by

$$a_{\sigma,h}(\boldsymbol{w}_h;\boldsymbol{u}_h,\boldsymbol{v}_h) := \sum_{E\in\mathcal{T}_h}\int_E \boldsymbol{\sigma}\big(\boldsymbol{x},\boldsymbol{\Pi}^{0,E}_{k-1}\nabla\boldsymbol{u}_h(\boldsymbol{x})\big) : \boldsymbol{\Pi}^{0,E}_{k-1}\nabla\boldsymbol{v}(\boldsymbol{x})\,\mathrm{d}E$$
$$+\,\alpha_E(\boldsymbol{w}_h)\,\mathcal{S}^E\big((I-\Pi^{\nabla,E}_k)\boldsymbol{u}_h,(I-\Pi^{\nabla,E}_k)\boldsymbol{v}_h\big)$$

for all $\boldsymbol{w}_h,\boldsymbol{u}_h,\boldsymbol{v}_h\in\boldsymbol{V}_h$, with $\mathcal{S}^E(\cdot,\cdot)$ the same stabilization form used for the linear case (7.10).

The scalar $\alpha_E(\boldsymbol{w}_h)>0$ is needed in order to introduce a scaling based on the constitutive law also in the stabilization, and takes the role of the μ parameter in (7.16). Here, since the problem is nonlinear and the constitutive tangent depends on the displacement $\boldsymbol{u}_h$, this parameter needs to depend on the displacements (but as usual is not required to be accurate, the only purpose being a stabilizing effect). Different choices can be taken for $\alpha_E(\boldsymbol{w}_h)$, for instance

$$\alpha_E(\boldsymbol{w}_h)=\left\|\frac{\partial\boldsymbol{\sigma}}{\partial\nabla\boldsymbol{u}}\big(\boldsymbol{x}_E,\boldsymbol{\Pi}^{0,E}_0\nabla\boldsymbol{w}_h\big)\right\|$$

with $\boldsymbol{x}_E$ denoting the barycenter of E and $\|\cdot\|$ representing any norm on the fourth order tensor space. We refer to the literature mentioned above and below for other possible choices of $\alpha_E(\boldsymbol{w}_h)$.

In order to solve the nonlinear problem (7.21) a typical approach in the engineering literature is using an incremental loading procedure combined with Newton iterations. Such approach can also be applied here, we refer to equation (24) of (Beirão da Veiga *et al.* 2015) for the details. Note moreover that the parameter α_E can be made dependent on $\boldsymbol{u}_h$ at the *previous* loading step, thus avoiding the calculation of the derivatives of α_E in the Newton iterations.

It is important to observe that the methodology here described couples very well with existing solid mechanics codes. For instance, given any "black-box" constitutive algorithm for the constitutive law $\boldsymbol{\sigma}$ and the associated tangent matrix, this can be embedded directly into the above method. This inherent simplicity was one of the reasons for the wide success that VEM enjoyed in the solid mechanics community. We close this section by mentioning some important generalizations, and recall that a wider overview on the VEM literature in solid mechanics can be found in the introduction to this section.

Almost incompressible materials. As already anticipated, simply by rendering the coefficient $\alpha_E(\boldsymbol{w}_h)$ dependent only on the deviatoric part of the strains, the scheme acquires robustness in the incompressible limit. Since such property is also related to the inf-sup condition in Lemma 7.3, either $k\geq 2$ or certain restrictions on the mesh are required (cfr the discussion in Section 7.3).

Inelastic materials. The extension to inelastic materials is trivial following the same approach as for standard finite elements. One needs to keep track of the history variables on each integration point during the incremental loading procedure and apply the inelastic constitutive law as a black-box algorithm. See for instance (Beirão da Veiga *et al.* 2015, Artioli *et al.* 2017*b*) for more details.

Large deformations. The approach for the large deformation case follows the same pattern, and is based on a projection of the displacement gradients followed by application of the constitutive law. Nevertheless the more complex geometric setting and the potential large variation of the involved variables requires some additional care. This may call for ad-hoc approximations of the determinant J of the displacement mapping and for suitable rules for calculating the stability parameter α_E. What makes VEM particularly valuable in large deformation analysis is the robustness of the method to mesh deformations, which is a critical aspect for such problems. We refer the reader to (Chi *et al.* 2017) for an introduction to VEM for large deformation problems.

8. The Stokes and Navier-Stokes problems

In the present section we review some core results on divergence-free VEM for incompressible fluid dynamics. The starting point is the construction introduced in (Beirão da Veiga, Lovadina and Vacca 2017) (see also (Antonietti, Beirão da Veiga, Mora and Verani 2014)) for the discretization of the Stokes problem.

In the above paper the authors propose a family of VEM velocity-pressure pairs of general "polynomial" order which, in addition to being inf-sup stable, have the important property that the discrete velocity space is contained in the discrete pressure space. As a consequence it leads to a stable scheme that guarantees a truly divergence-free velocity solution, as opposed to a relaxed divergence-free condition as it happens in standard FEM. There are many advantages of divergence-free schemes when compared to standard inf-sup stable ones, an example being that the discrete velocity error is not polluted by the pressure. Although the above VEM scheme is not pressure-robust (in the sense of (John, Linke, Merdon, Neilan and Rebholz 2017)) it still retains many advantages when compared with standard FEM (Boffi *et al.* 2013), in addition to the possibility of using general meshes.

Later, in (Vacca 2018, Beirão da Veiga, Lovadina and Vacca 2018*b*), the the method was extended also to the Navier-Stokes and Brinkman equations. In (Beirão da Veiga, Mora and Vacca 2019*b*, Beirão da Veiga, Dassi and Vacca 2018*a*), the authors investigated the discrete Stokes complex structure laying behind the VEM spaces, both in 2D and 3D, leading also to alternative schemes (for a glimpse at the related FEM literature we refer to (Arnold, Falk and Winther 2006*a*, Falk and Neilan 2013)). Computational and implementation aspects where further detailed and developed in (Dassi and Vacca 2020, Dassi and Scacchi 2020), while in (Chernov *et al.* 2021) the authors studied the hp version of the method. In (Liu, Li and Nie 2020, Frerichs and Merdon 2022) some right-hand side modifications were proposed to build a VEM scheme that is also pressure robust for the Stokes problem. In (Beirão da Veiga, Canuto, Nochetto and Vacca 2021) a model fluid interaction problem is analyzed using mesh cutting techniques in combination with the above VEM approach. There have been also other developments on VEM for fluid mechanics problems outside the divergence-free framework, some examples being non-conforming methods (Cangiani, Gyrya and Manzini 2016, Liu, Li and Chen 2017, Zhao, Zhang, Mao and Chen 2020, Liu and Chen 2019, Liu, Li and Chen 2019), non-standard mixed formulations (Cáceres, Gatica and Sequeira 2017, Gatica, Munar and Sequeira 2018*b*, Cáceres and Gatica 2016, Munar and Sequeira 2020, Gatica, Munar and Sequeira 2018*a*, Cáceres, Gatica and Sequeira 2018) and other derivations (Chen and Wang 2019, Wang, Wang and He 2020). Finally, a few references about the application of other polytopal technologies (such as polygonal FEM, polygonal DG, HHO, HDG) to fluid mechanic problems are (Natarajan 2020, Botti, Di Pietro and Droniou 2018, Di Pietro and Krell 2018, Aghili and Di Pietro 2018, Castañón Quiroz and Di Pietro 2020, Lipnikov, Vassilev and Yotov 2014, Cockburn, Fu and Qiu 2017, Antonietti, Verani, Vergara and Zonca 2019, Antonietti, Mascotto, Verani and Zonca 2022) while some references (among the many) on FEM divergence-free and pressure robust methods are (Guzmán and Scott 2019, Guzmán and Neilan 2018, Guzmán and Neilan 2014) and (Gauger, Linke and Schroeder 2019, Linke and Merdon 2016*b*, John *et al.* 2017, Linke and Merdon 2016*a*).

8.1. The Navier-Stokes equations

We here briefly review the steady Navier–Stokes equation on a polygonal simply connected domain $\Omega \subseteq \mathbb{R}^d$ with $d = 2, 3$ (for more details, see for instance (Girault and Raviart 1979)). We search a velocity field $\boldsymbol{u}$ and a pressure field p that satisfy

$$\begin{cases} -\,\nu\,\mathrm{div}(\boldsymbol{\varepsilon}(\boldsymbol{u})) + (\boldsymbol{\nabla}\boldsymbol{u})\,\boldsymbol{u} - \nabla p = \boldsymbol{f} & \text{in } \Omega, \\ \mathrm{div}\,\boldsymbol{u} = 0 & \text{in } \Omega, \\ \boldsymbol{u} = 0 & \text{on } \partial\Omega, \end{cases} \tag{8.1}$$

where $\nu \in \mathbb{R}$, $\nu > 0$ is the viscosity of the fluid and $\boldsymbol{f} \in [L^2(\Omega)]^d$ represents the volume source term. We here consider Dirichlet homogeneous boundary conditions only for simplicity, the extension to different boundary conditions being trivial. Let the continuous spaces

$$\boldsymbol{V} := \left[H^1_0(\Omega)\right]^d, \qquad Q := L^2_0(\Omega) = \left\{q \in L^2(\Omega) \quad \text{s.t.} \quad \int_\Omega q\,\mathrm{d}\Omega = 0\right\}.$$

The variational formulation of Problem (8.1) reads:

$$\begin{cases} \text{find } (\boldsymbol{u}, p) \in \boldsymbol{V} \times Q, \text{ such that} \\ \nu\, a(\boldsymbol{u}, \boldsymbol{v}) + c(\boldsymbol{u};\, \boldsymbol{u}, \boldsymbol{v}) + b(\boldsymbol{v}, p) = (\boldsymbol{f}, \boldsymbol{v}) & \text{for all } \boldsymbol{v} \in \boldsymbol{V}, \\ b(\boldsymbol{u}, q) = 0 & \text{for all } q \in Q \end{cases} \tag{8.2}$$

where the continuous forms are

$$
\begin{aligned}
a(\boldsymbol{u}, \boldsymbol{v}) &:= \int_\Omega \boldsymbol{\varepsilon}(\boldsymbol{u}) : \boldsymbol{\varepsilon}(\boldsymbol{v}) \, \mathrm{d}\Omega \,, \quad b(\boldsymbol{v}, q) := \int_\Omega q \, \operatorname{div} \boldsymbol{v} \, \mathrm{d}\Omega \,, \\
c(\boldsymbol{w};\, \boldsymbol{u}, \boldsymbol{v}) &:= \int_\Omega (\boldsymbol{\nabla} \boldsymbol{u}) \, \boldsymbol{w} \cdot \boldsymbol{v} \, \mathrm{d}\Omega \qquad \forall \boldsymbol{u}, \boldsymbol{v}, \boldsymbol{w} \in \boldsymbol{V}, \; q \in Q \,.
\end{aligned}
\tag{8.3}
$$

By definition, the velocity solution $\boldsymbol{u}$ lays in the kernel of the bilinear form $b(\cdot, \cdot)$, that corresponds to the functions in $\boldsymbol{V}$ with vanishing divergence

$$
\boldsymbol{Z} := \{\boldsymbol{v} \in \boldsymbol{V} \quad \text{s.t.} \quad \operatorname{div} \, \boldsymbol{v} = 0\}. \tag{8.4}
$$

We can observe by a direct computation that, for a fixed $\boldsymbol{w} \in \boldsymbol{Z}$, the trilinear form $c(\boldsymbol{w};\, \cdot, \cdot)$ is skew symmetric, i.e.

$$
\text{for a fixed } \boldsymbol{w} \in \boldsymbol{Z} \qquad c(\boldsymbol{w}; \boldsymbol{u}, \boldsymbol{v}) = -c(\boldsymbol{w}; \boldsymbol{v}, \boldsymbol{u}) \qquad \text{for all } \boldsymbol{u}, \boldsymbol{v} \in \boldsymbol{V}.
$$

Therefore, the trilinear form $c(\cdot;\, \cdot, \cdot)$, for $\boldsymbol{w} \in \boldsymbol{Z}$, is equal to its skew-symmetric part, defined as:

$$
c^{\text{skew}}(\boldsymbol{w};\, \boldsymbol{u}, \boldsymbol{v}) := \frac{1}{2}\big(c(\boldsymbol{w};\, \boldsymbol{u}, \boldsymbol{v}) - c(\boldsymbol{w};\, \boldsymbol{v}, \boldsymbol{u})\big) \qquad \text{for all } \boldsymbol{u}, \boldsymbol{v}, \boldsymbol{w} \in \boldsymbol{V}. \tag{8.5}
$$

It is well known that (see for instance (Girault and Raviart 1979, Boffi *et al.* 2013)) the problem (8.2) is well posed assuming suitable bounds on the external load $\boldsymbol{f}$ and the viscosity ν. Such "diffusion dominated" assumption requires

$$
\gamma := \frac{C \, \|\boldsymbol{f}\|_{Z^*}}{\nu^2} < 1 \,, \tag{8.6}
$$

where C denotes the continuity constant of $c(\cdot;\, \cdot, \cdot)$ on Z with respect to the H^1-norm. Note that the above assumption can be also stated by introducing the concept of Helmholtz–Hodge projector (see for instance (John *et al.* 2017, Lemma 2.6) and (Gauger *et al.* 2019, Theorem 3.3)).

Remark 8.1 (Stokes problem). The Stokes model is simply obtained by neglecting the nonlinear convective term in (8.1).

We close this section recalling the following useful polynomial decompositions, see also Section 6.1:

$$
\begin{aligned}
[\mathbb{P}_n(\mathcal{O})]^2 &= \nabla \mathbb{P}_{n+1}(\mathcal{O}) \oplus \big(\boldsymbol{x}^\perp \mathbb{P}_{n-1}(\mathcal{O})\big) \qquad && \text{if } \dim(\mathcal{O}) = 2, \\
[\mathbb{P}_n(\mathcal{O})]^3 &= \nabla \mathbb{P}_{n+1}(\mathcal{O}) \oplus \big(\boldsymbol{x} \wedge [\mathbb{P}_{n-1}(\mathcal{O})]^3\big) \qquad && \text{if } \dim(\mathcal{O}) = 3,
\end{aligned}
\tag{8.7}
$$

where $\boldsymbol{x}^\perp = (x_2, -x_1)$.

8.2. Virtual Element Spaces in 2D

In the present section we outline an overview of the "divergence-free" Virtual Element spaces in the 2D case. In order to ease the reader, we will start by the simpler spaces introduced in (Beirão da Veiga *et al.* 2017), which are sufficient to treat the Stokes problem, and afterwards review the enhanced spaces of (Vacca 2018, Beirão da Veiga *et al.* 2018*b*), which are suitable also for more complex problems such as Navier-Stokes and Brinkmann. We here work at the local level, that is defining the local spaces and the associated Degrees of Freedom at the element level.

Note that we here focus only on the **velocity** space; the simpler pressure space will be introduced later, directly at the global level.

Basic Virtual Elements

Let $k \in \mathbb{N}$, $k \geq 2$ represent the degree of the method (for the “lowest order” case $k = 1$, which is not part of the current family, we refer to (Antonietti *et al.* 2014)). We consider on each polygon $E \in \mathcal{T}_h$ the (local) discrete velocity virtual space

$$\begin{aligned} \boldsymbol{V}_k^{\mathrm{S}}(E) := \{\boldsymbol{v} \in [C^0(\overline{E})]^2 \ \text{ such that } \ \mathrm{rot}\boldsymbol{\Delta v} \in \mathbb{P}_{k-3}(E), \ \ \mathrm{div}\ \boldsymbol{v} \in \mathbb{P}_{k-1}(E)\,, \\ \boldsymbol{v}_{|\mathrm{e}} \in [\mathbb{P}_k(\mathrm{e})]^2 \ \ \forall \mathrm{e} \subset \partial E\} \end{aligned} \tag{8.8}$$

where as usual the operators above are to be interpreted in the distributional sense. We note that, in standard VEM fashion, the definition of $\boldsymbol{V}_k^{\mathrm{S}}(E)$ is associated to a PDE within the element, in this case a Stokes-like variational problem on E. Indeed, using (8.7) it is easy to check that the condition $\mathrm{rot}\boldsymbol{\Delta v} \in \mathbb{P}_{k-3}$ is equivalent to the existence of $q \in \mathbb{P}_{k-3}(E)$ such that $\boldsymbol{\Delta v} + \nabla s = \boldsymbol{x}^{\perp} q$ for some $s \in L_0^2(E)$; such equation, combined with the remaining conditions in (8.8), represents a Stokes problem on the element.

It is immediate to check that $[\mathbb{P}_k(E)]^2 \subseteq \boldsymbol{V}_k^{\mathrm{S}}(E)$, which is important for the approximation properties of the space, and that the dimension of $\boldsymbol{V}_h^{\mathrm{S}}(E)$ is (recalling that N_{e} denotes the number of edges of E),

$$\dim(\boldsymbol{V}_h^{\mathrm{S}}(E)) = 2k\, N_{\mathrm{e}} + (k-1)(k-2)/2 + k(k+1)/2 - 1 = 2k\, N_{\mathrm{e}} + k(k-1)$$

where the correction by minus one is related to the data compatibility condition ensuing from the Stokes theorem.

In $\boldsymbol{V}_k^{\mathrm{S}}(E)$ we set the following degrees of freedom:

$$\begin{aligned} &(\mathbf{D_1}):\ \text{the values of } \boldsymbol{v} \text{ at the vertexes of the polygon } E; \\ &(\mathbf{D_2}):\ \text{the edge moments } \int_{\mathrm{e}} \boldsymbol{v}\cdot\boldsymbol{p}\,\mathrm{de} \quad \forall \boldsymbol{p} \in [\mathbb{P}_{k-2}(\mathrm{e})]^2\ \forall \mathrm{e} \in \partial E; \\ &(\mathbf{D_3}):\ \text{the moments of } \mathrm{div}\ \boldsymbol{v} \quad \int_E (\mathrm{div}\ \boldsymbol{v}) p\,\mathrm{d}E \quad \forall p \in \mathbb{P}_{k-1}^0(E); \\ &(\mathbf{D_4}):\ \text{for } k \geq 3, \text{ the moments of } \quad \int_E \boldsymbol{v}\cdot\boldsymbol{x}^{\perp} p\,\mathrm{d}E \quad \forall p \in \mathbb{P}_{k-3}(E). \end{aligned} \tag{8.9}$$

Lemma 8.2. The degrees of freedom (8.9) are unisolvent for $\boldsymbol{V}_k^{\mathrm{S}}(E)$.

Proof. It is trivial to check that the number of the operators (8.9) is equal to the dimension of $\boldsymbol{V}_k^{\mathrm{S}}(E)$. Therefore we only need to check that, if $\boldsymbol{v} \in \boldsymbol{V}_h^{\mathrm{S}}(E)$ vanishes on all (8.9) then $\boldsymbol{v} = 0$. Recalling (8.8) and since ($\mathbf{D_1}$) and ($\mathbf{D_2}$) in (8.9) vanish, it follows immediately that $\boldsymbol{v}|_{\partial E} = 0$. Due to the Stokes theorem, such boundary condition also implies $\int_E \operatorname{div} \boldsymbol{v} \, \mathrm{d}E = 0$ which combined with $\operatorname{div} \boldsymbol{v} \in \mathbb{P}_{k-1}(E)$ (check (8.8)) and the fact that ($\mathbf{D_3}$) vanish implies $\operatorname{div} \boldsymbol{v} = 0$. As a consequence we can write $\boldsymbol{v} = \mathbf{rot}\, \psi$ for some $\psi \in H_0^1(E)$. As a final preliminary result, we note that, since $\mathrm{rot}\boldsymbol{\Delta v} \in \mathbb{P}_{k-3}$ and due to (8.7), one can write

$$\mathrm{rot}\boldsymbol{\Delta v} = \mathrm{rot}(\boldsymbol{x}^{\perp} q) \,, \qquad q \in \mathbb{P}_{k-3}(E) \,. \tag{8.10}$$

An integration by parts, $\boldsymbol{v}|_{\partial E} = 0$ and $\boldsymbol{v} = \mathbf{rot}\, \psi$ now yields

$$\int_E \nabla \boldsymbol{v} : \nabla \boldsymbol{v} = - \int_E \boldsymbol{v} \cdot \boldsymbol{\Delta v} = - \int_E \mathbf{rot}\, \psi \cdot \boldsymbol{\Delta v} \,,$$

which, combined with integration by parts, $\psi|_{\partial E} = 0$ and (8.10), yields

$$\begin{aligned} \int_E \nabla \boldsymbol{v} : \nabla \boldsymbol{v} &= \int_E \psi \cdot \mathrm{rot}\boldsymbol{\Delta v} = \int_E \psi \cdot \mathrm{rot}(\boldsymbol{x}^{\perp} q) \\ &= - \int_E \mathbf{rot}\, \psi \cdot (\boldsymbol{x}^{\perp} q) = - \int_E \boldsymbol{v} \cdot (\boldsymbol{x}^{\perp} q) = 0, \end{aligned}$$

where the last identity follows from the vanishing ($\mathbf{D_4}$) dofs. The above identity clearly implies $\psi = 0$ and the result follows recalling $\boldsymbol{v} = \mathbf{rot}\, \psi$. □

Remark 8.3. We observe that the degrees of freedom ($\mathbf{D_1}$)-($\mathbf{D_2}$) in (8.9) allow to compute $\boldsymbol{v}$ on the boundary of the element. Furthermore, the combination of the Stokes theorem and ($\mathbf{D_3}$) allow to compute the polynomial $\operatorname{div} \boldsymbol{v} \in \mathbb{P}_{k-1}(E)$. Therefore such two quantities are fully computable.

We next make an important observation. The dofs (8.9) allow to compute exactly (cf. (2.6) and (2.5) and Definition 2.2) the following projection operators:

$$\begin{aligned} &\Pi_k^{\nabla,E} \colon \boldsymbol{V}_k^{\mathrm{S}}(E) \to [\mathbb{P}_k(E)]^2 \,, \\ &\Pi_{k-2}^{0,E} \colon \boldsymbol{V}_k^{\mathrm{S}}(E) \to [\mathbb{P}_{k-2}(E)]^2 \,, \\ &\boldsymbol{\Pi}_{k-1}^{0,E} \colon \boldsymbol{\nabla} \boldsymbol{V}_k^{\mathrm{S}}(E) \to [\mathbb{P}_{k-1}(E)]^{2\times 2} \,. \end{aligned} \tag{8.11}$$

We show here only a proof for the first item, as the last two follow by analogous arguments. Looking at the definition of the H_0^1-projection (2.6) we see that, in order to determine, for any $\boldsymbol{v} \in \boldsymbol{V}_k^{\mathrm{S}}(E)$, the polynomial $\Pi_k^{\nabla,E} \boldsymbol{v}$ we need to compute

$$\int_E \boldsymbol{\nabla v} : \boldsymbol{\nabla p} \qquad \text{for all } \boldsymbol{p} \in [\mathbb{P}_k(E)]^2. \tag{8.12}$$

Employing the polynomial decomposition (8.7) for $\boldsymbol{\Delta}\, \boldsymbol{p} \in [\mathbb{P}_{k-2}(E)]^2$, we can write $\boldsymbol{\Delta}\, \boldsymbol{p} = \nabla q_{k-1} + \boldsymbol{x}^{\perp} q_{k-3}$ for some $q_{k-1} \in \mathbb{P}_{k-1}(E)$ and $q_{k-3} \in \mathbb{P}_{k-3}(E)$. Therefore, integrating by parts we deduce

$$\begin{aligned}\int_E \boldsymbol{\nabla v} : \boldsymbol{\nabla p} &= \int_{\partial E} \boldsymbol{v} \cdot (\boldsymbol{\nabla p})\boldsymbol{n} - \int_E \boldsymbol{v} \cdot \boldsymbol{\Delta p} \\ &= \int_{\partial E} \boldsymbol{v} \cdot (\boldsymbol{\nabla p})\boldsymbol{n} - \int_E \boldsymbol{v} \cdot (\nabla q_{k-1} + \boldsymbol{x}^\perp q_{k-3}) \\ &= \int_{\partial E} \boldsymbol{v} \cdot ((\boldsymbol{\nabla p})\boldsymbol{n} - q_{k-1}\boldsymbol{n}) + \int_E \operatorname{div} \boldsymbol{v}\, q_{k-1} - \int_E \boldsymbol{v} \cdot \boldsymbol{x}^\perp q_{k-3}.\end{aligned}$$

Recalling Remark 8.3 and ($\mathbf{D_4}$) in (8.9), the above identity yields that (8.12) is a computable expression.

We close this section mentioning a drawback of the above space. The properties above show that the degrees of freedom (8.9) allow to compute exactly the L^2-projection $\Pi^{0,E}_{k-2}$ onto $\mathbb{P}_{k-2}$, but not that onto $\mathbb{P}_k$.

Enhanced Virtual Elements

In this section we will apply the *enhancement approach* to define a new (velocity) virtual space $\boldsymbol{V}_k(E)$, to be used in place of the space $\boldsymbol{V}^{\mathrm{S}}_k(E)$, in such a way that the full projection $\Pi^{0,E}_k : \boldsymbol{V}_k(E) \to [\mathbb{P}_k(E)]^2$ is computable from the dofs (8.9), without increasing the dimension of the space nor spoiling other critical properties such as $[\mathbb{P}_k(E)]^2 \subseteq \boldsymbol{V}^{\mathrm{S}}_k(E)$. Such "enhancement approach" was introduced in (Vacca 2018, Beirão da Veiga *et al.* 2018*b*) taking inspiration from (Ahmad *et al.* 2013).

We preliminarily observe that in order to compute $\Pi^{0,E}_k \boldsymbol{v}$ we obviously need to compute

$$\int_E \boldsymbol{v} \cdot \boldsymbol{p}_k \,\mathrm{d}E \qquad \text{for any } \boldsymbol{p}_k \in [\mathbb{P}_k(E)]^2.$$

Using the polynomial decomposition (8.7), let $q_{k+1} \in \mathbb{P}_{k+1}(E)$ and $q_{k-1} \in \mathbb{P}_{k-1}(E)$ be such that $\boldsymbol{p}_k = \nabla q_{k+1} + \boldsymbol{x}^\perp q_{k-1}$. Then, using this and integrating by parts we have

$$\begin{aligned}\int_E \boldsymbol{v} \cdot \boldsymbol{p}_k \,\mathrm{d}E &= \int_E \boldsymbol{v} \cdot (\nabla q_{k+1} + \boldsymbol{x}^\perp q_{k-1})\,\mathrm{d}E \\ &= \int_{\partial E} \boldsymbol{v} \cdot \boldsymbol{n}\, q_{k+1}\,\mathrm{d}s - \int_E \operatorname{div} \boldsymbol{v}\, q_{k+1}\,\mathrm{d}E + \int_E \boldsymbol{v} \cdot \boldsymbol{x}^\perp q_{k-1}\,\mathrm{d}E.\end{aligned} \tag{8.13}$$

The last integral is not computable, since the dofs ($\mathbf{D_4}$) in (8.9) allow to compute $\int_E \boldsymbol{v} \cdot \boldsymbol{x}^\perp q$ only for polynomials $q \in \mathbb{P}_{k-3}(E)$ and not for $q \in \mathbb{P}_{k-1}(E)$.

Therefore, in order to construct $\boldsymbol{V}_k(E)$ we proceed as in the previous sections for the simpler Laplace problem: we first enlarge the space in order to have the computability of the missing moments, and then we introduce the so-called "enhanced constraints" to recover the right dimension of the space.

We then first introduce, on each element $E \in \mathcal{T}_h$, the augmented space

$$\boldsymbol{W}_k(E) := \{\boldsymbol{v} \in [C^0(\overline{E})]^2 \text{ such that } \mathrm{rot}\boldsymbol{\Delta v} \in \mathbb{P}_{k-1}(E),\ \ \mathrm{div}\, \boldsymbol{v} \in \mathbb{P}_{k-1}(E), \\ \boldsymbol{v}_{|\mathrm{e}} \in [\mathbb{P}_k(\mathrm{e})]^2 \ \ \forall \mathrm{e} \subset \partial E\}. \tag{8.14}$$

The degrees of freedom in $\boldsymbol{W}_k(E)$ will be, referring to (8.9),

$$(\mathbf{D_1}) - (\mathbf{D_2}) - (\mathbf{D_3}) \quad \text{plus} \quad (\mathbf{D_5}): \int_E \boldsymbol{v} \cdot \boldsymbol{x}^{\perp} p \,\mathrm{d}E \quad \forall p \in \mathbb{P}_{k-1}(E). \tag{8.15}$$

Although the space $\boldsymbol{W}_k(E)$ has the right computability and approximation properties, it has too many degrees of freedom. We therefore reduce it and introduce the *"enhanced"* VEM velocity space. We recall that, for any non negative integers $m \le n$, we denoted by $\mathbb{P}_{n/m}$ any subspace (fixed once and for all) of $\mathbb{P}_n$ such that

$$\mathbb{P}_n = \mathbb{P}_m \oplus \mathbb{P}_{n/m}.$$

We define:

$$\boldsymbol{V}_k(E) := \{\boldsymbol{v} \in [C^0(\overline{E})]^2 \text{ s. t. } \boldsymbol{v}_{|\mathrm{e}} \in [\mathbb{P}_k(\mathrm{e})]^2 \ \ \forall \mathrm{e} \subset \partial E,\ \mathrm{rot}\boldsymbol{\Delta v} \in \mathbb{P}_{k-1}(E), \\ \mathrm{div}\, \boldsymbol{v} \in \mathbb{P}_{k-1}(E),\ \int_E (\boldsymbol{v} - \Pi_k^{\nabla,E}\boldsymbol{v}) \cdot \boldsymbol{x}^{\perp} p \,\mathrm{d}E = 0 \ \ \forall p \in \mathbb{P}_{k-1/k-3}(E)\}. \tag{8.16}$$

We point out that the important property

$$[\mathbb{P}_k(E)]^2 \subseteq \boldsymbol{V}_k(E)$$

still holds.

Furthermore, we show that as dofs in $\boldsymbol{V}_k(E)$ we can take the same dofs set (8.9) introduced for $\boldsymbol{V}_k^{\mathrm{S}}(E)$.

Property 8.4. The degrees of freedom (8.9) are unisolvent for $\boldsymbol{V}_k(E)$.

Proof. A simple computation, following the same argument as in the previous section, easily shows that

$$\dim(\boldsymbol{W}_k(E)) = 2k\, N_{\mathrm{e}} + \frac{k(k+1)}{2} + \frac{k(k+1)}{2} - 1 = \dim(\boldsymbol{V}_k^{\mathrm{S}}(E)) + \dim(\mathbb{P}_{k-1/k-3}(E)).$$

Since $\boldsymbol{V}_k(E)$ is obtained from $\boldsymbol{W}_k(E)$ by enforcing $\dim(\mathbb{P}_{k-1/k-3}(E))$ linear constraints, from the above identity we immediately obtain

$$\dim(\boldsymbol{V}_h(E)) \ge \dim(\boldsymbol{V}_k^{\mathrm{S}}(E)).$$

Therefore, since the number of dofs in (8.9) is equal to $\dim(\boldsymbol{V}_k^{\mathrm{S}}(E))$, the proof is concluded if we show that any $\boldsymbol{v} \in \boldsymbol{V}_k(E)$ that vanishes on all dofs (8.9) must satisfy $\boldsymbol{v} = 0$. A key observation is the fact that the operator

$$\Pi_k^{\nabla,E} : \boldsymbol{W}_k(E) \to [\mathbb{P}_k(E)]^2\,,$$

only depends on (8.9); the proof is identical to that shown for $\boldsymbol{V}_k^{\mathrm{S}}(E)$ at the end of the previous section. As a consequence, since $\boldsymbol{v}$ vanishes on all linear operators (8.9), it holds $\Pi_k^{\nabla,E}(\boldsymbol{v}) = 0$. Therefore, from the definition of $\boldsymbol{V}_k(E)$, we also have

$$\int_E \boldsymbol{v} \cdot \boldsymbol{x}^\perp p \, \mathrm{d}E = 0 \qquad \forall p \in \mathbb{P}_{k-1/k-3}(E).$$

The combination of the above equation and the fact that ($\mathbf{D_4}$) in (8.9) vanish for $\boldsymbol{v}$ imply that the full enlarged operator set (8.15) vanishes for $\boldsymbol{v}$. The proof is concluded recalling that $\boldsymbol{v} \in \boldsymbol{V}_h(E) \subseteq \boldsymbol{W}_k(E)$ and that (8.15) is a set of unisolvent dofs for $\boldsymbol{W}_k(E)$. □

Finally, we have the following important result.

Property 8.5. The degrees of freedom (8.9) allow us to compute exactly (cf. (2.5))

$$\Pi_k^{0,E} : \boldsymbol{V}_k(E) \to [\mathbb{P}_k(E)]^2.$$

Proof. We start from equation (8.13) and observe that the first two terms on the right hand side are computable thanks to Remark 8.3, which clearly holds also for the new space $\boldsymbol{V}_k(E)$. We therefore are left with the third term $\int_E \boldsymbol{v} \cdot \boldsymbol{x}^\perp q_{k-1}$ which we split as

$$\int_E \boldsymbol{v} \cdot \boldsymbol{x}^\perp q_{k-1} \, \mathrm{d}E = \int_E \boldsymbol{v} \cdot \boldsymbol{x}^\perp p_{k-3} \, \mathrm{d}E + \int_E \boldsymbol{v} \cdot \boldsymbol{x}^\perp \widetilde{p} \, \mathrm{d}E$$

with $p_{k-3} \in \mathbb{P}_{k-3}(E)$ and $\widetilde{p} \in \mathbb{P}_{k-1/k-3}$. The first term above is computable from $\mathbf{D_4}$ and the second one follows from the property built in the definition of the space (8.16):

$$\int_E \boldsymbol{v} \cdot \boldsymbol{x}^\perp \widetilde{p} \, \mathrm{d}E = \int_E \Pi_k^{\nabla,E}(\boldsymbol{v}) \cdot \boldsymbol{x}^\perp \widetilde{p} \, \mathrm{d}E.$$

□

8.3. Virtual Element Spaces in 3D

The aim of this section is to present the divergence-free Virtual Element spaces in three dimensions. This is the natural extension of the 2D VEM of Section 3 combined with the ideas introduced for the 3D Laplace operators in Section 3.8. We will keep our exposition rather brief and refer the reader to (Beirão da Veiga *et al.* 2018*a*) for further details. As in the previous section, we here focus on the **velocity** space and work locally on the element.

As in Section 3.8, in order to define the **velocity** VEM space in 3D we proceed in two steps: we first introduce suitable VEM spaces related to the faces of the element, then we define the local spaces defined on the polyhedron.

Let as before $k \in \mathbb{N}$, $k \geq 2$ (for the lowest order case $k = 1$, that falls outside the current family, we refer for instance to the velocity space introduced in (Beirão da

Veiga *et al.* 2022*a*)). We define on each face f of an element $P \in \mathcal{T}_h$ the (scalar) face space

$$V_k(\mathrm{f}) := \{v \in C^0(\bar{\mathrm{f}}) \text{ such that } \Delta_2 v \in \mathbb{P}_{k+1}(\mathrm{f}),\ v_{|\mathrm{e}} \in \mathbb{P}_k(\mathrm{e})\ \ \forall \mathrm{e} \subset \partial \mathrm{f}$$
$$\int_{\mathrm{f}} (v - \Pi_k^{\nabla,\mathrm{f}} v)\, p \,\mathrm{df} = 0\ \ \forall p \in \mathbb{P}_{k+1/k-2}(\mathrm{f})\}. \tag{8.17}$$

Note that the space $V_k(\mathrm{f})$ is slightly different from that introduced in Section 3.8 for the Laplace problem, since the "enhancement" is here even more extreme; the reason for this choice will be clear in what follows. One can easily see that $V_k(\mathrm{f})$ satisfies $\mathbb{P}_k(\mathrm{f}) \subseteq V_k(\mathrm{f})$ and that a set of degrees of freedom for $V_k(F)$ is

$$\begin{aligned}
&(\mathbf{D_1}): \text{ the values of } v \text{ at the vertexes of the face f;}\\
&(\mathbf{D_2}): \text{ the edge moments } \int_{\mathrm{e}} v p \,\mathrm{de} \quad \forall p \in \mathbb{P}_{k-2}(\mathrm{e}), \forall \mathrm{e} \subset \partial \mathrm{f};\\
&(\mathbf{D_3}): \text{ the moments } \int_{\mathrm{f}} v p \,\mathrm{df} \quad \forall p \in \mathbb{P}_{k-2}(\mathrm{f}).
\end{aligned} \tag{8.18}$$

Furthermore, with arguments similar to those used in Section 3, one can check that the L^2 projection operator

$$\Pi_{k+1}^{0,\mathrm{f}} : V_k(\mathrm{f}) \to \mathbb{P}_{k+1}(\mathrm{f}) \tag{8.19}$$

is computable on the basis of the dofs (8.18). Note that thanks to the particular definition of $V_k(F)$ we are able to compute the projection in the richer space $\mathbb{P}_{k+1}(F)$.

We are now able to present the 3D VEM "divergence-free" space for velocities; we here present directly the more advanced space, suitable for both the Stokes and the Navier-Stokes problems.

$$\begin{aligned}
\boldsymbol{V}_k(P) := \{ &\boldsymbol{v} \in [C^0(P)]^3 \text{ s. t. } \mathbf{curl}\boldsymbol{\Delta v} \in [\mathbb{P}_{k-1}(P)]^3, \ \operatorname{div} \boldsymbol{v} \in \mathbb{P}_{k-1}(P),\\
&\boldsymbol{v}_{|\mathrm{f}} \subset [V_k(\mathrm{f})]^3 \ \ \forall \mathrm{f} \in \partial P,\\
&\int_P (\boldsymbol{v} - \Pi_k^{\nabla,P} \boldsymbol{v}) \cdot (\boldsymbol{x} \wedge \boldsymbol{p})\, \mathrm{d}P = 0 \ \ \forall \boldsymbol{p} \in [\mathbb{P}_{k-1/k-3}(P)]^3 \}.
\end{aligned} \tag{8.20}$$

The second line of (8.20) defines the space $\boldsymbol{V}_k(P)$ on the boundary of the element. The first line states that the virtual functions are obtained solving a Stokes-like problem in the element. Indeed, recalling (8.7) it can be checked that the condition $\mathbf{curl}\boldsymbol{\Delta v} \in \mathbb{P}_{k-1}$ is equivalent to the existence of $\boldsymbol{q} \in \mathbb{P}_{k-1}(P)$ such that $\boldsymbol{\Delta v} + \nabla s = \boldsymbol{x} \wedge \boldsymbol{q}$ for some $s \in L^2_0(P)$; such equation, combined with the condition $\operatorname{div} \boldsymbol{v} \in \mathbb{P}_{k-1}(P)$ in (8.8), represents a Stokes-like problem on the element. Finally, the last condition represents an "enhancement" constraint.

It is easy to check that $[\mathbb{P}_k(P)]^3 \subseteq \boldsymbol{V}_k(P)$. Furthermore, with arguments similar to the previous sections, one can show that the following linear operators constitute a set of unisolvent degrees of freedom for the space $\boldsymbol{V}_k(P)$:

$$
\begin{aligned}
&(\mathbf{D_1}) : \text{the values of } \boldsymbol{v} \text{ at the vertexes of the polyhedron } P;\\
&(\mathbf{D_2}) : \text{the moments } \textstyle\int_{\mathrm{e}} \boldsymbol{v}\cdot\boldsymbol{p}\,\mathrm{de} \quad \forall \boldsymbol{p}\in[\mathbb{P}_{k-2}(\mathrm{e})]^3\ \forall \text{ edge e} \subset \partial P;\\
&(\mathbf{D_3}) : \text{the face moments } \textstyle\int_{\mathrm{f}} \boldsymbol{v}\cdot\boldsymbol{p}\,\mathrm{df} \quad \forall \boldsymbol{p}\in[\mathbb{P}_{k-2}(\mathrm{f})]^3;\\
&(\mathbf{D_4}) : \text{the moments of div } \boldsymbol{v} : \textstyle\int_P(\mathrm{div}\,\boldsymbol{v})p\,\mathrm{d}P \quad \forall p\in\mathbb{P}^0_{k-1}(P)\,;\\
&(\mathbf{D_5}) : \text{for } k\geq 3, \text{ the ``moments'' of } \textstyle\int_P \boldsymbol{v}\cdot(\boldsymbol{x}\wedge\boldsymbol{p})\,\mathrm{d}P \quad \forall \boldsymbol{p}\in[\mathbb{P}_{k-3}(P)]^3\,.
\end{aligned}
\tag{8.21}
$$

Another critical property is that the 3-dimensional versions of the projections in (8.11) are computable on the space $\boldsymbol{V}_k(P)$. We here show only the proof for

$$\Pi_k^{0,P} : \boldsymbol{V}_k(P) \to [\mathbb{P}_k(P)]^3,$$

and observe that in order to compute $\Pi_k^{0,E}\boldsymbol{v}$ we need to compute

$$\int_P \boldsymbol{v}\cdot\boldsymbol{p}\,\mathrm{d}P \qquad \text{for any } \boldsymbol{p}\in[\mathbb{P}_k(P)]^3.$$

Using (8.7), let $q_{k+1}\in\mathbb{P}_{k+1}(P)$ and $\boldsymbol{q}_{k-1}\in[\mathbb{P}_{k-1}(P)]^3$ be such that $\boldsymbol{p} = \nabla q_{k+1} + \boldsymbol{x}\wedge\boldsymbol{q}_{k-1}$. In turn, the polynomial $\boldsymbol{q}_{k-1}$ can be split as $\boldsymbol{q}_{k-1} = \boldsymbol{q}_{k-3} + \widetilde{\boldsymbol{q}}_{k-1}$, with $\boldsymbol{q}_{k-3}\in[\mathbb{P}_{k-3}(P)]^3$ and $\widetilde{\boldsymbol{q}}_{k-1}\in[\mathbb{P}_{k-1/k-3}(P)]^3$. By an argument analog to that used in the 2D case, it is easy to check that div $\boldsymbol{v}\in\mathbb{P}_{k-1}(P)$ is computable using the above dofs. Then, an integration by parts and trivial steps yield

$$
\begin{aligned}
\int_P \boldsymbol{v}\cdot\boldsymbol{p}_k dP &= \int_P \boldsymbol{v}\cdot(\nabla q_{k+1} + \boldsymbol{x}\wedge\boldsymbol{q}_{k-1})\,\mathrm{d}P\\
&= \sum_{\mathrm{f}\subset\partial P}\int_{\mathrm{f}} \boldsymbol{v}\cdot\boldsymbol{n}\,q_{k+1}\,\mathrm{df} - \int_P \mathrm{div}\,\boldsymbol{v}\,q_{k+1}\,\mathrm{d}P + \int_P \boldsymbol{v}\cdot(\boldsymbol{x}\wedge\boldsymbol{q}_{k-1})\,\mathrm{d}P\\
&= \sum_{\mathrm{f}\subset\partial P}\int_{\mathrm{f}} \Pi^{0,\mathrm{f}}_{k+1}\boldsymbol{v}\cdot\boldsymbol{n}\,q_{k+1}\,\mathrm{df} - \int_P \mathrm{div}\,\boldsymbol{v}\,q_{k+1}\,\mathrm{d}P\\
&\quad + \int_P \boldsymbol{v}\cdot(\boldsymbol{x}\wedge\boldsymbol{q}_{k-3})\,\mathrm{d}P + \int_P \Pi^{\nabla,P}_k\boldsymbol{v}\cdot(\boldsymbol{x}\wedge\widetilde{\boldsymbol{q}}_{k-1})\,\mathrm{d}P.
\end{aligned}
\tag{8.22}
$$

All the above terms are computable. The first one since $\Pi^{0,\mathrm{f}}_{k+1}\boldsymbol{v}$ is computable on each face (see (8.19)), the second one since div $\boldsymbol{v}$ is known and computable, the third one using $(\mathbf{D_5})$ in (8.21) and the fourth one since $\Pi^{\nabla,P}_k\boldsymbol{v}$ is computable. Note that the first term motivates the need for the particular definition used in (8.17).

8.4. The discrete VEM problem

Let $\mathcal{T}_h$ be a decomposition of the domain $\Omega\subset\mathbb{R}^d$ with $d = 2, 3$ into general polytopal elements. In order to keep the same exposition in 2D and 3D, we will here indicate the generic element with the letter E (thus representing a polygon if $d = 2$ and a polyhedron if $d = 3$).

For any $E \in \mathcal{T}_h$, let $\boldsymbol{V}_k(E)$ denote one of the enhanced velocity VEM spaces introduced in the previous sections ((8.16) in 2D, (8.20) in 3D, respectively). The global velocity VEM space is defined by

$$\boldsymbol{V}_h := \{\boldsymbol{v} \in \boldsymbol{V} \ \text{ such that } \ \boldsymbol{v}_{|E} \in \boldsymbol{V}_k(E) \ \text{ for all } E \in \mathcal{T}_h\}\,, \tag{8.23}$$

and the global dofs are given by standard dofs assembly as in FEM. The discrete pressure space is given by the piecewise polynomial functions of degree $k-1$, i.e., the local and global pressure spaces are simply given by

$$\begin{aligned} &Q_h(E) := \mathbb{P}_{k-1}(E) \qquad \forall E \in \mathcal{T}_h\,, \\ &Q_h := \{q \in Q \quad \text{s.t.} \quad q_{|E} \in Q_h(E) \quad \text{for all } E \in \mathcal{T}_h\}\,. \end{aligned} \tag{8.24}$$

We recall the following results stating some interpolation properties of the velocity space (see Proposition 4.2. in (Beirão da Veiga *et al.* 2017) and Theorem 4.1 in (Beirão da Veiga *et al.* 2018*b*)) and the inf-sup stability of the pair $(\boldsymbol{V}_h, Q_h)$ (see Proposition 4.3 in (Beirão da Veiga *et al.* 2017)).

Proposition 8.6. Under the mesh assumption 2.1, let $\boldsymbol{v} \in [H^s(\mathcal{T}_h)]^d$ with $1 < s \leq k+1$. Then there exists $\boldsymbol{v}_h \in \boldsymbol{V}_h$ such that

$$\|\boldsymbol{v} - \boldsymbol{v}_h\|_0 + h\|\boldsymbol{\nabla}\boldsymbol{v} - \boldsymbol{\nabla}\boldsymbol{v}_h\|_0 \lesssim h^s\, |\boldsymbol{v}|_{s,\mathcal{T}_h}$$

where the hidden constant depends only on k and the shape regularity constant ϱ.

Proposition 8.7. Given the discrete spaces $\boldsymbol{V}_h$ and Q_h defined in (8.23) and (8.24) respectively, there exists a positive constant $\widehat{\beta}$, independent of h, such that

$$\sup_{\boldsymbol{v}_h \in \boldsymbol{V}_h,\ \boldsymbol{v}_h \neq \boldsymbol{0}} \frac{b(\boldsymbol{v}_h, q_h)}{\|\boldsymbol{\nabla}\boldsymbol{v}_h\|_0} \geq \widehat{\beta}\, \|q_h\|_0 \qquad \text{for all } q_h \in Q_h.$$

We now define computable discrete local forms, following a construction similar to that shown in Section 3.7:

$$a_h^E(\boldsymbol{u},\, \boldsymbol{v}) := \int_E \left(\boldsymbol{\Pi}_{k-1}^{0,E}\boldsymbol{\varepsilon}(\boldsymbol{u})\right) : \left(\boldsymbol{\Pi}_{k-1}^{0,E}\boldsymbol{\varepsilon}(\boldsymbol{v})\right)\, \mathrm{d}E + \mathcal{S}^E\left((I - \Pi_k^{0,E})\boldsymbol{u},\, (I - \Pi_k^{0,E})\boldsymbol{v}\right)\,, \tag{8.25}$$

$$c_h^{o,E}(\boldsymbol{w};\, \boldsymbol{u}, \boldsymbol{v}) := \int_E \left[\left(\boldsymbol{\Pi}_{k-1}^{0,E}\boldsymbol{\nabla}\,\boldsymbol{u}\right)\, \Pi_k^{0,P}\boldsymbol{w}\right] \cdot \Pi_k^{0,E}\boldsymbol{v}\, \mathrm{d}E\,, \tag{8.26}$$

$$c_h^{\mathrm{skew},E}(\boldsymbol{w};\, \boldsymbol{u}, \boldsymbol{v}) := \frac{1}{2}\left(c_h^{o,E}(\boldsymbol{w};\, \boldsymbol{u}, \boldsymbol{v}) - c_h^{o,E}(\boldsymbol{w};\, \boldsymbol{v}, \boldsymbol{u})\right)\,, \tag{8.27}$$

for all $\boldsymbol{w}, \boldsymbol{u}, \boldsymbol{v} \in \boldsymbol{V}_h(E)$, where clearly

$$\boldsymbol{\Pi}_k^{0,E}\boldsymbol{\varepsilon}(\boldsymbol{v}) = \frac{\boldsymbol{\Pi}_k^{0,E}\boldsymbol{\nabla}\,\boldsymbol{v} + (\boldsymbol{\Pi}_k^{0,E}\boldsymbol{\nabla}\,\boldsymbol{v})^{\mathrm{T}}}{2}$$

and the symmetric stabilizing form $\mathcal{S}^E \colon \boldsymbol{V}_h(E) \times \boldsymbol{V}_h(E) \to \mathbb{R}$ satisfies

$$\|\boldsymbol{\nabla}\boldsymbol{v}\|_{0,E}^2 \lesssim \mathcal{S}^E(\boldsymbol{v},\, \boldsymbol{v}) \lesssim \|\boldsymbol{\nabla}\boldsymbol{v}\|_{0,E}^2 \qquad \text{for all } \boldsymbol{v} \in \boldsymbol{V}_h(E) \cap \mathrm{Ker}(\Pi_k^{0,E}). \tag{8.28}$$

The condition above essentially requires the stabilizing term $\mathcal{S}^E(\boldsymbol{v}, \boldsymbol{v})$ to scale as $\|\boldsymbol{\nabla v}\|^2_{0,E}$. Possible choices for the stabilization are the same already discussed in Section 3.3.

The global virtual forms are defined by simply summing the local contributions:

$$a_h(\boldsymbol{u}, \boldsymbol{v}) := \sum_{E \in \mathcal{T}_h} a_h^E(\boldsymbol{u}, \boldsymbol{v}), \quad c_h(\boldsymbol{w}; \boldsymbol{u}, \boldsymbol{v}) := \sum_{E \in \mathcal{T}_h} c_h^{\text{skew},E}(\boldsymbol{w}; \boldsymbol{u}, \boldsymbol{v}), \tag{8.29}$$

for all $\boldsymbol{w}, \boldsymbol{u}, \boldsymbol{v} \in \boldsymbol{V}_h$. We point out that

- the symmetry of $a_h(\cdot, \cdot)$ together with (8.28) easily implies that $a_h(\cdot, \cdot)$ is continuous and coercive with respect to the H^1-norm;
- the discrete trilinear form $c_h(\cdot; \cdot, \cdot)$ is skew-symmetric and is continuous with respect to the H^1-norm.

Finally the discrete right hand side is defined by the computable quantity

$$(\boldsymbol{f}_h, \boldsymbol{v}) := \sum_{E \in \mathcal{T}_h} \int_E \Pi_k^{0,E} \boldsymbol{f} \cdot \boldsymbol{v} \, \mathrm{d}E = \sum_{E \in \mathcal{T}_h} \int_E \boldsymbol{f} \cdot \Pi_k^{0,E} \boldsymbol{v} \, \mathrm{d}E \quad \text{for all } \boldsymbol{v} \in \boldsymbol{V}_h \,. \tag{8.30}$$

Referring to the discrete spaces (8.23), (8.24), the discrete forms (8.29), the $b(\cdot, \cdot)$ form in (8.3) and the approximated load term (8.30), the virtual element approximation of the Navier-Stokes equation is given by

$$\begin{cases} \text{find } (\boldsymbol{u}_h, \, p_h) \in \boldsymbol{V}_h \times Q_h, \text{ such that} \\ \nu \, a_h(\boldsymbol{u}_h, \, \boldsymbol{v}_h) + c_h(\boldsymbol{u}_h; \, \boldsymbol{u}_h, \boldsymbol{v}_h) + b(\boldsymbol{v}_h, \, p_h) = (\boldsymbol{f}_h, \, \boldsymbol{v}_h) & \text{for all } \boldsymbol{v}_h \in \boldsymbol{V}_h, \\ b(\boldsymbol{u}_h, \, q_h) = 0 & \text{for all } q_h \in Q_h. \end{cases} \tag{8.31}$$

A crucial observation is that definitions (8.23) and (8.24), along with Proposition 8.7, imply that $\operatorname{div} \boldsymbol{V}_h = Q_h$. Therefore the discrete kernel is a subspace of the continuous kernel $\boldsymbol{Z}$ (cf. (8.4)):

$$\boldsymbol{Z}_h := \{\boldsymbol{v}_h \in \boldsymbol{V}_h \ \text{ such that } \ b(\boldsymbol{v}_h, q_h) = 0 \ \text{ for all } q_h \in Q_h\} \subseteq \boldsymbol{Z} \,. \tag{8.32}$$

Consequently, the second equation of (8.31) implies that the discrete velocity $\boldsymbol{u}_h \in \boldsymbol{V}_h$ is **exactly divergence-free**.

The well-posedness of the discrete problems is stated in the following theorem.

Theorem 8.8. Let $\widehat{C}$ represent the continuity constant of the form $c_h(\cdot; \cdot, \cdot)$ in Z_h. Under the data assumption

$$\widehat{\gamma} := \frac{\widehat{C} \, \|\boldsymbol{f}_h\|_{\boldsymbol{Z}_h'}}{\widehat{\alpha}^2 \nu^2} < 1 \,, \tag{8.33}$$

with the usual definition of dual norm, Problem (8.31) is well-posed.

8.5. Convergence results and exploring the divergence-free property

We here briefly underline the main benefits of the proposed VEM scheme, in addition to the capability (shared by any VEM scheme) of using general polytopal meshes. The divergence-free property and the kernel inclusion (8.32) entail a range of advantages:

- The error components partly decouple, as shown in the converge results below. Namely the influence of the pressure in the velocity error is weaker with respect to standard inf-sup stable elements (see (Beirão da Veiga *et al.* 2018*b*));
- the scheme in (8.31) is equivalent to a suitable reduced problem. The internal divergence-moments dofs (**D₃** in (8.18) for $d = 2$, **D₄** in (8.21) for $d = 3$) and the associated pressures dofs can be automatically ignored in the final linear system (see (Beirão da Veiga *et al.* 2017));
- the proposed Virtual Element enjoys an underlying discrete Stokes complex structure (see (Beirão da Veiga *et al.* 2019*b*, Beirão da Veiga *et al.* 2018*a*));
- the space $\boldsymbol{V}_h$ is uniformly stable also for the Darcy equation (see (Vacca 2018)).

We finally state a convergence result for the proposed Virtual Element scheme (8.31). We refer to Theorem 4.6 in (Beirão da Veiga *et al.* 2018*b*) for the proof.

Proposition 8.9. Under the assumptions (8.6), (8.33) and 2.1, let $(\boldsymbol{u},\ p) \in \boldsymbol{V} \times Q$ be the solution of Problem (8.2) and $(\boldsymbol{u}_h,\ p_h) \in \boldsymbol{V}_h \times Q_h$ be the solution of Problem (8.31). Assuming that $\boldsymbol{u}$ and $\boldsymbol{f}$ belong to $[H^{k+1}(\mathcal{T}_h)]^d$ and $p \in H^k(\mathcal{T}_h)$ we have

$$\|\boldsymbol{u} - \boldsymbol{u}_h\|_1 \leq\ h^k \chi_1(\boldsymbol{u}) +\ h^{k+2} \chi_2(\boldsymbol{f})\,, \tag{8.34}$$

$$\|p - p_h\|_0 \leq\ h^k \chi_3(p) +\ h^k \chi_4(\boldsymbol{u}) +\ h^{k+2} \chi_5(\boldsymbol{f})\,. \tag{8.35}$$

where the χ_i, $i = 1, .., 5$ are suitable functions independent of h (but which may depend on the material parameters, k and ϱ).

Note that the velocity error does not depend directly on the discrete pressures, but only indirectly through the presence of the *higher order* loading term in (8.34). Indeed, the velocity error of classical mixed FE methods would have an additional term, of order $O(h^k)$, depending on the exact pressure p. In some situations the partial decoupling of the errors stated in (8.34) induces a positive effect on the velocity approximation.

Remark 8.10. In the context of the approximation of the Navier–Stokes equation, a numerical method is said to be pressure-robust (see e.g. (John *et al.* 2017)) if the discrete velocity solution depends only on the Helmholtz–Hodge projector of the load $\boldsymbol{f}$ (as it happens for the exact velocity field). For instance, if the load is a gradient field then the continuous velocity vanishes, and the discrete velocity computed with a pressure-robust method vanishes as well. Thus method (8.31) is not pressure-robust, as it does not guarantee such property. On the other hand the dependence on the full load is much weaker with respect to standard mixed schemes thus leading, for instance, to a higher rate of convergence whenever the load is a gradient. Modified schemes have been proposed in (Liu *et al.* 2020, Frerichs and

Merdon 2022) in order to get a fully pressure-robust VEM scheme. Such approaches have the drawback of requiring a suitable Raviart-Thomas interpolation of the test functions with respect to a sub-triangulation of the mesh $\mathcal{T}_h$.

References

R. A. Adams (1975), *Sobolev spaces*, Vol. 65 of Pure and Applied Mathematics, Academic Press, New York-London.

J. Aghili and D. A. Di Pietro (2018), An Advection-Robust Hybrid High-Order Method for the Oseen Problem, *J. Sci. Comput.* **77**(3), 1310–1338.

B. Ahmad, A. Alsaedi, F. Brezzi, L. D. Marini and A. Russo (2013), Equivalent projectors for Virtual Element Methods, *Comput. Math. Appl.* **66**(3), 376–391.

P. F. Antonietti, L. Beirão da Veiga, D. Mora and M. Verani (2014), A stream virtual element formulation of the Stokes problem on polygonal meshes, *SIAM J. Numer. Anal.* **52**(1), 386–404.

P. F. Antonietti, L. Beirão da Veiga, S. Scacchi and M. Verani (2016), A C^1 Virtual Element Method for the Cahn-Hilliard equation with polygonal meshes, *SIAM J. Numer. Anal.* **54**(1), 34–57.

P. F. Antonietti, G. Manzini and M. Verani (2018), The fully nonconforming Virtual Element Method for biharmonic problems, *Math. Models Methods Appl. Sci.* **28**(2), 387–407.

P. F. Antonietti, L. Mascotto, M. Verani and S. Zonca (2022), Stability analysis of polytopic Discontinuous Galerkin approximations of the Stokes problem with applications to fluid-structure interaction problems, *Journal of Scientific Computing* **90**, Article number: 23.

P. F. Antonietti, M. Verani, C. Vergara and S. Zonca (2019), Numerical solution of fluid-structure interaction problems by means of a high order Discontinuous Galerkin method on polygonal grids, *Finite Elements in Analysis and Design* **159**, 1–14.

D. N. Arnold and G. Awanou (2011), The serendipity family of finite elements, *Found. Comput. Math.* **11**(3), 337–344.

D. N. Arnold, D. Boffi and R. S. Falk (2002), Approximation by quadrilateral finite elements, *Math. Comp.* **71**(239), 909–922.

D. N. Arnold, F. Brezzi, B. Cockburn and L. D. Marini (2001), Unified analysis of discontinuous Galerkin methods for elliptic problems, *SIAM J. Numer. Anal.* **39**(5), 1749–1779.

D. N. Arnold, R. S. Falk and R. Winther (2006*a*), Differential complexes and stability of finite element methods. I. The de Rham complex, in *Compatible spatial discretizations*, Vol. 142 of IMA Vol. Math. Appl., Springer, New York, pp. 24–46.

D. N. Arnold, R. S. Falk and R. Winther (2006*b*), Finite element exterior calculus, homological techniques, and applications, *Acta Numer.* **15**, 1–155.

E. Artioli, L. Beirão da Veiga, C. Lovadina and E. Sacco (2017*a*), Arbitrary order 2D Virtual Elements for polygonal meshes: Part I, elastic problem, *Computational Mechanics* **60**, 355–377.

E. Artioli, L. Beirão da Veiga, C. Lovadina and E. Sacco (2017*b*), Arbitrary order 2D Virtual Elements for polygonal meshes: Part II, inelastic problem, *Computational Mechanics* **60**, 643–657.

E. Artioli, S. de Miranda, C. Lovadina and L. Patruno (2018), A family of Virtual Element Methods for plane elasticity problems based on the Hellinger–Reissner principle, *Comput. Methods Appl. Mech. Engrg.* **340**, 978–999.

E. Artioli, S. Marfia and E. Sacco (2020), VEM-based tracking algorithm for cohesive/frictional 2d fracture, *Comp. Meth. Appl. Mech. Engnrg.* **365**, 112956.

G. Auchmuty and J. C. Alexander (2001), L^2 well-posedness of planar div-curl systems, *Arch. Ration. Mech. Anal.* **160**(2), 91–134.

G. Auchmuty and J. C. Alexander (2005), L^2-well-posedness of 3D div-curl boundary value problems, *Quart. Appl. Math.* **63**(3), 479–508.

B. Ayuso de Dios, K. Lipnikov and G. Manzini (2016), The nonconforming Virtual Element Method, *ESAIM Math. Model. Numer. Anal.* **50**(3), 879–904.

L. Beirão da Veiga, F. Dassi and G. Vacca (2018*a*), The Stokes complex for Virtual Elements in three dimensions, *Math. Models Methods Appl. Sci.* **30**(3), 477–512.

L. Beirão da Veiga, F. Dassi, G. Manzini and L. Mascotto (2022*a*), The Virtual Element Method for the 3D Resistive Magnetohydrodynamic model, ArXiv 2201.04417v1 [Math NA], submitted for publication.

L. Beirão da Veiga, F. Dassi, G. Manzini and L. Mascotto (2022*b*), Virtual elements for Maxwell's equations, *Computers & Mathematics with Applications* **116**, 82–99.

L. Beirão da Veiga, C. Lovadina and G. Vacca (2017), Divergence free Virtual Elements for the Stokes problem on polygonal meshes, *ESAIM Math. Model. Numer. Anal.* **51**(2), 509–535.

L. Beirão da Veiga, C. Lovadina and G. Vacca (2018*b*), Virtual elements for the Navier-Stokes problem on polygonal meshes, *SIAM J. Numer. Anal.* **56**(3), 1210–1242.

L. Beirao da Veiga and K. Lipnikov (2010), A mimetic discretization of the Stokes Problem with Selected Edge Bubbles, *SIAM J. Sci. Comput.* **32**, 875–893.

L. Beirão da Veiga and L. Mascotto (2022), Interpolation and stability properties of low-order face and edge virtual element spaces, *IMA Journal of Numerical Analysis*. drac008.

L. Beirão da Veiga, F. Brezzi and L. D. Marini (2013*a*), Virtual elements for linear elasticity problems, *SIAM J. Numer. Anal.* **51**(2), 794–812.

L. Beirão da Veiga, F. Brezzi, A. Cangiani, G. Manzini, L. D. Marini and A. Russo (2013*b*), Basic principles of Virtual Element Methods, *Math. Models Methods Appl. Sci.* **23**(1), 199–214.

L. Beirão da Veiga, F. Brezzi, F. Dassi, L. D. Marini and A. Russo (2017*a*), Virtual Element approximation of 2D magnetostatic problems, *Comput. Methods Appl. Mech. Engrg.* **327**, 173–195.

L. Beirão da Veiga, F. Brezzi, F. Dassi, L. D. Marini and A. Russo (2018*a*), A family of three-dimensional Virtual Elements with applications to magnetostatics, *SIAM J. Numer. Anal.* **56**(5), 2940–2962.

L. Beirão da Veiga, F. Brezzi, F. Dassi, L. D. Marini and A. Russo (2018*b*), Lowest order Virtual Element approximation of magnetostatic problems, *Comput. Methods Appl. Mech. Engrg.* **332**, 343–362.

L. Beirão da Veiga, F. Brezzi, L. D. Marini and A. Russo (2014), The hitchhiker's guide to the Virtual Element Method, *Math. Models Methods Appl. Sci.* **24**(8), 1541–1573.

L. Beirão da Veiga, F. Brezzi, L. D. Marini and A. Russo (2016*a*), $H(div)$ and $H(curl)$-conforming VEM, *Numer. Math.* **133**(2), 303–332.

L. Beirão da Veiga, F. Brezzi, L. D. Marini and A. Russo (2016*b*), Mixed Virtual Element Methods for general second order elliptic problems on polygonal meshes, *ESAIM Math. Model. Numer. Anal.* **50**, 727–747.

L. Beirão da Veiga, F. Brezzi, L. D. Marini and A. Russo (2016*c*), Serendipity nodal VEM spaces, *Comp. Fluids* **141**, 2–12.

L. Beirão da Veiga, F. Brezzi, L. D. Marini and A. Russo (2016*d*), Virtual Element Methods for general second order elliptic problems on polygonal meshes, *Math. Models Methods Appl. Sci.* **26**(4), 729–750.

L. Beirão da Veiga, F. Brezzi, L. D. Marini and A. Russo (2020), Polynomial preserving Virtual Elements with curved edges, *Mathematical Models and Methods in Applied Sciences* **30**(8), 1555–1590.

L. Beirão da Veiga, C. Canuto, R. H. Nochetto and G. Vacca (2021), Equilibrium analysis of an immersed rigid leaflet by the Virtual Element Method, *Math. Models Methods Appl. Sci.* pp. 1323–1372.

L. Beirão da Veiga, A. Chernov, L. Mascotto and A. Russo (2016*e*), Basic principles of hp Virtual Elements on quasiuniform meshes, *Mathematical Models and Methods in Applied Sciences* **26**(08), 1567–1598.

L. Beirão da Veiga, C. Lovadina and D. Mora (2015), A Virtual Element Method for elastic and inelastic problems on polytope meshes, *Comput. Methods Appl. Mech. Engrg.* **295**, 327–346.

L. Beirão da Veiga, C. Lovadina and A. Russo (2017*b*), Stability analysis for the Virtual Element Method, *Math. Models Methods Appl. Sci.* **27**(13), 2557–2594.

L. Beirão da Veiga, G. Manzini and L. Mascotto (2019*a*), A posteriori error estimation and adaptivity in hp Virtual Elements, *Numerische Mathematik* **143**(1), 139–175.

L. Beirão da Veiga, L. Mascotto and J. Meng (2022), Interpolation and stability estimates for edge and face Virtual Elements of general order, arXiv:2203.00303v2 [math.NA].

L. Beirão da Veiga, D. Mora and G. Vacca (2019*b*), The Stokes complex for Virtual Elements with application to Navier–Stokes flows, *J. Sci. Comput.* **81**(2), 990–1018.

L. Beirão da Veiga, A. Russo and G. Vacca (2019*c*), The Virtual Element Method with curved edges, *ESAIM Math. Model. Numer. Anal.* **53**(2), 375–404.

L. Beirão da Veiga, A. Chernov, L. Mascotto and A. Russo (2016), Basic principles of hp Virtual Elements on quasiuniform meshes, *Mathematical Models and Methods in Applied Sciences* **26**(8), 1567–1598.

M. F. Benedetto, S. Berrone, A. Borio, S. Pieraccini and S. Scialò (2016), A hybrid mortar Virtual Element Method for discrete fracture network simulations, *Journal of Computational Physics* **306**, 148–166.

M. F. Benedetto, A. Borio and S. Scialò (2017), Mixed virtual elements for discrete fracture network simulations, *Finite Elem. Anal. Des.* **134**, 55–67.

M. F. Benedetto, A. Borio, F. Kyburg, J. Mollica and S. Scialò (2022), An arbitrary order mixed virtual element formulation for coupled multi-dimensional flow problems, *Comput. Methods Appl. Mech. Engrg.* **391**, Paper No. 114204, 27.

S. Berrone and A. Raeli (2022), Efficient partitioning of conforming virtual element discretizations for large scale discrete fracture network flow parallel solvers, *Engineering Geology* **306**, 106747.

S. Bertoluzza, M. Pennacchio and D. Prada (2019), High order VEMs on curved domains, *Rend. Lincei Mat. Appl.* **30**(2), 391–412.

D. Boffi, F. Brezzi and M. Fortin (2013), *Mixed finite element methods and applications*, Vol. 44 of Springer Series in Computational Mathematics, Springer, Heidelberg.

A. Bossavit (1988), Mixed finite elements and the complex of Whitney forms, in *The mathematics of Finite Elements and applications, VI (Uxbridge, 1987)*, Academic Press, London, pp. 137–144.

L. Botti, D. A. Di Pietro and J. Droniou (2018), A Hybrid High-Order discretisation of the Brinkman problem robust in the Darcy and Stokes limits, *Comput. Methods Appl. Mech. Engrg.* **341**, 278–310.

S. C. Brenner and L. R. Scott (2008), *The mathematical theory of finite element methods*, Vol. 15 of Texts in Applied Mathematics, third edition, Springer, New York.

S. C. Brenner and L.-Y. Sung (2018), Virtual Element Methods on meshes with small edges or faces, *Math. Models Methods Appl. Sci.* **28**, 1291–1336.

S. C. Brenner, Q. Guan and L.-Y. Sung (2017), Some estimates for Virtual Element Methods, *Comput. Methods Appl. Math.* **17**(4), 553–574.

S. C. Brenner, L.-Y. Sung and Z. Tan (2021), A C^1 Virtual Element Method for an elliptic distributed optimal control problem with pointwise state constraints, *Math. Models Methods Appl. Sci.* **31**(14), 2887–2906.

F. Brezzi and L. D. Marini (2013), Virtual element methods for plate bending problems, *Comput. Methods Appl. Mech. Engrg.* **253**, 455–462.

F. Brezzi and L. D. Marini (2021), Finite elements and Virtual Elements on classical meshes, *Vietnam J. Math.* **49**(3), 871–899.

F. Brezzi, R. S. Falk and L. D. Marini (2014), Basic principles of mixed Virtual Element Methods, *ESAIM Math. Model. Numer. Anal.* **48**(4), 1227–1240.

E. Cáceres and G. N. Gatica (2016), A mixed Virtual Element Method for the pseudostress–velocity formulation of the Stokes problem, *IMA J. of Numer. Anal.* **37**(1), 296–331.

E. Cáceres, G. N. Gatica and F. A. Sequeira (2017), A mixed Virtual Element Method for the Brinkman problem, *Math. Mod. and Meth. in Appl. Sci.* **27**(04), 707–743.

E. Cáceres, G. N. Gatica and F. A. Sequeira (2018), A mixed Virtual Element Method for quasi-Newtonian Stokes flows, *SIAM J. Numer. Anal.* **56**(1), 317–343.

A. Cangiani, E. Georgoulis, T. Pryer and O. Sutton (2017), A posteriori error estimates for the Virtual Element Method, *Numerische Mathematik* **137**(4), 857–893.

A. Cangiani, V. Gyrya and G. Manzini (2016), The nonconforming Virtual Element Method for the Stokes equations, *SIAM J. Numer. Anal.* **54**(6), 3411–3435.

S. Cao and L. Chen (2018), Anisotropic error estimates of the linear Virtual Element Method on polygonal meshes, *SIAM Journal on Numerical Analysis* **56**(5), 2913–2939.

S. Cao, L. Chen and R. Guo (2022*a*), Immersed Virtual Element Methods for Maxwell interface problems in three dimensions, arXiv:2202.09987 [math.NA].

S. Cao, L. Chen, R. Guo and F. Lin (2022*b*), Immersed Virtual Element Methods for elliptic interface problems in two dimensions, *Journal of Scientific Computing* **93**, Article number:12.

D. Castañón Quiroz and D. A. Di Pietro (2020), A Hybrid High-Order method for the incompressible Navier–Stokes problem robust for large irrotational body forces, *Comput. Math. Appl.* **79**(9), 2655–2677.

L. Chen and J. Huang (2018), Some error analysis on Virtual Element Methods, *Calcolo* **55**(1), Paper No. 5, 23.

L. Chen and F. Wang (2019), A Divergence Free Weak Virtual Element Method for the Stokes Problem on Polytopal Meshes, *J. Sci. Comput.* **78**(2), 864–886.

A. Chernov, C. Marcati and L. Mascotto (2021), p- and hp- Virtual Elements for the Stokes problem, *Adv. Comput. Math.* **47**, Article number:24.

H. Chi, L. Beirao da Veiga and G. Paulino (2017), Some basic formulations of the Virtual Element Method (VEM) for finite deformations, *Computer Methods in Applied Mechanics and Engineering* **318**, 148–192.

H. Chi, A. Pereira, I. Menezes and G. Paulino (2020), Virtual element method (VEM)-based topology optimization: an integrated framework, *Struct. and Mult. Optim.* **62**, 1089–1114.

E. Chin and N. Sukumar (2021), Scaled boundary cubature scheme for numerical integration over planar regions with affine and curved boundaries, *Computer Methods in Applied Mechanics and Engineering* **380**, Paper number 113796.

E. Chin, J. Lasserre and N. Sukumar (2015), Numerical integration of homogeneous functions on convex and nonconvex polygons and polyhedra, *Computational Mechanics* **56**(6), 967–981.

C. Chinosi and L. D. Marini (2016), Virtual Element Method for fourth order problems: L^2-estimates, *Computers and Mathematics with Applications* **72**(8), 1959–1967.

P. G. Ciarlet (1978), *The finite element method for elliptic problems*, Studies in Mathematics and its Applications, Vol. 4, North-Holland Publishing Co., Amsterdam-New York-Oxford.

M. Cihan, B. Hudobivnik, J. Korelc and P. Wriggers (2022), A Virtual Element Method for 3d contact problems with non-conforming meshes, *Comput. Methods Appl. Mech. Engrg.* p. 115385.

B. Cockburn, G. Fu and W. Qiu (2017), A note on the devising of superconvergent HDG methods for Stokes flow by M-decompositions, *IMA J. Numer. Anal.* **37**(2), 730–749.

F. Dassi and S. Scacchi (2020), Parallel block preconditioners for three-dimensional virtual element discretizations of saddle-point problems, *Comput. Methods Appl. Mech. Engrg.* **372**, Article number:113424.

F. Dassi and G. Vacca (2020), Bricks for mixed high-order Virtual Element Method: projectors and differential operators, *Appl. Numer. Math.* **155**, 140–159.

F. Dassi, P. Di Barba and A. Russo (2020*a*), Virtual element method and permanent magnet simulations: potential and mixed formulations, *IET Science, Measurement & Technology* **14**(10), 1098–1104.

F. Dassi, A. Fumagalli, A. Scotti and G. Vacca (2022), Bend 3d mixed virtual element method for Darcy problems, *Comput. Math. Appl.* **119**, 1–12.

F. Dassi, C. Lovadina and M. Visinoni (2020*b*), A three-dimensional Hellinger–Reissner Virtual Element Method for linear elasticity problems, *Comput. Methods Appl. Mech. Engrg.* **364**, 112910.

D. A. Di Pietro and S. Krell (2018), A Hybrid High-Order method for the steady incompressible Navier-Stokes problem, *J. Sci. Comput.* **74**(3), 1677–1705.

R. S. Falk and M. Neilan (2013), Stokes complexes and the construction of stable finite elements with pointwise mass conservation, *SIAM J. Numer. Anal.* **51**(2), 1308–1326.

D. Frerichs and C. Merdon (2022), Divergence-preserving reconstructions on polygons and a really pressure-robust Virtual Element Method for the Stokes problem, *IMA J. Numer. Anal.* **42**(1), 597–619.

A. L. Gain, G. H. Paulino, L. S. Duarte and I. F. M. Menezes (2015), Topology optimization using polytopes, *Comput. Methods Appl. Mech. Engrg.* **293**, 411–430.

F. Gardini, G. Manzini and G. Vacca (2019), The nonconforming Virtual Element Method for eigenvalue problems, *ESAIM: Mathematical Modelling and Numerical Analysis* **53**(3), 749–774.

G. N. Gatica, M. Munar and F. A. Sequeira (2018*a*), A mixed Virtual Element Method for a nonlinear Brinkman model of porous media flow, *Calcolo* **55**, Article number: 21.

G. N. Gatica, M. Munar and F. A. Sequeira (2018*b*), A mixed Virtual Element Method for the Navier–Stokes equations, *Math. Mod. and Meth. in Appl. Sci.* **28**(14), 2719–2762.

N. Gauger, A. Linke and P. Schroeder (2019), On high-order pressure-robust space discretisations, their advantages for incompressible high Reynolds number generalised Beltrami flows and beyond., *SMAI J. Comput. Math.* **5**, 88–129.

V. Girault and P.-A. Raviart (1979), *Finite element approximation of the Navier-Stokes equations*, Vol. 749 of Lecture Notes in Mathematics, Springer-Verlag, Berlin-New York.

J. Guzmán and M. Neilan (2014), Conforming and divergence-free Stokes elements on general triangular meshes, *Math. Comp.* **83**(285), 15–36.

J. Guzmán and M. Neilan (2018), Inf-Sup Stable Finite Elements on Barycentric Refinements Producing Divergence–Free Approximations in Arbitrary Dimensions, *SIAM J. Numer. Anal.* **56**(5), 2826–2844.

J. Guzmán and L. R. Scott (2019), The Scott-Vogelius finite elements revisited, *Math. Comp.* **88**(316), 515–529.

R. Hiptmair (2001), Discrete Hodge operators, *Numer. Math.* **90**(2), 265–289.

A. Hussein, F. Aldakheel, B. Hudobivnik, P. Wriggers, P.-A. Guidault and O. Allix (2019), A computational framework for brittle crack-propagation based on efficient Virtual Element Method, *Finite Elements in Analysis and Design* **159**, 15–32.

V. John, A. Linke, C. Merdon, M. Neilan and L. G. Rebholz (2017), On the divergence constraint in mixed finite element methods for incompressible flows, *SIAM Rev.* **59**(3), 492–544.

A. Linke and C. Merdon (2016*a*), On velocity errors due to irrotational forces in the Navier-Stokes momentum balance, *J. Comput. Phys.* **313**, 654–661.

A. Linke and C. Merdon (2016*b*), Pressure-robustness and discrete Helmholtz projectors in mixed finite element methods for the incompressible Navier-Stokes equations, *Comput. Methods Appl. Mech. Engrg.* **311**, 304–326.

K. Lipnikov, D. Vassilev and I. Yotov (2014), Discontinuous Galerkin and mimetic finite difference methods for coupled Stokes-Darcy flows on polygonal and polyhedral grids, *Numer. Math.* **126**(2), 321–360.

X. Liu and Z. Chen (2019), The nonconforming Virtual Element Method for the Navier-Stokes equations, *Adv. Comput. Math.* **45**(1), 51–74.

X. Liu, J. Li and Z. Chen (2017), A nonconforming Virtual Element Method for the Stokes problem on general meshes, *Comput. Methods Appl. Mech. Engrg.* **320**, 694–711.

X. Liu, R. Li and Z. Chen (2019), A Virtual Element Method for the coupled Stokes–Darcy problem with the Beaver–Joseph–Saffman interface condition, *Calcolo* **56**(4), Article number:48.

X. Liu, R. Li and Y. Nie (2020), A divergence-free reconstruction of the nonconforming Virtual Element Method for the Stokes problem, *Comput. Methods Appl. Mech. Engrg.* **372**, Article number:113351.

L. Mascotto, I. Perugia and A. Pichler (2019), A nonconforming Trefftz Virtual Element Method for the Helmholtz problem, *Math. Models Methods Appl. Sci.* **29**(9), 1619–1656.

C. Mattiussi (1997), An analysis of finite volume, finite element, and finite difference methods using some concepts from algebraic topology, *J. Comput. Phys.* **133**(2), 289–309.

D. Mora, G. Rivera and R. Rodríguez (2015), A Virtual Element Method for the Steklov eigenvalue problem, *Math. Models Methods Appl. Sci.* **25**(8), 1421–1445.

D. Mora, G. Rivera and R. Rodriguez (2017), A posteriori error estimates for a Virtual Element Method for the steklov eigenvalue problem, *Comput. Math. Appl.* **74**(9), 2172–2190.

M. Munar and F. A. Sequeira (2020), A posteriori error analysis of a mixed Virtual Element Method for a nonlinear Brinkman model of porous media flow, *Comput. Math. Appl.* **80**(5), 1240–1259.

S. Natarajan (2020), On the application of polygonal finite element method for Stokes flow – A comparison between equal order and different order approximation, *Comput. Aided Geom. Design* **77**, Article number:101813.

K. Park, H. Chi and G. Paulino (2020), Numerical recipes for elastodynamic Virtual Element Methods with explicit time integration, *Int. J. Num. Meth. Engnrg.* **121**, 1–31.

K. Park, H. Chi and G. Paulino (2021), B-bar Virtual Element Method for nearly incompressible and compressible materials, *Meccanica* **56**, 1423–1439.

J. C. Simo and T. J. Hughes (2006), *Computational inelasticity*, Vol. 7, Springer Science & Business Media.

G. Vacca (2018), An H^1-conforming virtual element for Darcy and Brinkman equations, *Math. Models Methods Appl. Sci.* **28**(1), 159–194.

F. Wang and J. Zhao (2021), Conforming and nonconforming Virtual Element Methods for a Kirchhoff plate contact problem, *IMA J. Numer. Anal.* **41**(2), 1496–1521.

G. Wang, Y. Wang and Y. He (2020), A Posteriori Error Estimates for the Virtual Element Method for the Stokes Problem, *J. Sci. Comput.* **84**(2), Article number:37.

P. Wriggers and B. Hudobivnik (2017), A low order virtual element formulation for finite elasto-plastic deformations, *Computer Methods in Applied Mechanics and Engineering* **327**, 459–477.

P. Wriggers, B. Reddy, W. Rust and B. Hudobivnik (2017), Efficient virtual element formulations for compressible and incompressible finite deformations, *Comput. Mech.* **60**, 253–268.

P. Wriggers, W. Rust and B. Reddy (2016), A Virtual Element Method for contact, *Comput. Mech.* **58**, 1039–1050.

J. Zhao, S. Chen and B. Zhang (2016), The nonconforming Virtual Element Method for plate bending problems, *Math. Models Methods Appl. Sci.* **26**(09), 1671–1687.

J. Zhao, B. Zhang, S. Mao and S. Chen (2020), The nonconforming Virtual Element Method for the Darcy–Stokes problem, *Comput. Methods Appl. Mech. Engrg.* **370**, Article number:113251.